

UNCLASSIFIED

AD NUMBER	
AD356143	
CLASSIFICATION CHANGES	
TO:	unclassified
FROM:	confidential
LIMITATION CHANGES	
TO:	Approved for public release, distribution unlimited
FROM:	Distribution authorized to U.S. Gov't. agencies and their contractors; Administrative/Operational Use; NOV 1964. Other requests shall be referred to Directorate of Armament Dev., Det. 4, AFSC, Eglin AFB, FL.
AUTHORITY	
AFATL ltr, 28 Oct 1975; AFATL ltr, 28 Oct 1975	

THIS PAGE IS UNCLASSIFIED

NOTICE: When government or other drawings, specifications or other data are used for any purpose other than in connection with a definitely related government procurement operation, the U. S. Government thereby incurs no responsibility, nor any obligation whatsoever; and the fact that the Government may have formulated, furnished, or in any way supplied the said drawings, specifications, or other data is not to be regarded by implication or otherwise as in any manner licensing the holder or any other person or corporation, or conveying any rights or permission to manufacture, use or sell any patented invention that may in any way be related thereto.

NOTICE:

THIS DOCUMENT CONTAINS INFORMATION -  
AFFECTING THE NATIONAL DEFENSE OF  
THE UNITED STATES WITHIN THE MEAN-  
ING OF THE ESPIONAGE LAWS, TITLE 18,  
U.S.C., SECTIONS 793 and 794. THE  
TRANSMISSION OR THE REVELATION OF  
ITS CONTENTS IN ANY MANNER TO AN  
UNAUTHORIZED PERSON IS PROHIBITED  
BY LAW.

356143

CATALOGED BY DDC  
AS AD No.

ATL-TR-64-74

Copy 157 Copies.

(U) RESEARCH ON THE PROJECTION OF MULTILAYERED FRAGMENTS

by

Edward C. Poston, Jr.

3 5 6 1 4 3

November 1964

This document contains information affecting the national defense of the United States within the meaning of the Espionage Laws, Title 18, U.S.C., Sections 793 and 794. Its transmission or the revelation of its contents in any manner to an unauthorized person is prohibited by law.

Directorate of Armament Development  
Det 4, Research and Technology Division  
Air Force Systems Command  
Eglin Air Force Base, Florida

GROUP-4  
DOWNGRADED AT 3-YEAR INTERVALS;  
DECLASSIFIED AFTER 12 YEARS

Best Available Copy

PAGES \_\_\_\_\_  
ARE  
MISSING  
IN  
ORIGINAL  
DOCUMENT

FOR ERRATA

AD 3 5 6 1 4 3

THE FOLLOWING PAGES ARE CHANGES

TO BASIC DOCUMENT

Best Available Copy

HEADQUARTERS  
AIR PROVING GROUND CENTER  
AIR FORCE SYSTEMS COMMAND  
UNITED STATES AIR FORCE  
Eglin Air Force Base, Florida 32542



REPLY TO: FGLOR  
ATTN OF:

15 January 1965

SUBJECT: Errata for ATL-TR-64-74, Research on the Projection  
of Multilayered Fragments

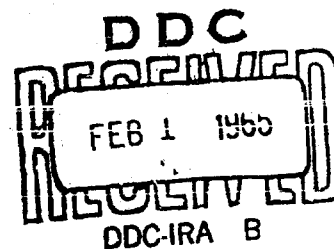
TO: Initial Recipients

1. The authors for subject report should be changed from Edward C. Poston, Jr., to JOHN K. CROSBY and C. F. ALLEN.
2. Request pen and ink corrections be made on the Cover, Title Page, and DD Form 1473 at the back of the report.

*Louis J. Vogel*  
LOUIS J. VOGEL

STINFO and Technical Reports Branch

356143



Best Available Copy

*Research & Tech Div*

Qualified requesters may obtain copies from DDC. Orders will be expedited if placed through the librarian or other person designated to request documents from DDC.

This document contains information affecting the national defense of the United States within the meaning of the Espionage Laws (Title 18, U.S.C., sections 793 and 794). Transmission or revelation in any manner to an unauthorized person is prohibited by law.

When US Government drawings, specifications, or other data are used for any purpose other than a definitely related government procurement operation, the government thereby incurs no responsibility nor any obligation whatsoever; and the fact that the government may have formulated, furnished, or in any way supplied the said drawings, specifications, or other data is not to be regarded by implication or otherwise, as in any manner licensing the holder or any other person or corporation, or conveying any rights or permission to manufacture, use, or sell any patented invention that may in any way be related thereto.

Do not return this copy. When not needed, destroy in accordance with pertinent security regulations.

**CONFIDENTIAL**

(U) RESEARCH ON THE PROJECTION OF MULTILAYERED FRAGMENTS

by

Edward C. Poston, Jr.

**CONFIDENTIAL**



## FOREWORD

---

(U) This report describes the work performed by Poulter Research Laboratories of Stanford Research Institute under Contract No. AF 08(635)-2951. This project was originated and funded by the Weapons Division, Research and Technology Branch (ATWR) Detachment 4, RTD, Eglin Air Force Base, Florida. In addition to acknowledging this support, the authors wish to thank the following members of the Stanford Research Institute staff for their major contributions to the project. Mr. Roy McLeod is responsible for the high quality of over one hundred flash X-ray records which were indispensable in the evaluation of the many designs studied. Mr. Lee Parker performed the later work on shock initiation of explosives using flying plates. The Q Code programming and running of the program were performed by Mr. John O. Erkman. The advice and encouragement of Dr. David Bernstein are also gratefully acknowledged.

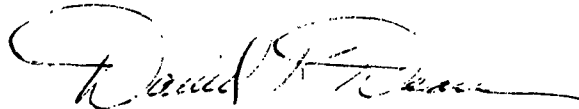
# CONFIDENTIAL

## ABSTRACT (C)

---

(C, gp 4) This report describes a research program directed toward developing methods for explosive acceleration of multiple fragment layers to a uniform velocity. Seven methods which achieve such velocity uniformity in varying degrees are described. Other aspects of these methods which received attention included fragment density in the fragment cloud, fragment velocity, fragment cloud growth rate, and damage to fragments. Appendices are included which discuss theoretical calculations of the performance of one method, special instrumentation developed and used during the project, and fabrication methods for the fragment pack. A final appendix gives a complete listing of the shots fired during the project.

This report has been reviewed and is approved.



DAVID K. DEAN  
Colonel, USAF  
Chief, Weapons Division

# CONFIDENTIAL

## CONTENTS

---

1.	INTRODUCTION .....	1
2.	SUMMARY .....	5
3.	GENERAL PROCEDURE .....	7
	A. Concept and Literature Search .....	7
	B. Modification .....	7
	C. Solid Plate Velocity Uniformity .....	7
	D. Fragment Plate Velocity Uniformity .....	7
	E. Fragment Trajectory Distribution .....	8
	F. Fragment Recovery .....	8
4.	VELOCITY UNIFORMITY .....	9
	A. Flying Plate Acceleration .....	9
	B. Electrical Backwards Initiation .....	18
	C. MDF Backwards Initiation .....	26
	D. Shock-Induced Backwards Initiation .....	34
	E. Spaced and Buffered Plates .....	46
	F. NOL Two-Stage Design .....	52
	G. Expanded Metal Studies .....	60
	H. Miscellaneous Designs .....	71
5.	FRAGMENT TRAJECTORY DISTRIBUTION .....	75
	A. Measurement Technique .....	75
	B. Summary of Results .....	80
6.	FRAGMENT DAMAGE .....	85
	A. Flying Plate Shot .....	85
	B. Felted Metal Shots .....	86
	C. Hollow Sphere Shots .....	86
7.	CONCLUSIONS AND RECOMMENDATIONS .....	89
	A. Conclusions .....	89
	B. Recommendations .....	90
APPENDIX I	SIMPLE CALCULATIONS OF FLYING PLATE ACCELERATIONS (U) .....	91
APPENDIX II	Q CODE CALCULATIONS (U) .....	101

## CONTENTS (Continued)

---

APPENDIX III	INSTRUMENTATION (U) . . . . .	111
APPENDIX IV	FRAGMENT PACK FABRICATION TECHNIQUES (U) . .	123
APPENDIX V	COMPLETE SHOT TABULATION (U). . . . .	131
REFERENCES	. . . . .	145

# CONFIDENTIAL

## ILLUSTRATIONS

---

Fig. 1 (U)	Acceleration of Multiple Layers by a Shock Wave (U) . . .	2
Fig. 2 (U)	Design of Flying Plates Shots (U) . . . . .	10
Fig. 3 (U)	Aluminum Flying Plate Shot, No. 9978 (C) . . . . .	11
Fig. 4 (U)	Sixteen-Layer Flying Plate Shot, No. 9644 (C) . . . . .	12
Fig. 5 (U)	Major Pieces Recovered from Plate Acceleration Shots (U) . . . . .	14
Fig. 6 (U)	Heavy Plates, 1 inch thick, Accelerated by 3 inches of Comp B (U) . . . . .	15
Fig. 7 (U)	Design for Shot No. 9817 Using Pressure Transducers (U) . . . . .	16
Fig. 8 (U)	Design for Second Transducer Shot, No. 9818 (U) . . . . .	17
Fig. 9 (U)	Breakdown of Thin Aluminum Foil Bridgewires (U) . . . . .	21
Fig. 10 (U)	Three-Point Electrical Backwards Initiation Design (U) . . . . .	22
Fig. 11 (U)	Electrical Backwards Initiation Shots (U) . . . . .	24
Fig. 12 (C)	Standard MDF Shot Design and Modifications (U) . . . . .	27
Fig. 13 (U)	Double-Scale MDF Shot with 1/4-inch Balls, No. 10,203 (C) . . . . .	29
Fig. 14 (U)	Double-Scale MDF Shot with 1/8-inch Balls, No. 10,204 (C) . . . . .	30
Fig. 15 (C)	Modified MDF Shots (U) . . . . .	31
Fig. 16 (U)	Modified MDF Shot, No. 10,254. Flash X-ray at 580 $\mu$ sec (U) . . . . .	32
Fig. 17 (U)	Early Shot Design for Shock-Induced Backwards Initiation Studies (U) . . . . .	35
Fig. 18 (U)	Modified Shock-Induced Backwards Initiation Design (U) . .	36
Fig. 19 (U)	Shock-Induced Backwards Initiation Shot Operating Satisfactorily, No. 9240 (U) . . . . .	37
Fig. 20 (C)	Shock-Induced Backwards Initiation X-ray Shots. (U) . . .	38
Fig. 21 (U)	Mousetrap Design for Delayed Shock Initiation of Comp B (U) . . . . .	39
Fig. 22 (U)	Pressure vs Particle Velocity Plots for Shock-Initiated Backwards Initiation Design (U) . . . . .	39

CONFIDENTIAL

# CONFIDENTIAL

## ILLUSTRATIONS (Continued)

---

Fig. 23 (U)	Framing Camera Records of Two Shock-Initiated Backwards Initiation Experiments (U) . . . . .	41
Fig. 24 (U)	X-Ray Records of Two Shock-Initiated Backwards Initiation Experiments (U) . . . . .	43
Fig. 25 (U)	Spaced Layer Shot Design (U) . . . . .	46
Fig. 26 (U)	Spaced Plate Shot, No. 9711 (U) . . . . .	48
Fig. 27 (C)	Spaced Fragment Plate Shot Assembly (C) . . . . .	49
Fig. 28 (C)	Spaced Plate Shots with Fragments and 60 lb/ft <sup>3</sup> Foam (C) . . . . .	50
Fig. 29 (C)	NOL Design Modified for Multilayer Acceleration (C) . . .	53
Fig. 30 (C)	Assembly and Setup of NOL Design Shots (U) . . . . .	55
Fig. 31 (C)	NOL Design Shots (U) . . . . .	56
Fig. 32 (U)	NOL Shots with Fragments (U) . . . . .	57
Fig. 33 (C)	Two-Inch NOL Shots with Various Inner Explosive Arrangements (C) . . . . .	59
Fig. 34 (U)	Distance-Time Plot of Explosively Shocked, Low-Density Metal (U) . . . . .	61
Fig. 35 (C)	Evacuated Metal Felt Shot Design (U) . . . . .	62
Fig. 36 (U)	X-ray Records of Evacuated Metal Felt Shots (U) . . . . .	63
Fig. 37 (C)	Compressed Fragments Recovered from 4-Layer Low-Density Shots (C) . . . . .	64
Fig. 38 (C)	Felted Nickel Shot with Quasi-Plane-Wave Initiation (U) . .	65
Fig. 39 (U)	Felted Nickel X-ray Shot, No. 10,392 - 970 $\mu$ sec (U) . . .	66
Fig. 40 (U)	Nickel Fragments Recovered from Shot No. 10,392 (U) . .	66
Fig. 41 (U)	Assembly of Felted Nickel Fragments Separated by 0.005-inch Mylar, Shot No. 10,480 (C) . . . . .	67
Fig. 42 (U)	Felted Nickel X-ray Shot with Fragments Separated by 0.005-inch Mylar, No. 10,480 (C) . . . . .	68
Fig. 43 (U)	Recovered Fragments from Felted Nickel Shot with Mylar Separation, No. 10,480 (U) . . . . .	69
Fig. 44 (U)	Aluminum Foam Buffer Shot, No. 10,270 (U) . . . . .	73
Fig. 45 (U)	Record from Shot Interlayered with 0.0165-inch Lead, No. 10,237 (U) . . . . .	74

CONFIDENTIAL

# CONFIDENTIAL

## ILLUSTRATIONS (Continued)

---

Fig. 46 (U)	First Fragment Distribution Target, Showing Hits from Shot No. 9607 (U) . . . . .	76
Fig. 47 (U)	Fragment Hit Distribution, Shot No. 9607 (U) . . . . .	78
Fig. 48 (U)	Fragment Hit Distribution, Shot No. 9771 (U) . . . . .	79
Fig. 49 (U)	Six-Point MDF Peripheral Backwards Initiation (U) . . . . .	82
Fig. 50 (U)	Peripheral Initiation Design, Shot No. 9799 (U) . . . . .	83
Fig. 51 (U)	Hit Pattern from 3-inch NOL Design, Shot No. 10,398 (U) . . . . .	84
Fig. 52 (U)	Typical Fragments Recovered from Range Shot No. 9445 (U) . . . . .	85
Fig. 53 (C)	Recovered Hollow Brass Balls (U) . . . . .	87
Fig. 54 (C)	Transfer Ratios Between Flying Plate and Fragment Pack for Various Density Ratios (C) . . . . .	95
Fig. 55 (U)	Pressure vs Distance for Shock Wave Induced in an Aluminum Target by the Impact of an Aluminum Plate (Space Coordinates are Lagrangian) (U) . . . . .	105
Fig. 56 (U)	Particle Velocity vs Distance for Shock Wave Induced in an Aluminum Target by the Impact of an Aluminum Plate (Space Coordinates are Lagrangian) (U) . . . . .	106
Fig. 57 (U)	Free-Surface Velocity vs Distance into Target (U) . . . . .	107
Fig. 58 (U)	Calculated Impact of 1-Inch Stack of Steel Plates (U) . . . . .	108
Fig. 59 (U)	Standard X-ray Setup (U) . . . . .	114
Fig. 60 (U)	Shot Setup with Two-Film Cassettes, Shot No. 10,203 (U) . . . . .	115
Fig. 61 (U)	Smear Camera Record of Backwards Initiation, Shot No. 9330 (U) . . . . .	117
Fig. 62 (U)	Evaporated Gold-on-Mylar Switch Arrangement (U) . . . . .	118
Fig. 63 (U)	Foil Switch and Fiber Optics Shot, No. 9497 (U) . . . . .	121
Fig. 64 (U)	Smear Camera Record with Foil Switch Closures Entered, Shot No. 9625 (U) . . . . .	122
Fig. 65 (U)	Soldered Hexagonal Fragment Layer Cast in Cerrobend (U) . . . . .	126
Fig. 66 (U)	Round Fragments Cast in a Round Tube with Cerrobend Filler (U) . . . . .	127

CONFIDENTIAL

## ILLUSTRATIONS (Continued)

---

Fig. 67 (U)	Round Fragments in a Hexagonal Tube Potted in Epoxy (U) . . . . .	128
Fig. 68 (U)	Stacking 1/8-inch Balls in the Double-Scale Mold (U) . . . .	129
Fig. 69 (U)	Standard 1/8-inch Ball Pack (U) . . . . .	129
Fig. 70 (U)	Standard Pack with Two Double-Scale Packs (U) . . . . .	130



# CONFIDENTIAL

## TABLES

---

Table 1 (U)	Flying Plate Spall Control Shots (U) . . . . .	13
Table 2 (U)	Results of Pressure Transducer Shots (U) . . . . .	18
Table 3 (C, gp 4)	Selected Flying Plate Shots (U) . . . . .	19
Table 4 (C, gp 4)	Electrical Backwards Initiation Shots (U) . . . . .	25
Table 5 (C, gp 4)	MDF Backwards Initiation Shots (U) . . . . .	33
Table 6 (U)	Shock-Induced Backwards Initiation Shots with Comp B (U). . . . .	44
Table 7 (U)	Shock-Induced Backwards Initiation Shots with PBX (U). . . . .	45
Table 8 (C, gp 4)	Shots with Spaced and Buffered Plates (U) . . . . .	51
Table 9 (C, gp 4)	Selected NOL Design Shots (U) . . . . .	58
Table 10 (C, gp 4)	Low-Density Fragment Shots (C). . . . .	70
Table 11 (C, gp 4)	Simultaneous Forward-Backward Initiation (U) . . .	71
Table 12 (C, gp 4)	Fragment Trajectory Shots (C). . . . .	81
Table 13 (C, gp 4)	Comparison of Various Designs (U). . . . .	89
Table 14 (C, gp 4)	Designs for Maximum Velocity for Various Fragment Materials and Total Weight (U) . . . . .	97
Table 15 (C, gp 4)	Designs for Various Total Warhead Weights which Maximize Momentum, Energy, and Lethality (C) . . . . .	98
Table 16 (C, gp 4)	Flying Plate Shots (U) . . . . .	134
Table 17 (C, gp 4)	Electrical Backwards Initiation Shots (U) . . . . .	136
Table 18 (C, gp 4)	MDF Backwards Initiation Shots (U) . . . . .	137
Table 19 (C, gp 4)	Shock-Induced Backwards Initiation Shots (U) . . . .	138
Table 20 (U)	Flying Plate Shock-Induced Backwards Initiation (U) . . . . .	139
Table 21 (C, gp 4)	Spaced and Buffered Plate Shots (C) . . . . .	140
Table 22 (C, gp 4)	NOL Design Shots (U) . . . . .	144
Table 23 (C, gp 4)	Low-Density Fragment Shots (C) . . . . .	143
Table 24 (C, gp 4)	Miscellaneous Shots (U). . . . .	144

CONFIDENTIAL

# CONFIDENTIAL

## 1. INTRODUCTION

(C, gp 4) This project was devoted to the preliminary development of concepts which can be used to design a warhead which will project a large number of preformed fragments from one end of an explosive charge. The major specification of the proposed warhead which required research to satisfy was that a fairly uniform velocity be given to all fragments, even though they had to be arranged originally in several layers. If this could be done, a thin, disc-shaped cloud of fragments would result.

(U) When a thick metal plate is accelerated by an impulse from a detonating layer of explosive on one side of it, the velocities given to various parts of the plate may vary greatly with position. Depending on the strength of the plate material and on the velocity gradients present, the plate may either overcome these velocity differences by retaining its integrity and moving off at some average velocity, or it may fracture and move off in pieces traveling at different velocities.

(U) If the solid plate is replaced by a pack of fragments held together by joints of negligible strength, the fragments will separate easily, and each will move off with the velocity typical of its original location. This behavior has long been used<sup>1</sup> as a method of determining the pressure-distance curve of a plane shock because, in this case, the momentum given to each plate of a stack of thin plates is roughly proportional to the momentum in a portion of the accelerating shock wave which is twice the plate thickness. Thus the outermost plate traps the momentum of the leading edge of the shock and typically moves off at the highest velocity, whereas plates successively farther in trap momentum from later, lower pressure portions of the wave and move off at lower velocities. An approximate schematic representation of this process is shown in Figure 1.

(U) Figure 1(a) shows a plane shock traveling through a stack of plates. As such a shock passes a given plane in the stack, the pressure and density jump almost instantaneously to the shocked values. The material at this plane

# CONFIDENTIAL

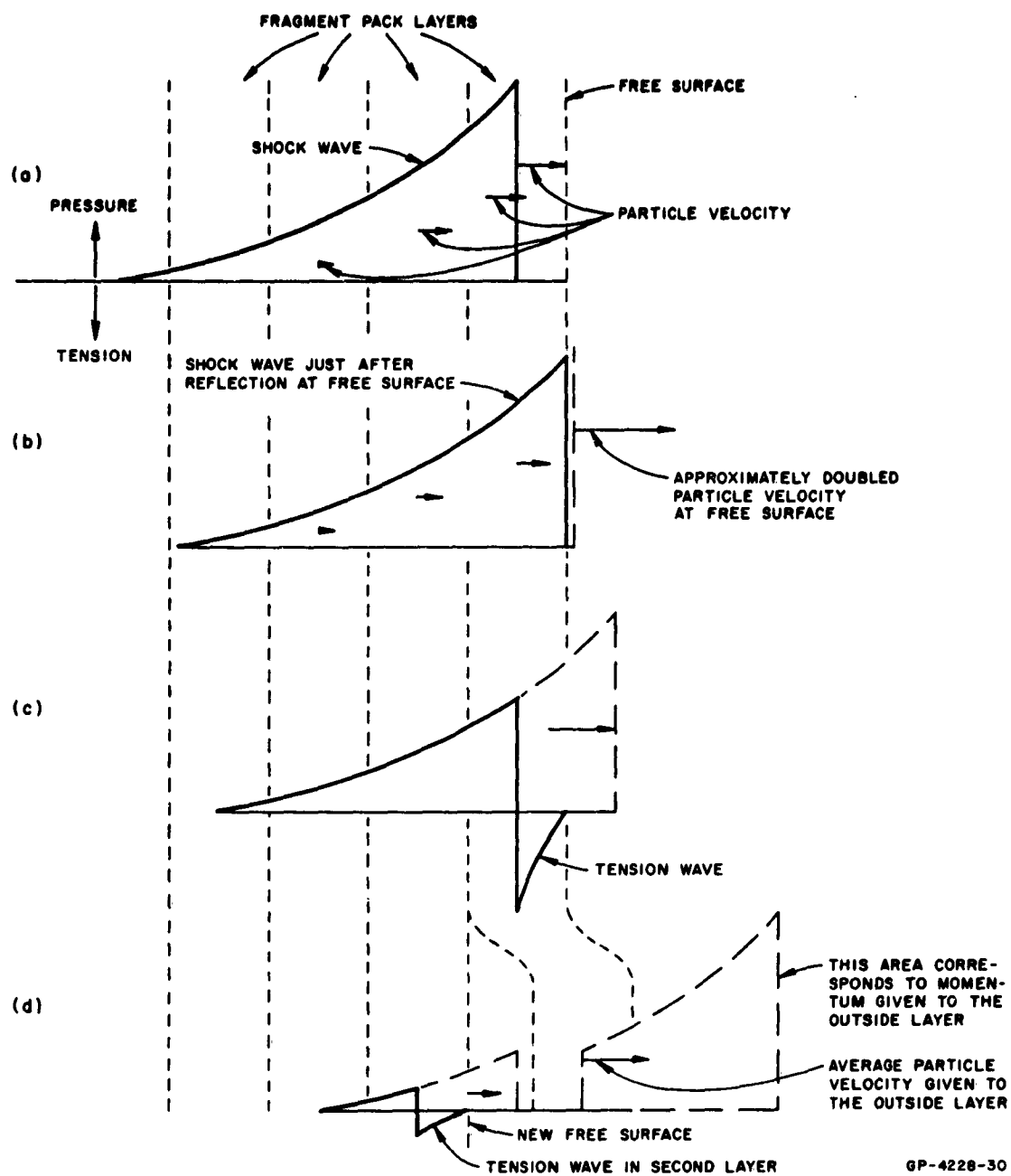


FIGURE 1 (U) ACCELERATION OF MULTIPLE LAYERS BY A SHOCK WAVE (U)  
 [Figure and caption combined (U)]

# CONFIDENTIAL

is also accelerated to some peak particle velocity which depends on the equation of state of the material and the peak pressure. As the shock front moves away from this plane, the pressure, density, and particle velocity at the plane all fall back toward the initial preshock values. When such a shock reaches a free boundary, as shown in Figure 1(b), it is reflected as a rarefaction wave of equal but opposite amplitude to the shock. This rarefaction keeps the free-surface pressure at zero and approximately doubles the particle velocity there. As the rarefaction travels back into the fragment pack, a net tension is developed at the rarefaction front since the negative peak value of the rarefaction wave has an absolute magnitude greater than the local positive pressure caused by the tail of the shock. When a joint of negligible strength between fragment layers is reached, this tension separates the layers, thus producing a new free surface and starting the process all over again as shown in Figure 1(d). However, since the high pressure and high particle velocity portion of the shock has been trapped in the first fragment layer, subsequent layers will end up with lower and lower particle velocities, with the exact values depending on the shape of the original shock wave.

(U) It should be emphasized that the above discussion ignores several aspects of shock propagation, such as decay of the initial shock, finite rise times in the reflected wave, material motion during shock front motion, and effects of gaps between fragment layers and between fragments in one layer. It is included here only to make clear the gross behavior to be expected from such a system.

(C, gp 4) From this discussion it is easy to see that one way to achieve uniform velocity for fragments originating in all the layers is to apply a constant pressure to one side of the fragment pack for a time equal to at least two shock traversal times through the pack. Another method is to accept the usual sharp pulse from the explosive but to modify it during passage through the fragment pack so that essentially uniform fragment velocities result. Both methods received attention during the project, and several techniques were developed using each of them.

(C, gp 4) In addition to the requirement of uniform fragment velocity, the original contract also specified that the warhead place "80 percent of the total number of pellets within a circular, hexagonal, or square pattern of uniform

# CONFIDENTIAL

# CONFIDENTIAL

distribution", and that it deliver "80 percent of the fragments to a range of 25 feet in air with a mass loss of less than 5 percent (less than 20 percent pellet breakup)". These aspects of the warhead performance were judged to be comparatively easy to control. Because of this and because they would be most affected by details of the later design of an operational warhead, they were not given as much attention as the problem of uniformity of fragment velocity. The tests that were made, however, indicated that there should be little difficulty in achieving the desired performance.

(U) Technical effort on this project started in September of 1962 with goals set out in R&D Exhibit No. ASQWR 61-11. After a year, the contract was extended and at that time R&D Exhibit No. ASQWR 61-11A was substituted. Experimental work was completed in August of 1964.

# CONFIDENTIAL

**CONFIDENTIAL**

## **2. SUMMARY**

(C, gp 4) During this project seven methods for projection of multiple layers of fragments from the end of an explosive charge were developed, which, in varying degrees, produce a cloud of fragments with uniform velocity. The velocity variation achieved went from 1 or 2 percent up to  $\pm 15$  percent, the fragment velocity varied from 0.17 to 0.68 mm/ $\mu$ sec, and the fraction of the total mass represented by fragments varied from 10 to 82 percent. Of course, low variation, high velocity, and high mass fraction in fragments were not all present in one design. However, a wide enough variety of combinations is available so that tailoring of performance to end item requirements should be fairly straightforward.

(C, gp 4) In addition to tests for velocity uniformity, additional shots were fired to determine the distribution of fragments in the fragment cloud. In some cases when some areas of the cloud appeared to have a low fragment density, changes were made in the design to correct this fault. Four methods were checked in this way, and all appeared capable of delivering a cloud of adequate density uniformity.

(U) Damage to fragments was not considered to be very likely in most of the designs studied, since the fragments used were chunky and comparatively gentle accelerations were produced. Even hollow brass balls were found to survive acceleration fairly well, and all other recovered fragments showed inconsequential damage.

(U) Two special techniques were developed during the project. The first used vacuum-deposited gold circuits to monitor the position of a detonation front deep in a piece of explosive without seriously disturbing the processes of initiation or detonation. The second used fiber optics probes to bring optical signals out through a thick metal barrier so that they could be recorded by a smear camera.

**CONFIDENTIAL**

# CONFIDENTIAL

## 3. GENERAL PROCEDURE

(C, gp 4) The development and testing of each of the seven methods developed for velocity control followed essentially similar paths. These consisted of six major steps:

### A. CONCEPT AND LITERATURE SEARCH

(U) The original concept for most of the methods originated in the staff of the Laboratories and resulted from the long experience we have had with problems of this kind. Other methods were suggested by various sources including the technical representatives of the sponsor, a report on calculations by some Naval Ordnance Laboratories personnel, and a suggestion made some years ago by Picatinny Arsenal personnel.

### B. MODIFICATION

(U) Quite often the source of the original concept was in work with a goal quite different from that of this project. It was therefore often necessary to modify the design or the emphasis in the design before experimenting to determine feasibility.

### C. SOLID PLATE VELOCITY UNIFORMITY

(C, gp 4) In order to get a first approximation to the ultimate performance of each method, the fragment pack was simulated by a stack of solid steel plates. Usually eight plates, each 2 inches in diameter and 1/8 inch thick, were used. After acceleration by the explosive, the flight of these plates was observed by the double flash X-ray camera. This procedure made it possible to fire several shots and to modify the design as necessary without destroying a large number of expensive fragment packs.

### D. FRAGMENT PLATE VELOCITY UNIFORMITY

(C, gp 4) When a method had been made to operate satisfactorily in tests with solid plates, similar shots were fired with fragment plates. As expected, these usually showed that the fragments behaved in essentially the same way as the solid plates had. In some methods the velocity uniformity was not good

CONFIDENTIAL

# CONFIDENTIAL

within a layer, even though the layer-to-layer differential was small. In these cases additional work was sometimes done to attempt to reduce the intra-layer variation.

## E. FRAGMENT TRAJECTORY DISTRIBUTION

(C, gp 4) In order to check on the fragment density in various parts of the fragment cloud produced by a design, firings were made against a large target covered with cardboard. After the shot a record was made of the hit density at all points on the target. When a hit pattern with undesirable features was recorded, such as an area of significantly lower density somewhere in the pattern, efforts were made to correct it.

## F. FRAGMENT RECOVERY

(U) It became obvious early in the project that damage to the fragments was not likely to be severe in any of the methods studied. Some estimate of this damage could be made by close examination of the flash X-ray records, and this was supplemented by occasional fragments recovered as a by-product of other tests. In the few cases where the survival of the fragments was in doubt, styrofoam and water recovery systems were used, usually in connection with an X-ray shot.



# CONFIDENTIAL

## 4. VELOCITY UNIFORMITY

(C, gp 4) In all, seven methods for uniform acceleration were developed during the two years of the project. In this report the word "method" will be used to denote one of these seven major techniques; "design" will be used to denote a particular manifestation of one method: flying plate method, aluminum flying plate design; NOL method, 3-inch NOL design. This section briefly describes the development of each method and contains tables summarizing the performance achieved by various designs.

### A. FLYING PLATE ACCELERATION

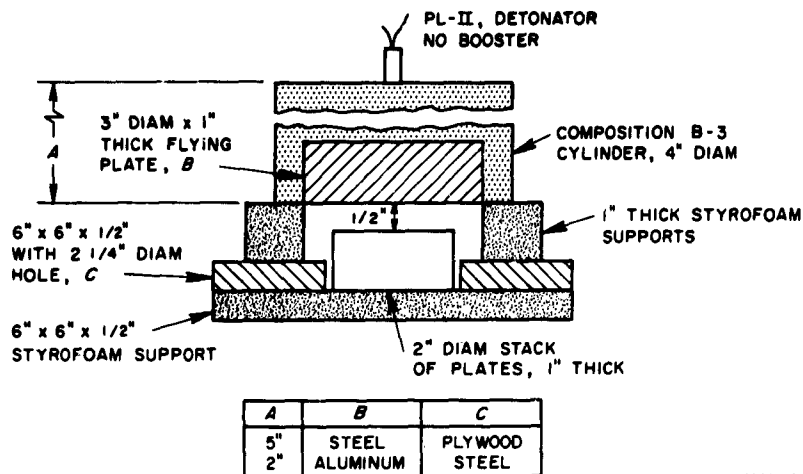
#### 1. Theory

(C, gp 4) When a solid metal plate strikes a multilayer fragment pack, two shock waves will originate at the plane of impact; one will travel forward into the fragment pack, and one will travel back into the plate. The pressure at the impact plane will remain at its original value until one of these shocks reaches a free surface and the resulting relief wave passes back through the pack, or the plate, to the impact plane. If the time for this process to occur via the plate is made at least as long as the time required via the fragment pack, the condition of a constant pressure pulse on the fragment pack will have been met, and all the fragments in the pack should be accelerated to the same velocity.

(C, gp 4) Appendix I gives the details of a simple calculation of the performance of various possible combinations of materials for the flying plate and for the fragments. Based on the results of this calculation, designs employing two materials, steel and aluminum, for flying plates were chosen for development. The steel plate design was expected to provide high velocity fragments although at a high cost in wasted weight, whereas the aluminum plate design was expected to be more efficient in terms of weight but to yield a lower velocity.

CONFIDENTIAL

CONFIDENTIAL



GA-4228-16

FIGURE 2 (U) DESIGN OF FLYING PLATE SHOTS (U)  
[Figure and caption combined (U)]

## 2. Experiments

(C, gp 4) A typical early shot design is shown in Figure 2. In later shots it was found that the aluminum plate design gave more uniform fragment velocity when both the plate and the explosive were 4 inches in diameter. When this change was made, the uniformity achieved by this design was quite remarkable. Figure 3 shows the X-ray records of the fragment cloud produced by such a design at a point about 7 inches from the shot. A large film and a single X-ray flash were used here so that the entire cloud could be recorded. Figure 4 shows another plate shot in which 16 fragment layers were accelerated, each containing about 800 fragments. Note here that even after 13 inches of travel, the main fragment cloud has not become appreciably thicker than its original 1 inch.

(C, gp 4) Although steel flying plates were apparently accelerated to velocities close to  $1.0 \text{ mm}/\mu\text{sec}$  by the explosive assembly shown in Figure 2, the fragment velocity fell far short of this figure. Since this is not predicted either by the simple calculations discussed in Appendix I or by the more sophisticated calculations discussed in Appendix II, some additional research was done to attempt to understand and improve the performance.

CONFIDENTIAL

**CONFIDENTIAL**

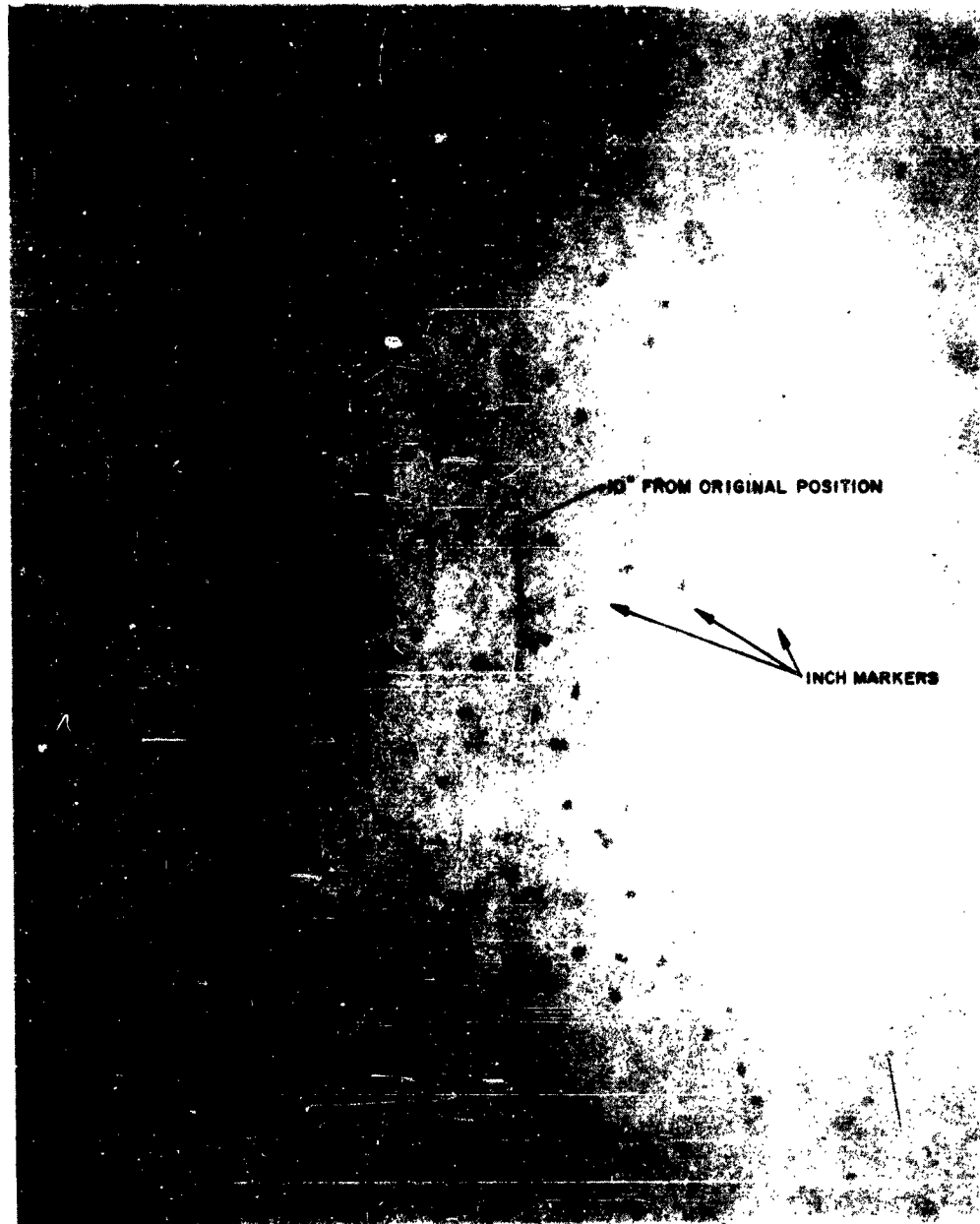


Figure 3 (U) Aluminum Flying Plate Shot, No. 9978 (C).

**CONFIDENTIAL**

CONFIDENTIAL



Figure 4 (U) Sixteen-Layer Flying Plate Shot, No. 9644 (C).

CONFIDENTIAL

**CONFIDENTIAL**

(C, gp 4) On the assumption that the poor performance of the steel flying plate design was due to spalling and breakup of the steel before impact on the fragment pack, several shots were made without fragment packs or plate stacks of any kind. The X ray was used to measure plate velocity and the major pieces of the plates were recovered to check on spalling.

(U) Table 1 gives details of four designs tried in the series, and Figure 5 shows the major spall recovered after each shot. As can be seen from Figure 5 the two shots utilizing a simple foam rubber buffer between explosive and steel gave little improvement, although the 1/2-inch buffer appeared to be better than the 1-inch buffer when maximum thickness of the spall was used as a criterion. In order to eliminate some of the radial breakup of the steel, two shots were fired with a 2 3/8-inch core of steel surrounded by a ring of 1/2-inch radial thickness. This design did reduce the spalling considerably, as can be seen in the figure, but both the shot using 1/2-inch foam barrier and that using none lost approximately one-half of the central flying plate mass by spalling.

Table 1 (U)  
FLYING PLATE SPALL CONTROL SHOTS (U)

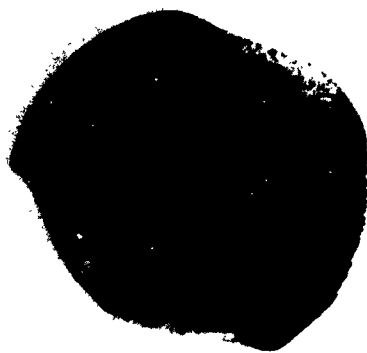
Shot No.	Rubber Thickness (inches)	HE and Steel o.d. (inches)	Steel i.d. for Two-Piece Plates (inches)	Velocity (mm/ $\mu$ sec)	Spall Thickness (inch)
9449	1/2	3	-	0.51	0.64
9450	1	3	-	0.40	0.53
9490	1/2	3 3/8	2 3/8	0.56	0.69
9491	0	3 3/8	2 3/8	0.70	0.69

All shots used 4 inches of C-3 explosive of the same outside diameter as steel.

(U) It is interesting to note the marked difference in the smoothness of the spall in the last two cases. The very smooth spall observed in the shot without foam rubber buffer is a result of the shock rarefaction caused by the 131-kbar phase transition in iron.<sup>2</sup> The similar shot using a foam rubber buffer apparently produces a somewhat lower shock pressure so that this shock rarefaction does not occur, and only the more usual smeared-out rarefaction wave is present. Thus the spalling plane is not well defined, and a rough break results.

**CONFIDENTIAL**

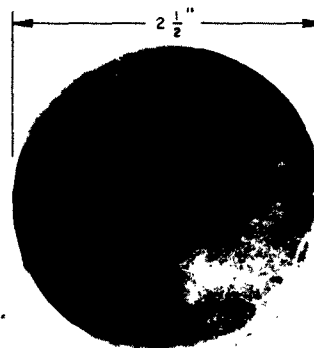
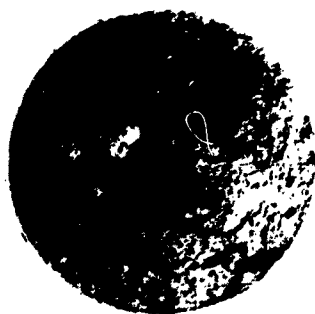
CONFIDENTIAL



SHOT 9450, 1" FOAM RUBBER

SHOT 9449, 1/2" FOAM RUBBER

PLAIN PLATES



GP 4228-20

SHOT 9490, 1/2" FOAM RUBBER

SHOT 9491, NO RUBBER

PLATES SURROUNDED BY 1/2" STEEL RING

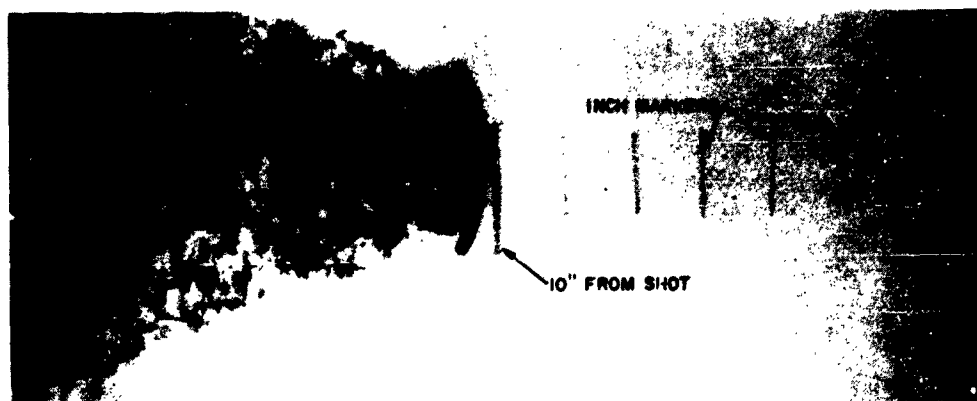
Figure 5 (U) Major Pieces Recovered from Plate Acceleration Shots (U).

CONFIDENTIAL

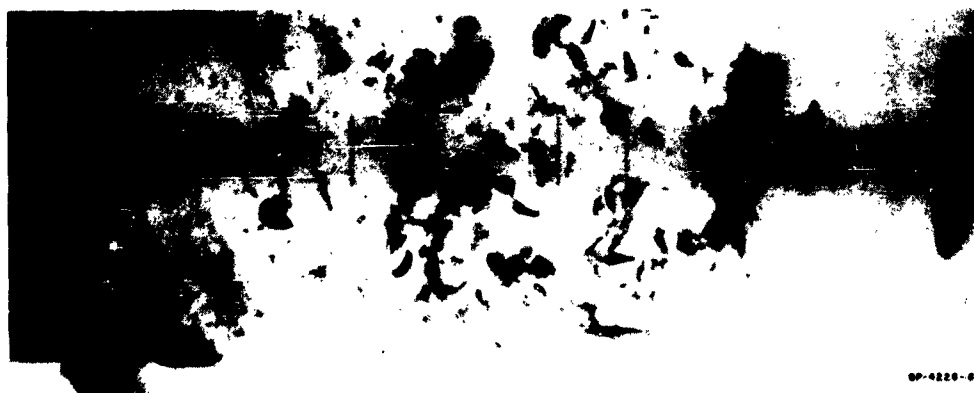
# CONFIDENTIAL

(U) In order to make sure that plates of other dense materials could not be used instead of steel, two shots similar to these spalling shots were fired, one with a brass plate and the other with a nickel plate. Figure 6 shows the X-ray pictures from these shots. It was quite obvious from these records that no improvement in performance could be expected by switching to either of these materials.

(C, gp 4) To check further on the processes of fragment acceleration, measurements were made of the pressure pulse waveform generated in the



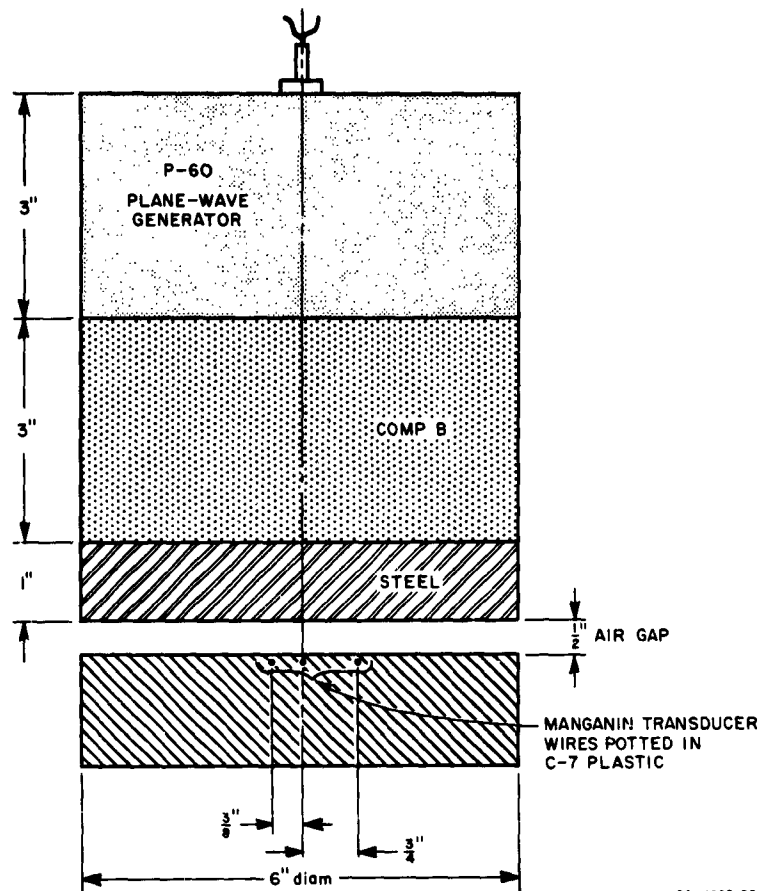
SHOT 10,146-BRASS PLATE, 280  $\mu$ sec



SHOT 10,255-NICKEL PLATE, 580  $\mu$ sec

Figure 6 (U) Heavy Plates, 1 Inch Thick, Accelerated by 3 Inches of Comp B (U).

CONFIDENTIAL



GA-4228-89

FIGURE 7 (U) DESIGN FOR SHOT NO. 9817 USING PRESSURE TRANSDUCERS (U)  
[Figure and caption combined (U)]

plastic of a Manganin wire resistance pressure transducer.<sup>3</sup> Figure 7 shows the design of the first of these shots.

(U) The interpretation of the records from the three transducers in this shot is as follows:

Zero Position: The plate strikes the transducer and generates a pressure of 100 kbar in the transducer. (This indicates a plate velocity of  $1.25 \text{ mm}/\mu\text{sec}$ .) The pressure pulse lasts  $1 \mu\text{sec}$ , indicating that the transducer was hit by a spall 2.5 mm thick from the 25-mm plate. The flying plate was bowed because the arrival times at the  $3/8$ - and  $3/4$ -inch positions were later and

CONFIDENTIAL



# CONFIDENTIAL

of lower pressure than at the center. The pulse at the 3/8-inch position is shorter than the center pulse, indicating a thinner spall than at the center. The pressure was lower also -- 95 kbar, which is consistent with bowed plate considerations. The pulse at the 3/4-inch position is slightly longer than either the 0 or 3/8-inch pulse. This implies a thicker spall section above the transducer element at the 3/4-inch position. Where the ragged upper surface of most spalls is considered, the variation of pulse length is understandable.

(U) The second shot of this series was similar to Shot 9491 where a two-piece plate was used. The shot configuration is shown in Figure 8. A smooth spall is generated by this type of shot, and it was hoped that a reliable waveform could be recorded. However, the spall had a much lower velocity than expected, and the only portion of the waveform recorded on the oscilloscope was the initial pressure step. (Scope sweep stopped before the total waveform could be recorded.) Table 2 summarizes the results of these two shots.

(C, gp 4) At this point it appeared that the only way to achieve the full velocity potential of a steel flying plate design was to scale up the explosive and two-piece plate used in Shot 9491, so that the resulting spall would be thick enough to accelerate the fragment pack all by itself. Such scaling up would result in a very high percentage of wasted weight, and since other methods of acceleration were showing promise of achieving high velocities, it was decided to stop work on the steel plate design.

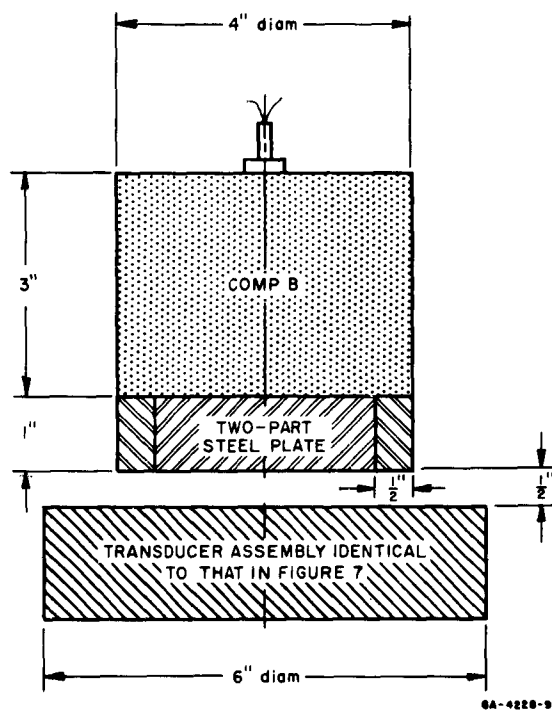


FIGURE 8 (U) DESIGN FOR SECOND TRANSDUCER SHOT, NO. 9818 (U)  
[Figure and caption combined (U)]

# CONFIDENTIAL

Table 2 (U)

## RESULTS OF PRESSURE TRANSDUCER SHOTS (U)

Shot No.	Radial Distance in Gage (inch)	Pressure in Gage (kbar)	Corresponding Plate Velocity (mm/ $\mu$ sec)	Spall Thickness (mm)	Comments
9817	0	100	1.25	2.5	6-inch diameter plane-wave shot
	3/8	95	1.20	2	
	3/4	88	1.14	5	
9818	0	41	0.63	---	Two-piece steel plate
	3/8	39	0.60	---	

### 3. Summary

(C, gp 4) Table 3 lists a selection of typical flying plate designs and their performances. As was shown in Figures 3 and 4, the performance of aluminum plate designs is very good indeed as far as velocity uniformity is concerned. Even with this light material for the plate, however, less than one-third of the warhead mass is represented by the fragments.

(C, gp 4) The steel plate designs shown in Table 3 seem to give velocities only slightly higher than the aluminum plate designs, and, in addition to having higher velocity variations, the mass percentage in fragments is very low indeed.

## B. ELECTRICAL BACKWARDS INITIATION

### 1. Theory

(C, gp 4) When a mass of explosives in contact with a fragment pack is initiated at the plane between them and the detonation front moves away from the pack, the pressure pulse on the pack is quite different from that produced when the more usual initiation procedure is used and the detonation front moves toward the pack. The peak pressure produced is much lower in the backwards initiation case, but it maintains its initial level until the detonation front reaches a free surface and reflects as a relief wave. Thus quite reasonable thicknesses of explosive can be used directly to accelerate a fragment pack to a uniform velocity.

# CONFIDENTIAL

Table 3 (C, gp-4)  
SELECTED FLYING PLATE SHOTS (U)

Shot No.	Plate Diameter and Material*	Explosive Geometry (thickness behind plate x diam.)	Pack Makeup**	Velocity (mm/ $\mu$ sec)	% Mass in Pack	Comments
9243	4" Al	1 1/2" x 4"	1/8" solid plates	0.25 $\pm$ <1%	27	16 layers of 1/16" x 1/16" brass cylinders, 852 per layer.  1636 hollow brass balls stacked in 8 layers in hex mold and potted.
9266	4" Al	1" x 4"	1/8" frag. plates	0.23, low spread	30	
9644	4" Al	1" x 4"	1/16" frag. plates	0.24, low spread	29	
10181	4" Al	1" x 4"	1/8" ball pack	0.41, low spread	14	1" plate-to-pack distance.
9302	3" Steel	4" x 4", plate inserted 1"	1/16" solid plates	0.34 $\pm$ 2.5%	14	
9268	3" Steel	4" x 4", plate inserted 1"	1/8" solid plates	0.34 $\pm$ 3%	14	
9935	3" Steel	2" x 4", plate inserted 1/2"	1/8" frag. plates	0.26 $\pm$ 9%	19	1" plate-to-pack distance.
9980	3" Steel	2" x 4", plate inserted 1/2"	1/8" frag. plates	0.28 $\pm$ 6%	19	

\* All plates were 1" thick.

\*\* All 1/8" fragment plates had 217 brass cylinders, 1/8" x 1/8", in hexagonal array potted in epoxy, 8 plates per pack. Solid plates were steel. Pack diameter was about 2" in all cases.

# CONFIDENTIAL

(U) Three different methods for producing the initiation at the desired plane were investigated. In this section a method will be described which involves electrical initiation of the explosive at the desired location.

## 2. Shot design

(C, gp 4) The requirements of an electrical backwards initiation system are that it be extremely thin so it will not interfere with the transmission of shock from the explosive to the fragment pack, and that it initiate the explosive as near to the explosive - fragment pack interface as possible. In addition, any air gaps between the explosive and the fragment pack are not desirable since they will produce perturbations in the shape of the pressure pulse transmitted to the fragment pack. In order to achieve such a system the electrical "bridge-wire" to be used has been constructed of aluminum foil which has wide leads necking down to a narrow center for the "wire". Such a device we will call a "bridge foil".

(U) Mylar tape with an evaporated aluminum coating was tried first as the bridge foil material because construction of the system with this tape would be very simple and straightforward. Framing camera pictures were taken to check the electrical breakdown when such a bridge foil is pulsed. Figure 9(a) shows the results of this test and illustrates the reason for rejection of this tape for this application. The breakdown rapidly evaporates the aluminum from the Mylar backing, and most of the energy is therefore dissipated over a large area as the electrical arcs reach across the expanding gap between the remaining solid aluminum areas. Figure 9(b) shows the behavior of a bridge foil made of 0.001-inch aluminum foil. In this case it is seen that the aluminum is thick enough so that energy dissipation occurs at a very localized spot at the neck; therefore the energy density at this spot will be high enough to initiate an explosive. This material was therefore selected for this application.

(U) Theoretically, the initiation of the explosive should take place over the entire interface simultaneously, but in practice this is impossible. An approach toward this goal can be made, however, if initiation at three points is achieved, and the shot design shown in Figure 10 was developed to do this. The booster pellets shown were pressed in two stages. First the outside cup was pressed out of graphitized tetryl, and then this cup was filled with low

# CONFIDENTIAL

CONFIDENTIAL

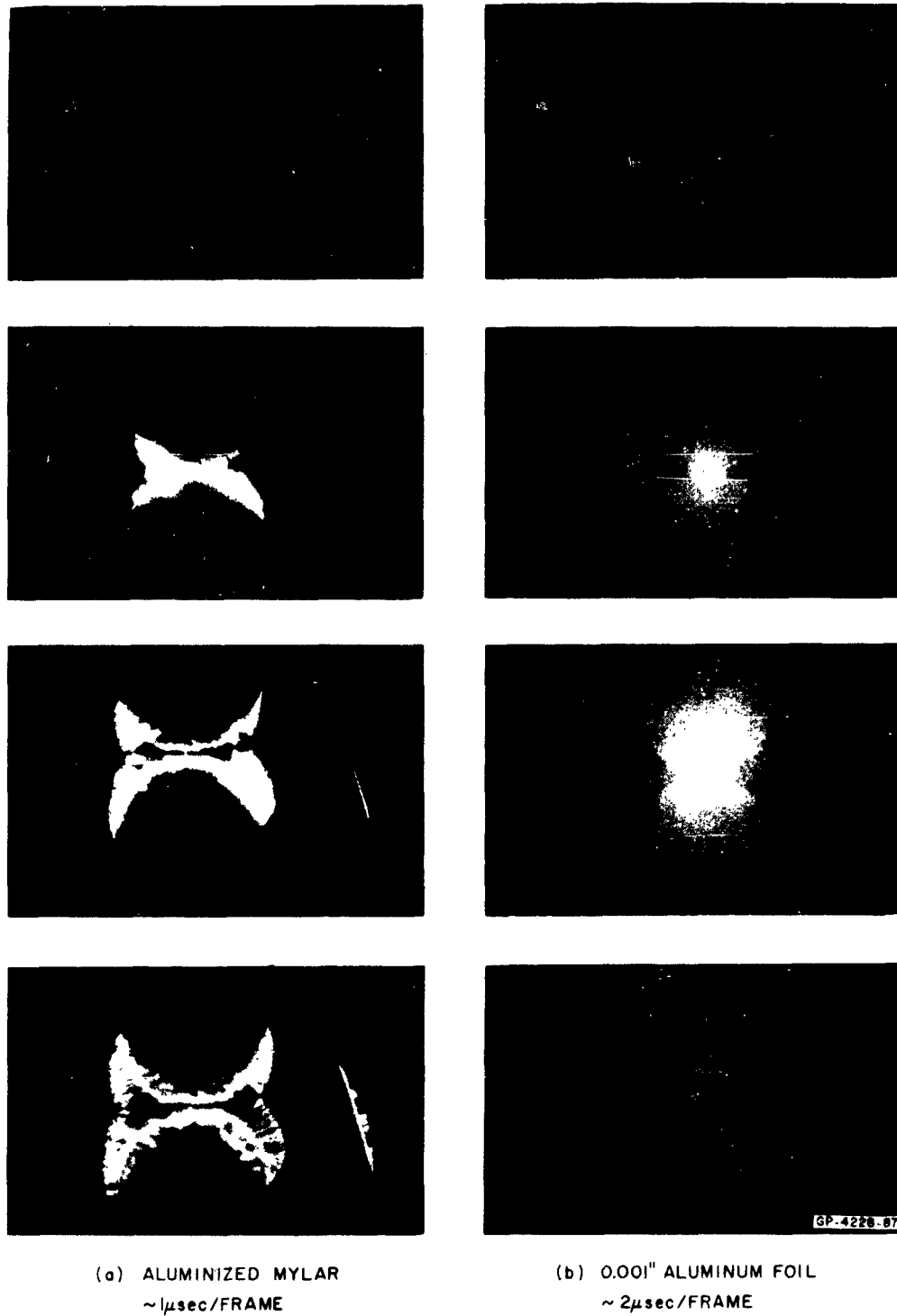
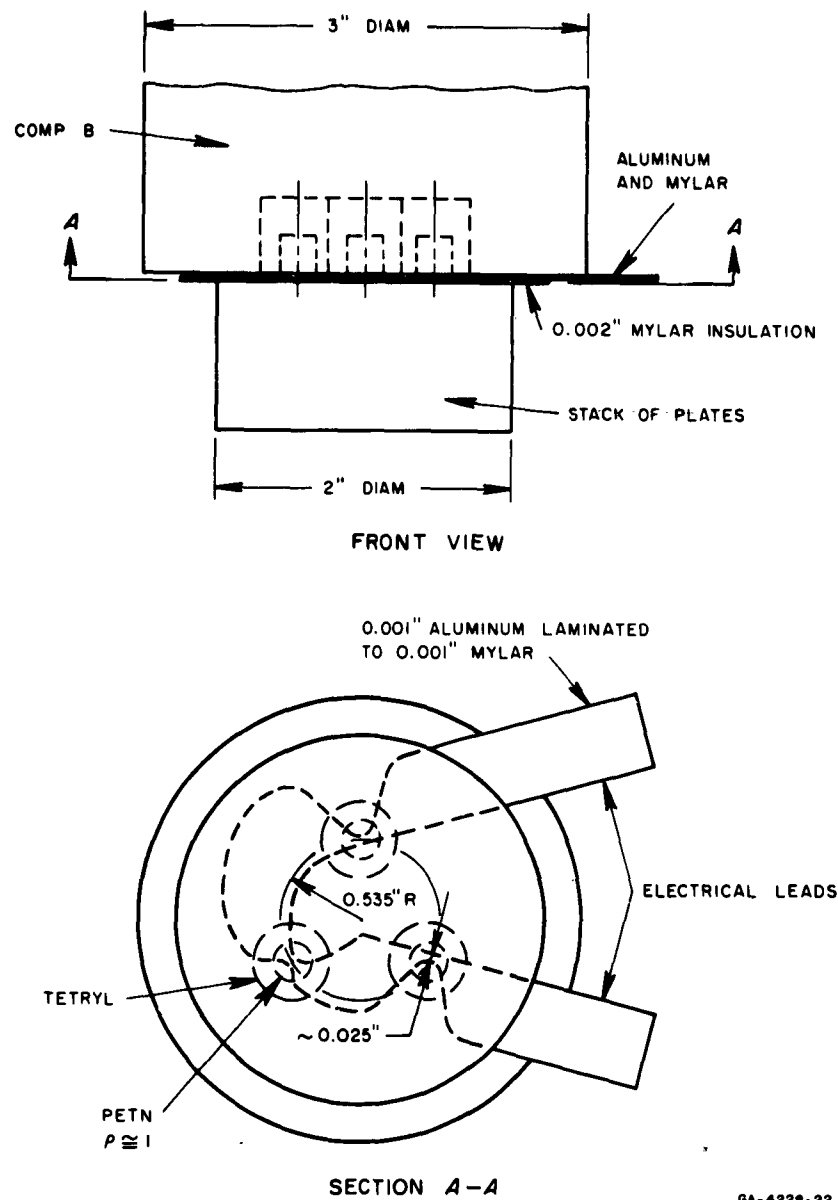


Figure 9 (U) Breakdown of Thin Aluminum Foil Bridgewires (U).

CONFIDENTIAL



GA-4226-22

FIGURE 10 (U) THREE-POINT ELECTRICAL BACKWARDS INITIATION DESIGN (U)  
[Figure and caption combined (U)]

# CONFIDENTIAL

density PETN. These boosters were inserted in holes machined into the Composition B main charge so that they were flush with the surface, and the bridge foil was laid across. The 0.001-inch-aluminum foil was laminated to 0.001 inch of Mylar for added strength before cutting and was insulated from the metal plate stack by 0.002 inch of Mylar, so the total thickness of materials between the explosive and the stack was only 0.004 inch.

### 3. Experiments

(C, gp 4) When this design was fired with a stack of solid steel plates, the results were very encouraging. Velocities were almost as high as those achieved by steel flying plate designs, and velocity variations were low. The next two shots used fragment plates and gave even higher velocities and the fragment clouds shown in Figure 11. The somewhat domed clouds seen in this figure are apparently typical of the method because the cloud shape did not seem to be significantly changed by the change from single to three-point initiation.

(U) A long series of shots with solid plates was fired after this successful start in order to investigate the effect of reduced explosive loading.

### 4. Summary

(C, gp 4) Table 4 lists the most significant electrical backwards initiation shots fired. These shots showed that very large reductions in explosive weight can be made with only slight effect on both velocity and velocity variation. The fraction of the total weight which is fragment weight can be as high as 50 percent for a design with velocity and velocity spread comparable to the best designs using this method. For the somewhat lower velocities resulting from 2-inch-diameter charges, this fraction can be as high as 70 percent before velocity variation passes the  $\pm 5$  percent mark. Even a 2-inch design with 85 percent of its weight in fragments performs fairly well, since the velocity is only 7 percent lower than the 70 percent design and the velocity variation has only risen to  $\pm 9$  percent.

(C, gp 4) If high velocity is required in a design which uses the space in a fixed-diameter warhead efficiently, the last two shots in the table suggest one way in which this can be achieved. These shots show that almost all of the

# CONFIDENTIAL

CONFIDENTIAL

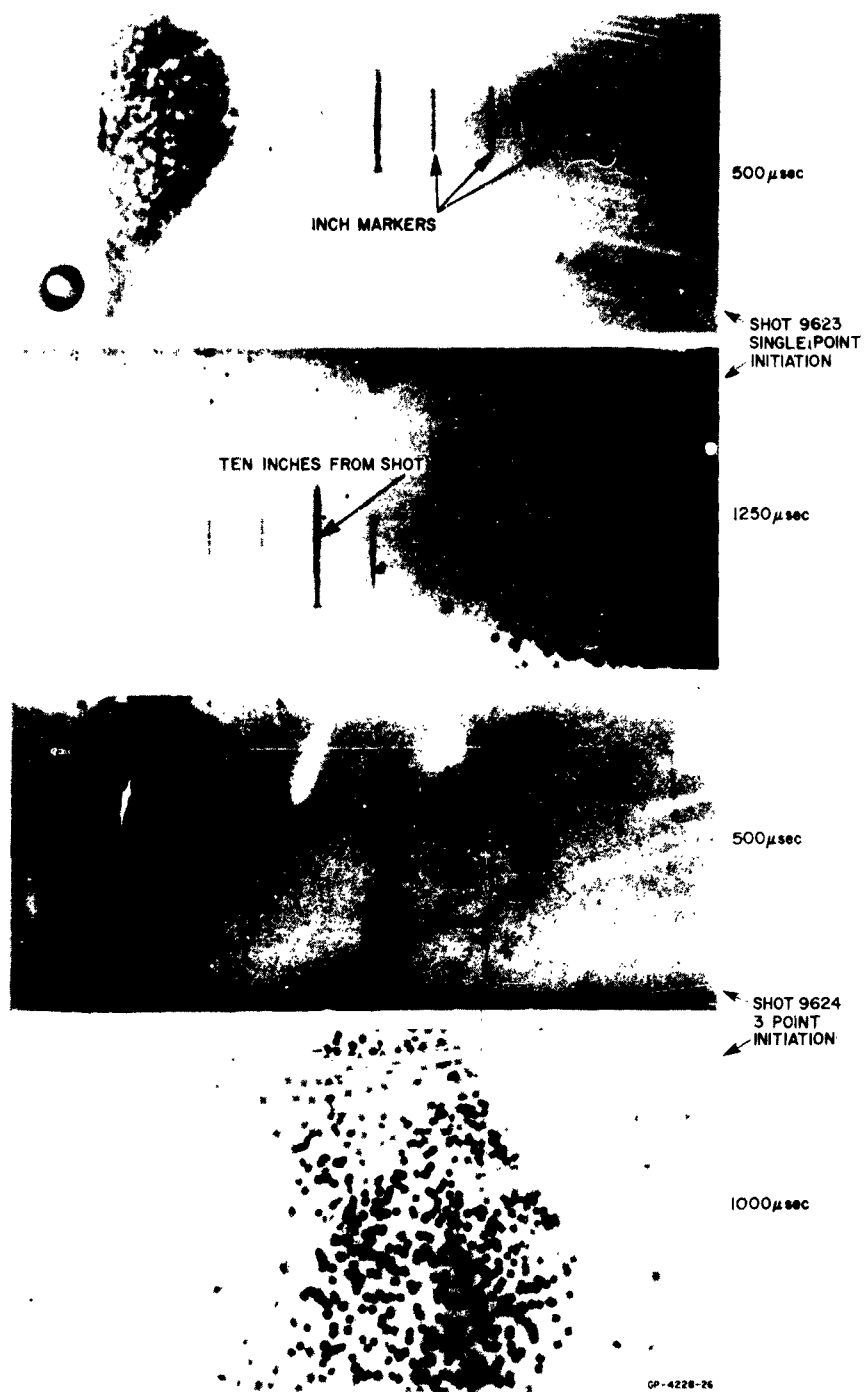


Figure 11 (U) Electrical Backwards Initiation Shots (U).

CONFIDENTIAL



CONFIDENTIAL

Table 4 (C, gp-4)  
ELECTRICAL BACKWARDS INITIATION SHOTS (U)

Shot No.	Explosive Geometry (thickness behind pack x diam.)	Initiation Points	Pack Makeup*	Velocity (mm/ $\mu$ sec)	% Mass in Frags.	Comments
9608	4" x 3"	1	1/8" Solid	0.32 $\pm$ <2%	35	
9609	4" x 3"	3	1/8" Solid	0.32 $\pm$ 3%	35	
9623	4" x 3"	1	1/8" Frag.	0.38 $\pm$ <2%	33	Domed cloud,
9624	4" x 3"	3	1/8" Frag.	0.39 $\pm$ 3%	33	Domed cloud.
9643	4" x 2"	1	1/8" Solid	0.19 $\pm$ 4%	54	
9703	3" x 3"	1	1/8" Solid	0.32 $\pm$ 1%	41	
9704	2" x 3"	1	1/8" Solid	0.31 $\pm$ 1 1/2%	51	
9705	1" x 3"	1	1/8" Solid	0.26 $\pm$ 2%	68	
9706	3" x 2"	1	1/8" Solid	0.19 $\pm$ 4%	62	
9707	2" x 2"	1	1/8" Solid	0.19 $\pm$ 5%	70	
9708	1" x 2"	1	1/8" Solid	0.17 $\pm$ 9%	82	
9709	2" x 2"	1	1/8" Solid	0.25 $\pm$ 3%	51	HE clad with 1/8" steel.
9710	2" x 2"	1	1/8" Solid	0.30 $\pm$ 2 1/2%	39	Clad with 1/4" steel.

\* Fragment plates had 217 brass cylinders, 1/8" x 1/8", in hexagonal array in epoxy, 8 plates per pack.  
Solid plates were steel.

CONFIDENTIAL

# CONFIDENTIAL

velocity lost when the explosive is reduced in diameter from 3 to 2 inches can be recovered by confining the 2-inch charge on all sides with steel. Naturally, the fragment weight fraction goes down when this is done, but under some circumstances this may still be desirable because for a given maximum warhead diameter about twice as many fragments can be fitted in when HE and fragment pack are the same diameter as can be fitted in when the HE has a diameter 50 percent greater than the fragment pack.

## C. MDF BACKWARDS INITIATION

### 1. Theory

(U) Two major drawbacks to the electrical backwards initiation design discussed above are: that although there are no primary explosives present in the train, the presence of low density PETN in permanent contact with the main charge of HE is somewhat hazardous; and that, on the other hand, low density PETN is still insensitive enough to require a very vigorous electrical discharge through the bridge foil in order to initiate it (the discharge of 4 to 8  $\mu$ f condenser charged to 5000 volts was commonly used here). These two factors might make application of electrical backwards initiation to a warhead difficult in normal safety precautions had to be observed, and if space and weight for an electrical supply of this magnitude were not readily available.

(C, gp 4) In order to eliminate these drawbacks and still retain the advantages of the backwards initiation concept, a system was developed which used a mild detonating fuse (MDF) to lead the detonation to the explosive - fragment pack interface. This MDF could then be initiated by any of the standard fuzing techniques, and normal safeing and arming mechanisms could be incorporated.

### 2. Experiments

(C, gp 4) Figure 12 shows the basic design tested and several variations of it fired later in the project. Since the MDF contained only 5 or 10 grains of explosive per foot, it could be threaded right through the main charge without causing detonation if a small amount of buffering material was put around it. Where initiation was desired, a booster of pressed tetryl was added to increase reliability. Operation of this design was checked first by

# CONFIDENTIAL

CONFIDENTIAL

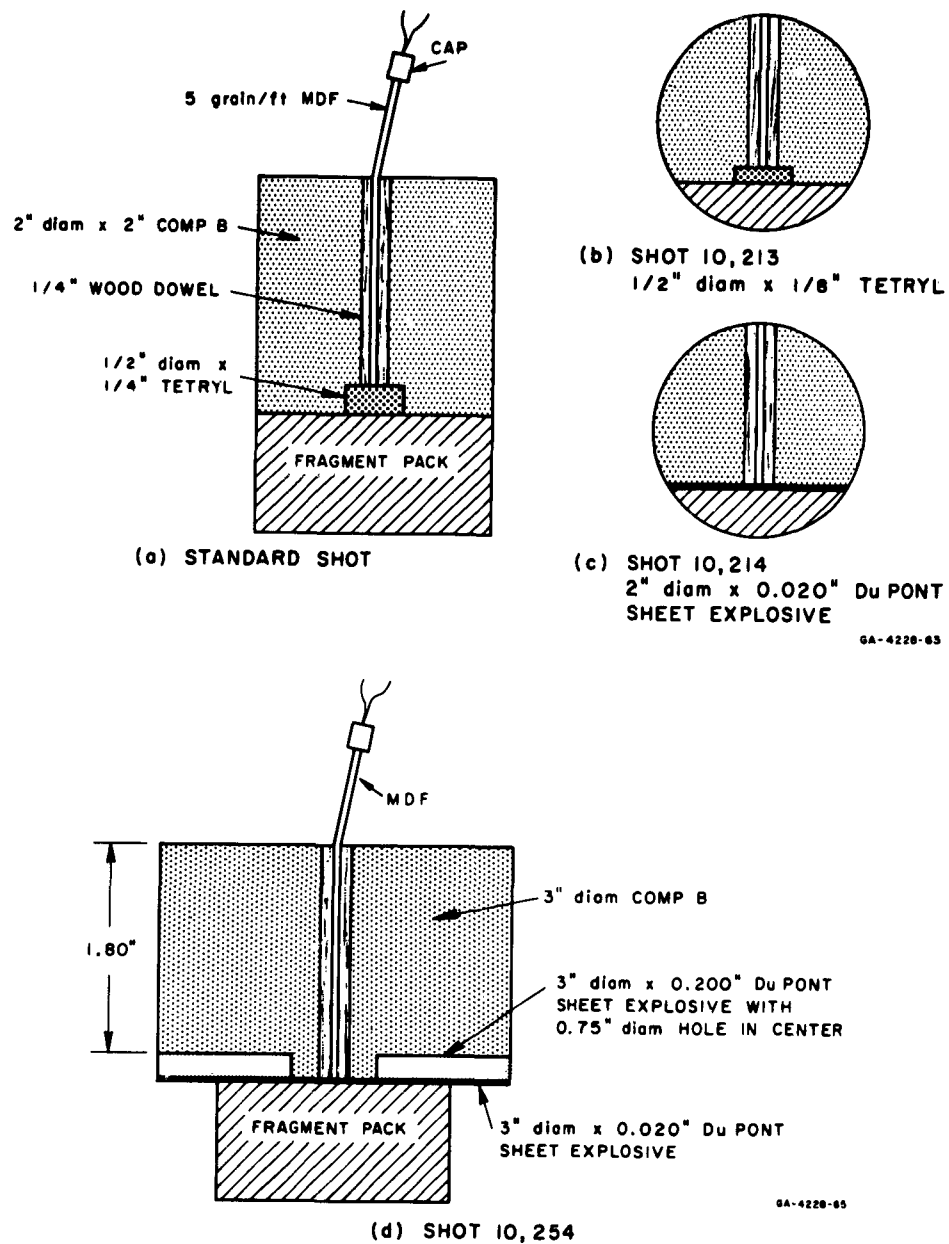


FIGURE 12 (C) STANDARD MDF SHOT DESIGN AND MODIFICATIONS (U)  
[Figure and caption combined (C, gp 4)]

CONFIDENTIAL

# CONFIDENTIAL

firing in front of the framing camera to make sure that initiation took place at the desired location and that no significant damage was done to the main charge by the MDF before initiation. When these shots proved the design satisfactory, X-ray shots with solid and fragment plates were fired.

These X-ray shots showed that the velocities produced by this method were very close to those produced by similar electrical backwards initiation designs. The only major difference was in the fragment cloud, which was more bowl shaped.

(C, gp 4) Figure 13 shows the cloud formed by a 4-inch diameter, double-scale shot, using 1/4-inch balls for fragments. It is clear from this figure that the cloud is in the form of a hollow bowl. Note especially in the 1640  $\mu$ sec record the contrast between the sharp images of the balls on the side of the bowl near the film cassette and the fuzzy images of those on the other side. Such a bowl, while not as pretty as the plate-like clouds produced by the aluminum flying plate method, may still be satisfactory for some applications, but nevertheless it is probably not optimum. In particular, the portion of the cloud marked "nose" in Figure 13 has been separated from the main structure of the cloud, and this at least is undesirable. Figure 14 shows one record from a similar 4-inch shot which had 14,000 1/8-inch brass balls in the fragment pack and which therefore shows the detailed structure of the cloud more clearly.

(C, gp 4) Two possible causes for the bowl shape appear reasonable. The 1/4-inch separation between the point of main charge initiation, the MDF-tetryl interface, and the desired point, the Comp-B fragment pack interface, will cause portions of the fragment pack near the axis to be struck by a detonation front traveling toward the pack instead of away from it, and these portions will thus initially attain a somewhat higher velocity. The increase in velocity will eventually be largely overshadowed by the acceleration resulting from the detonation of the much larger mass of explosive behind the initiation point, but it may still have some effect. This is particularly true in the center and would readily explain the formation of the nose.

(C, gp 4) A second explanation, which seems more likely when the similarity with the electrical backwards initiation shots is considered, is that the more rapid release of the gas pressure near the periphery, due to the

# CONFIDENTIAL

CONFIDENTIAL

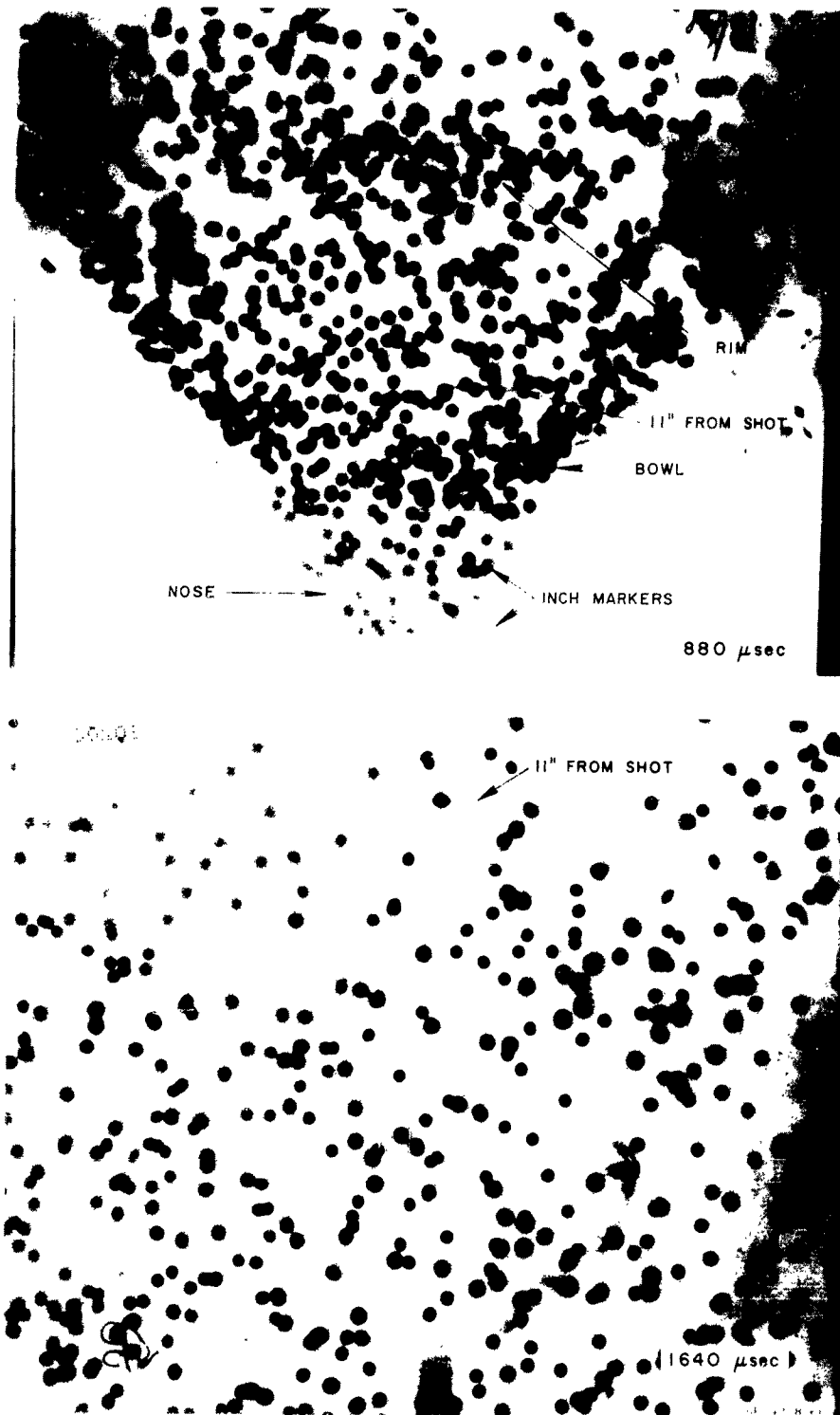


Figure 13 (U) Double-Scale MDF Shot with 1/4-Inch Balls,  
No. 10,203 (C).

CONFIDENTIAL

**CONFIDENTIAL**

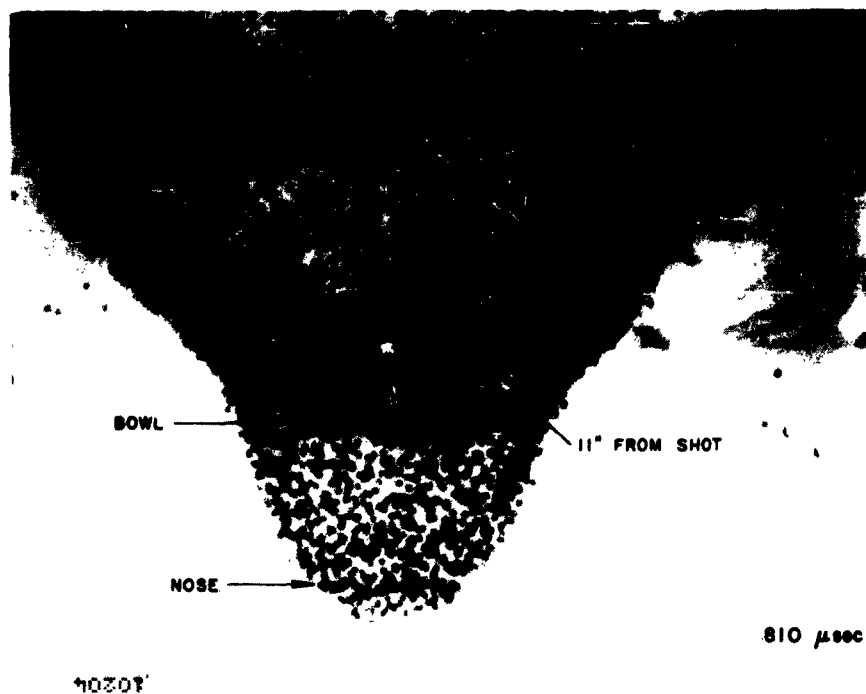


Figure 14 (U) Double-Scale MDF Shot with 1/8-Inch Balls, No. 10,204 (C).

nearness of the free surface of the explosive, may simply reduce the impulse supplied to those peripheral parts of the fragment pack.

(U) To test these hypotheses, four modified shots were constructed embodying the booster designs shown in Figure 12. The design using 0.020-inch Du Pont sheet explosive was made in 4-inch diameter as well as 2 inch in order to investigate the importance of edge effects.

(C, gp 4) Figure 15 shows the records from the two shots which reduced the initiation point height. The first of these was intended to be a duplicate of the large-scale shots discussed earlier in this section. In this case the initiation point height was also to scale since a booster pellet of half-thickness was used. As can be seen in Figure 15, the general shape of the fragment cloud is very similar to the double-scale shots, even including the nose. Velocities measured for various parts of the pattern also agreed very well with those of the large shot with 1/4-inch balls.

**CONFIDENTIAL**

# CONFIDENTIAL

(C, gp 4) The second shot moved the initiation point as close to the explosive-fragment pack interface as possible by replacing the booster with a 0.020-inch layer of DuPont sheet explosive, EL-506D. The record in Figure 15 shows that this change from an initiation point height of 0.125 inch to 0.020 inch went a long way toward eliminating the undesirable features of the fragment cloud shape. The cloud velocity in this shot was about 0.26 mm/ $\mu$ sec, with about  $\pm 7$  percent variation in the longitudinal component.

(C, gp 4) Some difficulty was experienced when the initiation of sheet explosive by MDF was attempted again in a large diameter shot. One shot failed at the MDF - sheet explosive joint and another apparently at the sheet explosive - Comp B joint. Finally, the design shown in Figure 12(d) was successfully fired and the resulting fragment cloud is shown in Figure 16. This

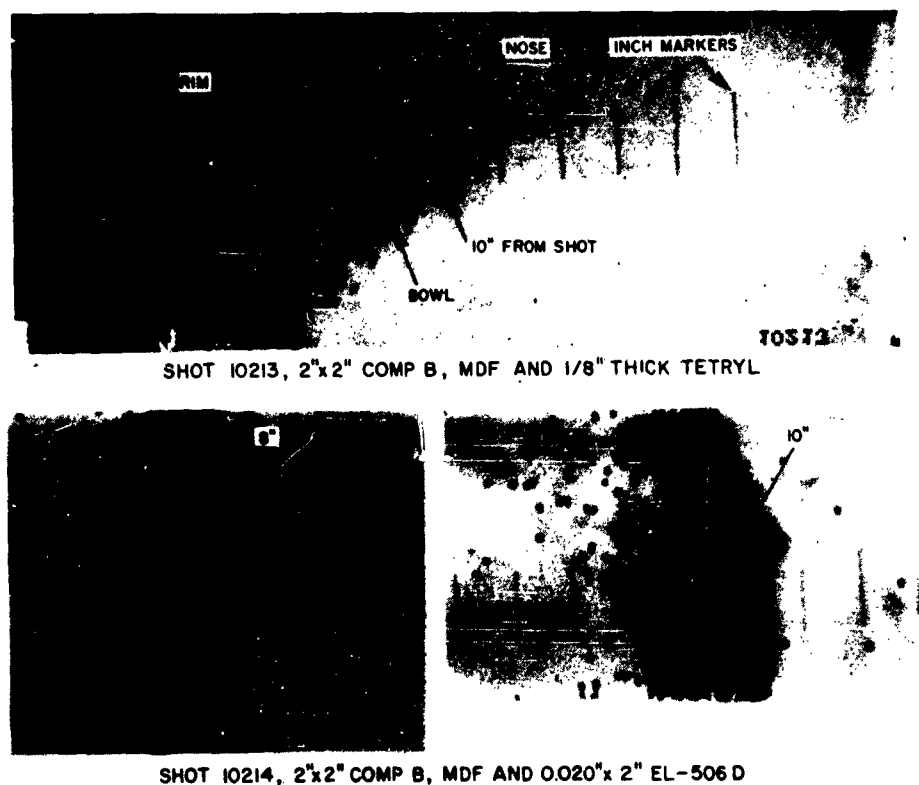


Figure 15 (C) Modified MDF Shots (U).

# CONFIDENTIAL

figure suggests that edge effects are not nearly as important as the boosting details, at least as far as the shape of the fragment cloud is concerned.

### 3. Summary

(U) Table 5 summarizes the work done on MDF backwards initiation designs. Comparison of this table with Table 4 shows that although variations in the design of MDF shots have not been as extensively investigated as they were for the electrical designs, it appears that the performances of the two will be essentially identical.

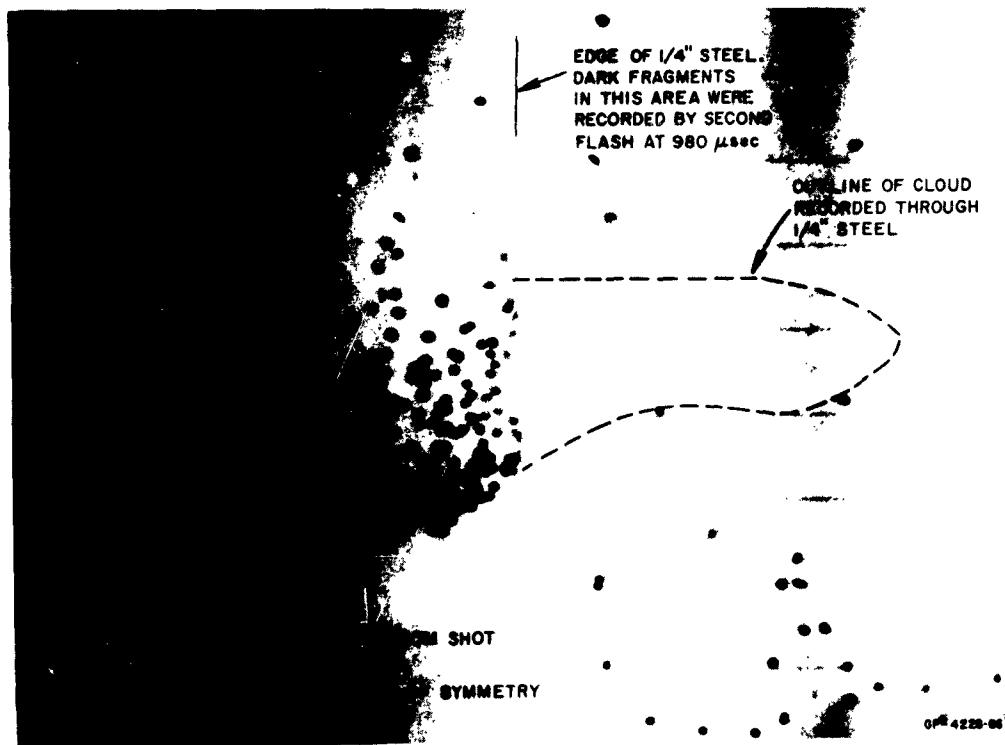


Figure 16 (U) Modified MDF Shot, No. 10,254. Flash X-Ray at 580  $\mu$ sec (U).

# CONFIDENTIAL



CONFIDENTIAL

Table 5 (C, gp-4)  
MDF BACKWARDS INITIATION SHOTS (U)

Shot No.	Explosive Geometry (thickness behind pack x diam.)	Initiation Geometry	Pack Makeup	Velocity (mm/ $\mu$ sec)	% Mass in Pack	Comments
9772	2" x 2"	Fig. 12(a)	1/8" solid plates	0.18 $\pm$ 6%	70	
9773	2" x 2"	Fig. 12(a)	1/8" solid plates	0.18 $\pm$ 6%	70	
10, 180	2" x 2"	Fig. 12(a)	1/8" ball pack	0.51	45	Hollow balls, domed cloud.
10, 203	4" x 4"	Fig. 12(a)	1/4" ball pack	Nose, 0.43 Bowl, 0.38 Rim, 0.28	55	1636 1/4" brass balls, domed cloud.
10, 204	4" x 4"	Fig. 12(a)	1/8" ball pack	Nose, 0.47 Bowl, 0.39 Rim, 0.26	58	14, 152 1/8" brass balls in 16 layers.
10, 213	2" x 2"	Fig. 12(b)	1/8" ball pack	Same as 10, 203	58	Exact 1/2 scale of 10, 203.
10, 214	2" x 2"	Fig. 12(c)	1/8" ball pack	0.26 $\pm$ 7%	58	Much flatter cloud.
10, 254	2" x 3"	Fig. 12(d)	1/8" ball pack	0.42 $\pm$ 6%	38	Cloud similar to 10, 214.

CONFIDENTIAL

## D. SHOCK-INDUCED BACKWARDS INITIATION

### 1. Theory

(C, gp 4) The objective of this effort was to develop a backwards initiation system which required no foils, no boosters, and no holes in the main explosive at or near the interface with the fragment pack. This would be accomplished by means of an initiator at the back of the explosive, away from the fragment pack. Instead of initiating the explosive directly, however, this device would only shock it to a level slightly below that required for initiation. The shock, or low-order detonation, would then propagate up to the front of the explosive where the higher pressure caused by its reflection from the metal fragments would cause it to become a high-order detonation. This detonation would then propagate back through the explosive, causing the desired pressure history at the explosive-fragment pack interface.

### 2. Experiments

(U) Initial work was based on a design suggested by Cosner,<sup>4</sup> who used a steel barrier to attenuate the shock from one explosive charge before it struck another. Figure 17 shows a typical design for early shots of this series. Modifications to this design which were tried at later stages of the project included the addition of a low-density ( $\rho \approx 1.0$  g/cc) wafer of PETN between the Comp B and the lower steel slug, the increase of the Comp B diameter to 3 inches, and encasing the Comp B in a steel cylinder. A design embodying all of these modifications shown in Figure 18 was found to operate fairly reliably. The framing camera records in Figure 19 show the shock going down the tube and signalling through the row of observation holes as it goes. Then a high-order detonation is initiated at the PETN wafer (3-inch diameter in this shot) and progresses back up the charge.

(C, gp 4) Since the modified design shown in Figure 18 appeared to work well when observed by the framing camera, two shots of this design were fired in front of the X ray in order to measure the resulting plate and fragment velocities. The first of these used solid steel plates, and the second used fragment plates made up out of brass cylinders cast in a Cerrobend matrix.

**CONFIDENTIAL**

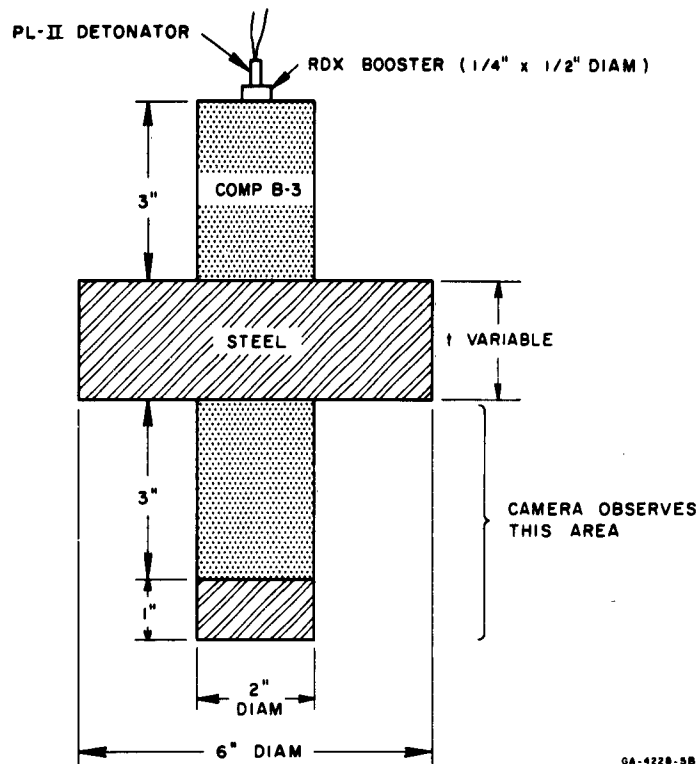


**FIGURE 17 (U) EARLY SHOT DESIGN FOR SHOCK-INDUCED BACKWARDS INITIATION STUDIES (U)**  
[Figure and caption combined (U)]

(C, gp 4) Figure 20 shows the records obtained from these two shots and includes tentative identification of the origins of various groups of fragments in the second shot. The large velocity variation shown in these records suggests either that the detonation was initiated too high in the explosive, or that the explosive coming down around the sides of the plate stack contributed additional velocity to the outside layers.

(C, gp 4) Two additional shots of this design were fired to check on the position of the initiation of the high-order detonation. The first, using a fiber optics technique, showed that the point of initiation was about 1 1/4 inches above the top of the plate stack. The second shot supplemented the fiber optics with electrical switches embedded in the explosive; this shot also recorded an initiation point between 1 1/4 and 1 3/4 inches from the plate stack. These shots are discussed in more detail in Appendix III since they are now of interest

**CONFIDENTIAL**

# CONFIDENTIAL

primarily because of their instrumentation. For the discussion here it is sufficient to note that their results strongly suggest that the X-ray shots shown in Figure 20 experienced similar early initiation, and that this was the main cause of the velocity variation seen in these shots.

## (a) Flying plate — shocked Comp B shots

(U) Before attempting to remedy this defect of early initiation, we decided to work on the more serious drawback of this design: the requirement for a heavy steel buffer to attenuate the donor charge shock down to the desired pressure level. To do this, a design was developed which used an explosively accelerated aluminum flying plate, 1/4 inch thick, to shock the main charge of explosive. Figure 21 shows the details of inclined plate or mousetrap geometry used to accelerate the aluminum. The foam rubber was added between the sheet explosive and the aluminum to prevent spalling of the aluminum. The angle of tilt was so chosen that the aluminum plate was parallel to the top of the Comp B charge upon arrival, impacted simultaneously at all points on the top, and therefore induced a plane shock in the Comp B.

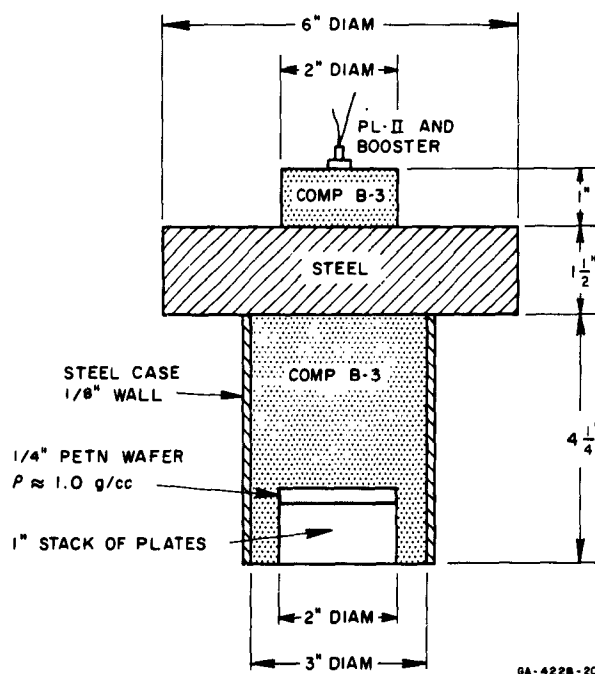


FIGURE 18 (U) MODIFIED SHOCK-INDUCED BACKWARDS INITIATION DESIGN (U)  
[Figure and caption combined (U)]

CONFIDENTIAL

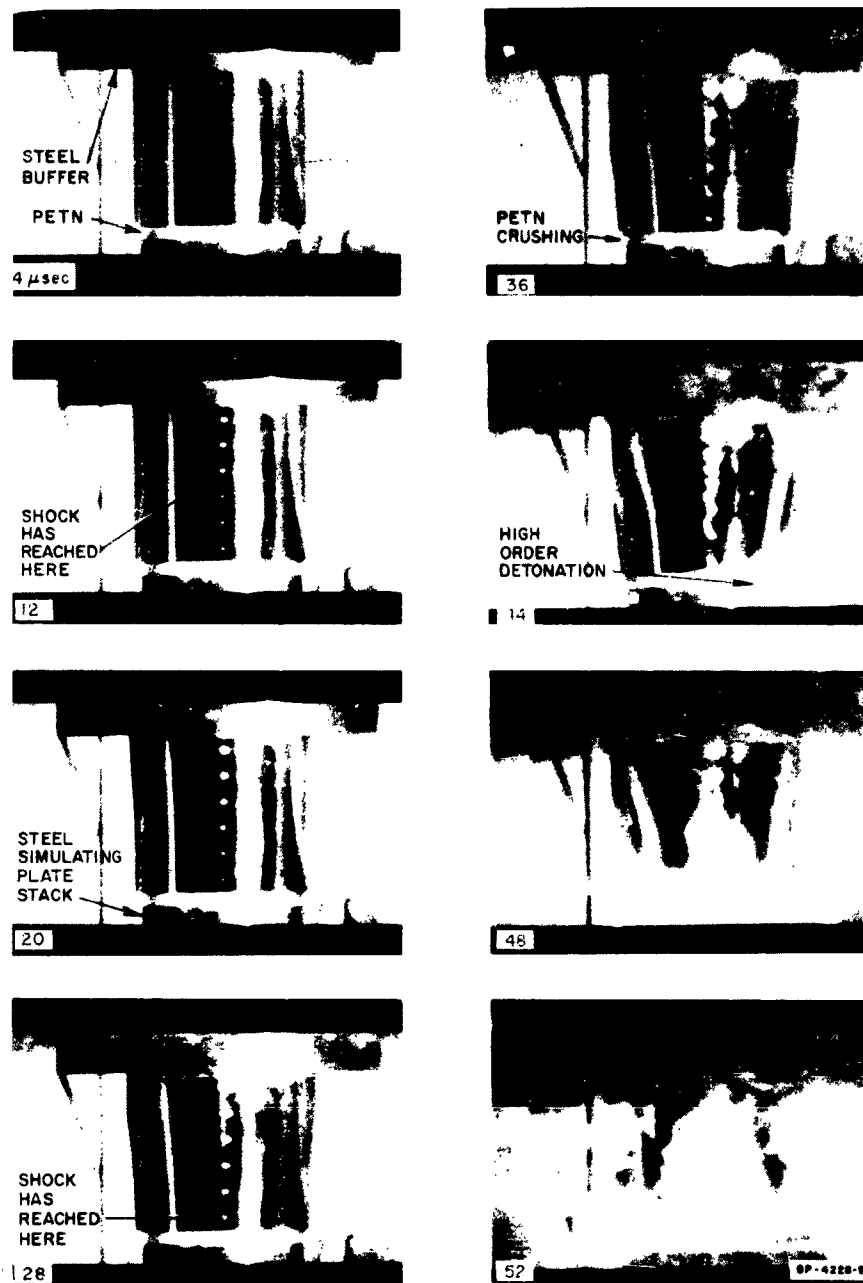


Figure 19 (U) Shock-Induced Backwards Initiation Shot Operating Satisfactorily, No. 9240 (U).

CONFIDENTIAL

CONFIDENTIAL

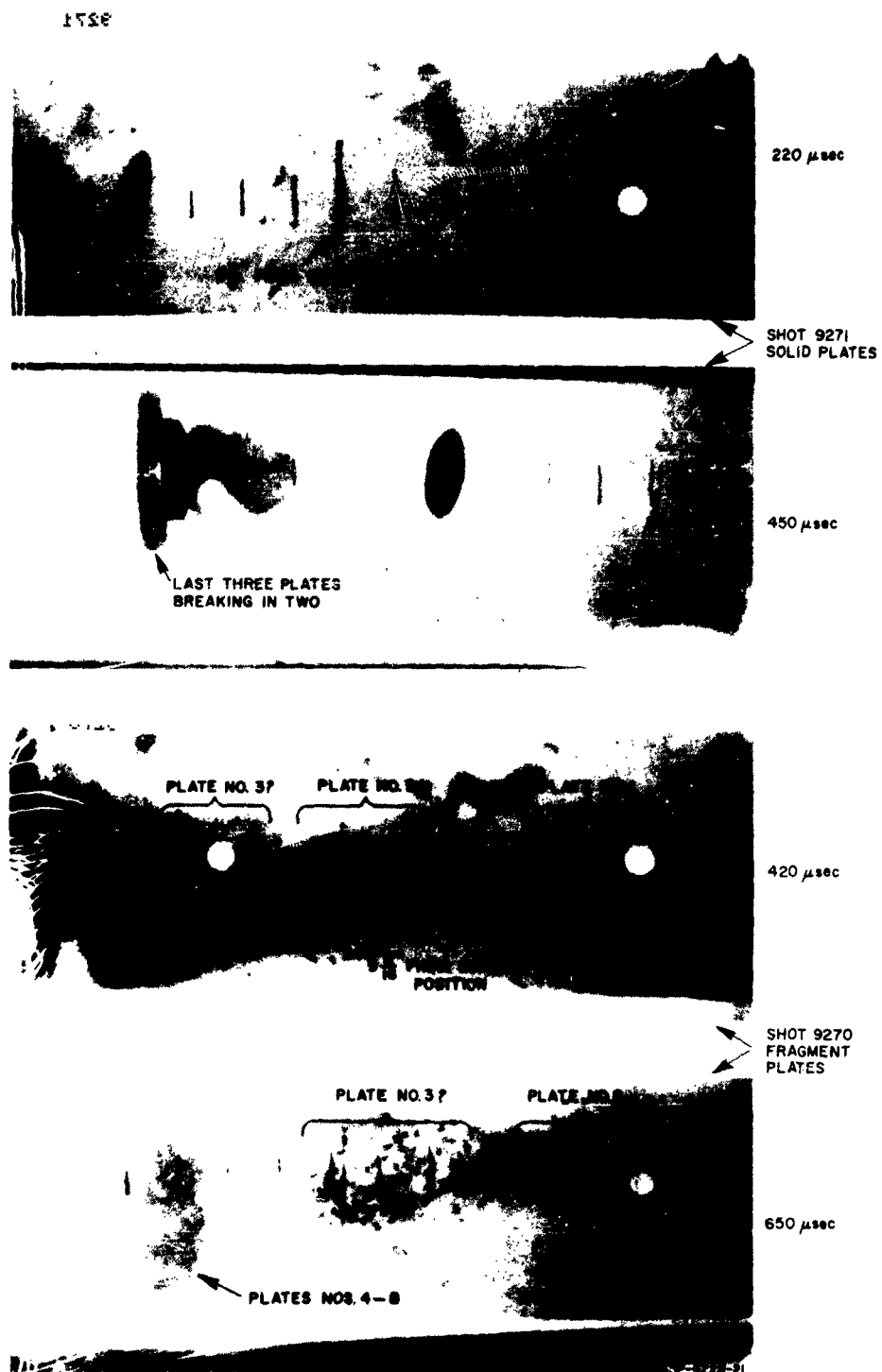


Figure 20 (C) Shock-Induced Backwards Initiation X-ray Shots (U).

CONFIDENTIAL

CONFIDENTIAL

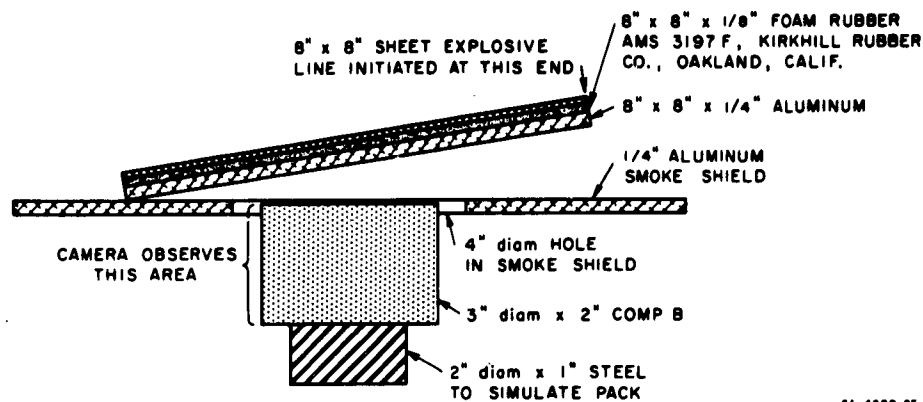


FIGURE 21 (U) MOUSETRAP DESIGN FOR DELAYED SHOCK INITIATION OF COMP B (U)  
[Figure and caption combined (U)]

(C, gp 4) The behavior of the various components of this assembly can be estimated from a knowledge of the equations of state of the components.<sup>5,6</sup> In particular, if the equations of state are put in the form of pressure vs velocity curves, a diagram such as that shown in Figure 22 can be constructed. For

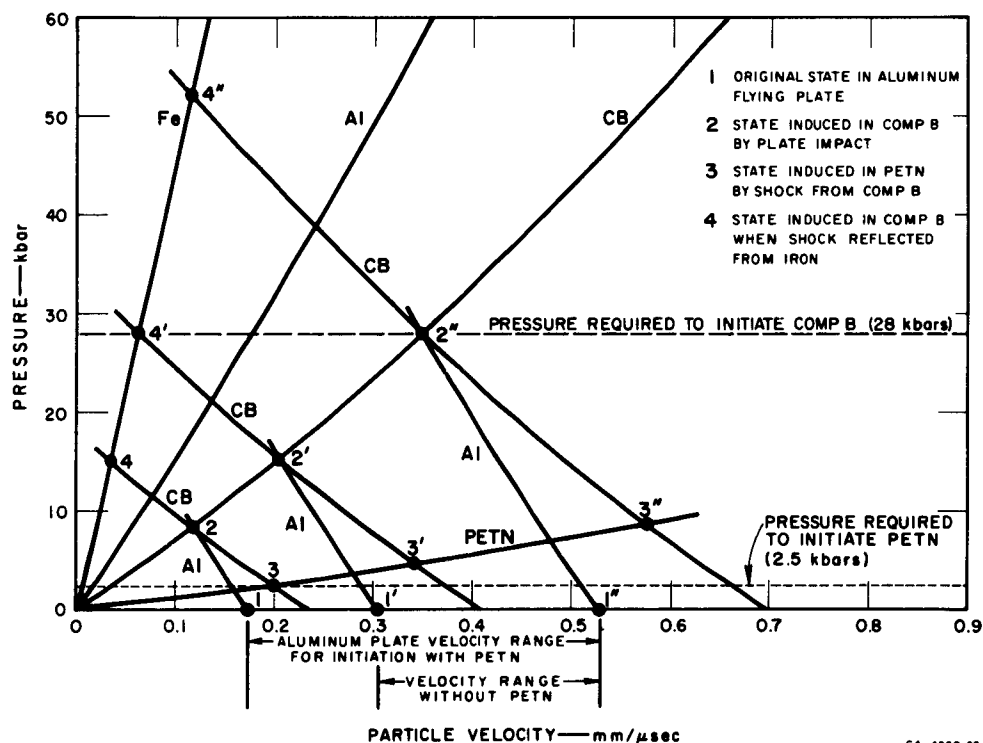


Figure 22 (U) Pressure vs Particle Velocity Plots for Shock-Initiated Backwards Initiation Design (U).

CONFIDENTIAL

# CONFIDENTIAL

example, if it is assumed that we have a shock-free aluminum flying plate traveling at  $0.175 \text{ mm}/\mu\text{sec}$ , its state is represented by the point marked 1 in the figure. When this plate strikes Comp B, a shock is induced in both materials, and the Comp B is accelerated to some particle velocity while the aluminum is slowed down; the state in both materials is then that shown at point 2. When the shock in the Comp B reaches the PETN, the reaction with the PETN (a material with a pressure-particle velocity curve of lower slope) will result in a rarefaction wave moving back into the Comp B and a shock wave moving into the PETN. The state in the PETN will then be shown by point 3. In the case being discussed the pressure at point 3 should be just high enough to cause initiation of PETN. If steel (a material with a curve of higher slope) is substituted for PETN, however, a shock will be reflected back into the Comp B, the pressure will rise, and a state in the Comp B shown at point 4 will result. In the case being discussed the Comp B pressure at point 4 is not as high as the 28-kbar level necessary for initiation, but if the aluminum flying plate velocity is raised to  $0.305 \text{ mm}/\mu\text{sec}$  it will reach this level and should initiate. This figure shows that in order to achieve the pressure required for initiation of the PETN, the aluminum flying plate velocity must be  $0.175 \text{ mm}/\mu\text{sec}$  or higher, and that the maximum allowable aluminum flying plate velocity (that is, one which will not directly initiate the Comp B) is  $0.528 \text{ mm}/\mu\text{sec}$ . Note, also, that if an aluminum flying plate velocity just under the maximum allowable level is chosen, the pressure induced in Comp B upon shock reflection from a steel barrier or fragment pack should be 52 kbar, well over the 28 kbar required for initiation of Comp B.

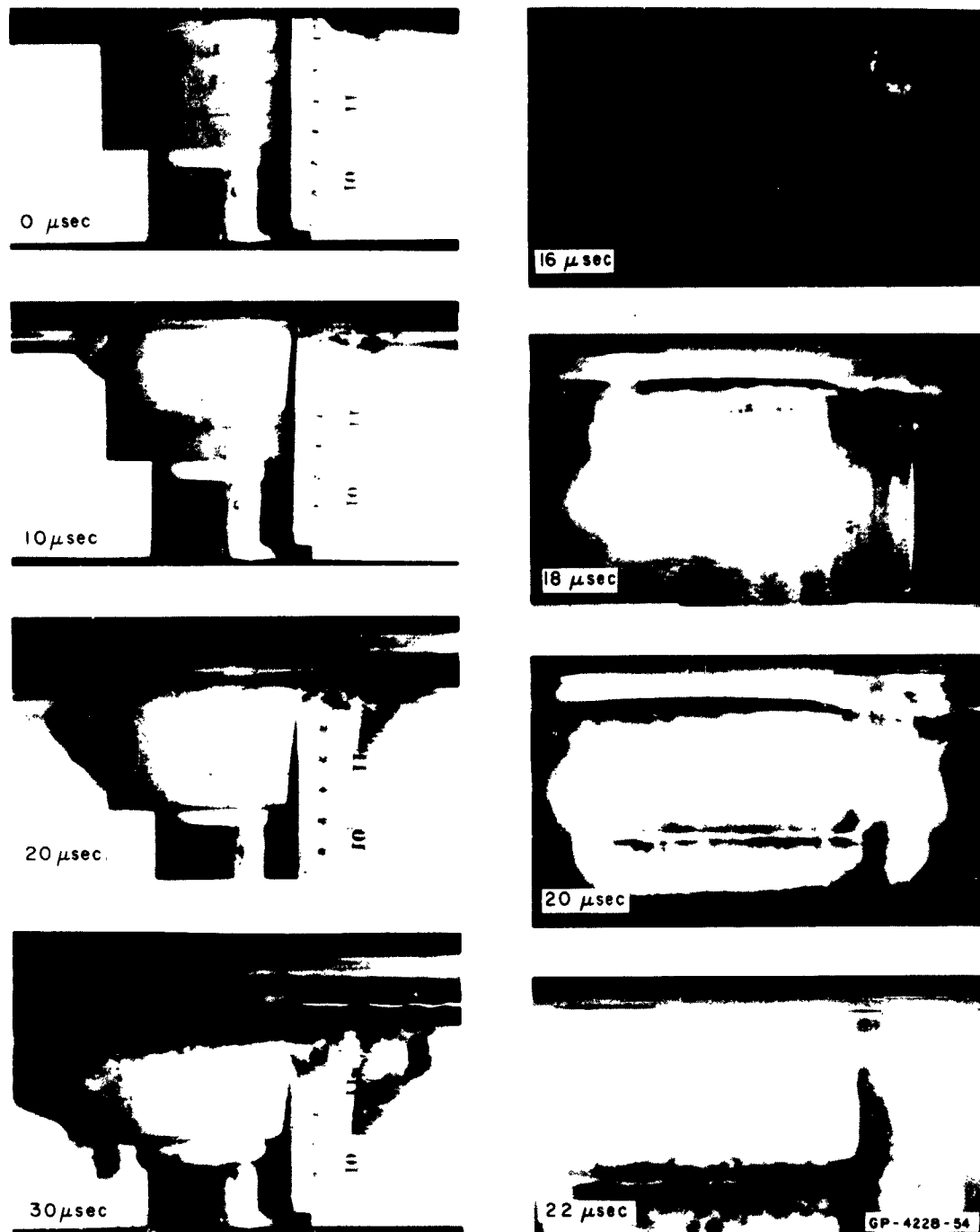
(U) It should be emphasized that this simple model of shock propagation and reflection ignores attenuation of the shock, both from relief waves coming in from the rear free surface of the flying plate and from the attenuation due to rarefactions from the curved cylindrical surface of the charge. Thus the pressure at any time significantly removed from initial impact of the aluminum on the Comp B is likely to be considerably lower than that shown here.

(U) For initial tests two designs were chosen which would yield flying plate velocities of  $0.37 \text{ mm}/\mu\text{sec}$  and  $0.52 \text{ mm}/\mu\text{sec}$ , both within the supposedly safe range for initiation of the PETN. Figure 23 shows selected frames from

# CONFIDENTIAL



CONFIDENTIAL



SHOT NO. 10,088,  
ALUMINUM PLATE VELOCITY: 0.37 mm/ $\mu$ sec

SHOT NO. 10,089,  
ALUMINUM PLATE VELOCITY: 0.52 mm/ $\mu$ sec  
LIGHT SOURCE FAILED

Figure 23 (U) Framing Camera Records of Two Shock-Initiated Backwards Initiation Experiments (U).

CONFIDENTIAL

# CONFIDENTIAL

the framing camera sequence of these two shots. As can be seen, Shot No. 10,088 did not provide a shock wave strong enough to initiate the lower PETN wafer, although some sort of reaction appears to be taking place in the later frames. Shot No. 10,089 did, however, operate satisfactorily, and this design was used for the following two tests.

(C, gp 4) After this successful framing camera shot, two shots were fired in front of the flash X ray to observe how this design accelerated a stack of plates. Shot No. 10,108 used solid steel plates, and Shot No. 10,119 used a fragment pack. Figure 24 shows the X-ray records from these two shots and illustrates the very good velocity uniformity achieved by the solid plate shot and the somewhat less perfect uniformity displayed by the fragment shot. The improvement over the performance shown in Figure 20 is quite remarkable, however, and it thus appears that this method of backwards initiation should yield results comparable to the two methods discussed earlier.

(U) The most important defect now remaining in this design was the presence of the fragile, and sensitive, low density PETN wafer in the assembly. Since the theoretical analysis summarized in Figure 22 suggested that elimination of this material should be possible, a series of 4 shots was fired to attempt it. These, and the two shots including PETN, are listed in Table 6.

(U) The four Comp B shots without PETN showed such inconsistencies, both among themselves and when compared to earlier shots, that it was decided to abandon Comp B as an explosive for this study. It might be possible to determine what combination of density and RDX concentration variations and what cracks or other casting defects are responsible for the observed behavior, but it did not seem worthwhile to do so for this project.

## (b) Plastic-bonded HMX tests

(U) A pressed explosive, such as 9404 PBX, can be expected to be much more consistent than Comp B. In addition, it is somewhat more energetic than Comp B and has a higher detonation velocity -- both attributes of potential value in this application. Accordingly, a short series of shots was fired with this material to check on its behavior when shocked. The shot design was the same as that used for the last Comp B shots except that since PBX

# CONFIDENTIAL

CONFIDENTIAL

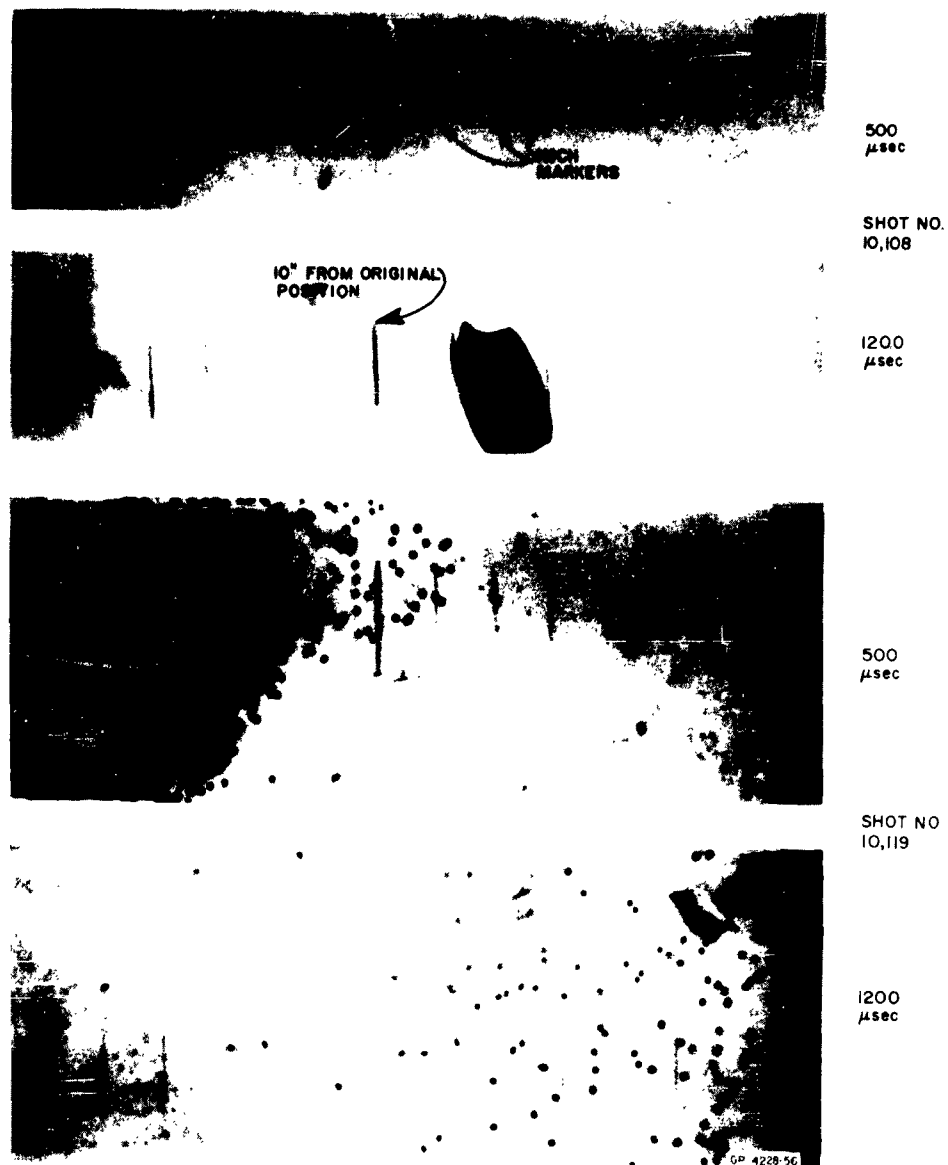


Figure 24 (U) X-Ray Records of Two Shock-Initiated Backwards Initiation Experiments (U).

CONFIDENTIAL

CONFIDENTIAL

Table 6 (U)  
SHOCK-INDUCED BACKWARDS INITIATION SHOTS WITH COMP B (U)

Shot No.	Plate Velocity (mm/ sec)	Driving HE (inch)	Booster under Comp B	Flipover Point (inches from top)	Comments
10, 088	0.37	0.100	PETN	None	Some reaction, no detonation. PETN went first.
10, 089	0.52	0.145	PETN	2.0	
10, 186	0.47	0.137	None	None	
10, 187	0.52	0.148	None	1.4	
10, 196	0.47	0.137	None	1.4	
10, 197	0.52	0.148	None	None	Comp B, 1 inch high.

All shots tested 3-inch-diameter by 2-inch-long Comp B cylinders except as noted. Shot setup shown in Figure 21.

CONFIDENTIAL

was available only in 3-inch-diameter cylinders 3 inches long. This explosive shape was used. Table 7 summarizes the results of these shots. These data are much more encouraging than those for Comp B and suggest that it should be possible to make the concept work if a 3-inch-diameter by 2-inch-high cylinder were used with a flying plate velocity of 0.42 mm/ $\mu$ sec. Unfortunately, PBX of this shape was not available to us, and we were therefore unable to test this conclusion.

Table 7 (U)  
SHOCK-INDUCED BACKWARDS  
INITIATION SHOTS WITH PBX (U)

Shot No.	Plate Velocity (mm/ $\mu$ sec)	Driving HE (inch)	Flipover Point (inches from top)
10,219	0.52	0.148	1.0
10,220	0.37	0.100	None
10,232	0.47	0.137	1.3
10,233	0.42	0.116	2.2
10,276	0.42	0.116	2.0
10,277	0.42	0.116	3.0
10,304	0.40	0.110	2.1
10,355	0.40	0.107	None

All shots tested 3-inch-diameter by 3-inch-long cylinders of 9404 PBX (HMX, plastic bonded) and were otherwise identical to the Comp B shot shown in Figure 21.

### 3. Summary

(U) Although this method has not been developed and tested as fully as most of the others discussed in this report, its feasibility has at least been demonstrated. A design incorporating Comp B will probably never operate reliably unless PETN is added, and this addition cancels most of the advantages of the method. Plastic-bonded HMX looks very promising, however, and additional research with it seems warranted. This should lead to a backwards initiation design which would be quite simple to manufacture, since no narrow holes or booster cavities would be required, and which would be safe and simple to initiate.

# CONFIDENTIAL

## E. SPACED AND BUFFERED PLATES

### 1. Theory

(C, gp 4) Early work in this project showed that although flying plate techniques worked very well when judged by the uniformity of fragment velocity, the magnitude of this velocity was somewhat lower than expected. This was because the momentum of the flying plate was not all transferred to the fragment pack, as theory predicted, but was shared between the two so that they were observed traveling off at about the same velocity. This observation suggested that it might be possible to substitute a layer of fragments for the flying plate and thus eliminate the wasted weight of the solid flying plate.

### 2. Experiments

(C, gp 4) Figure 25 shows one possible design for a warhead employing such a scheme. A single plate is thrown into another single plate, these two together then pick up two more; these four, the final four — at which point the entire stack has been accelerated. The spacing between plates was made

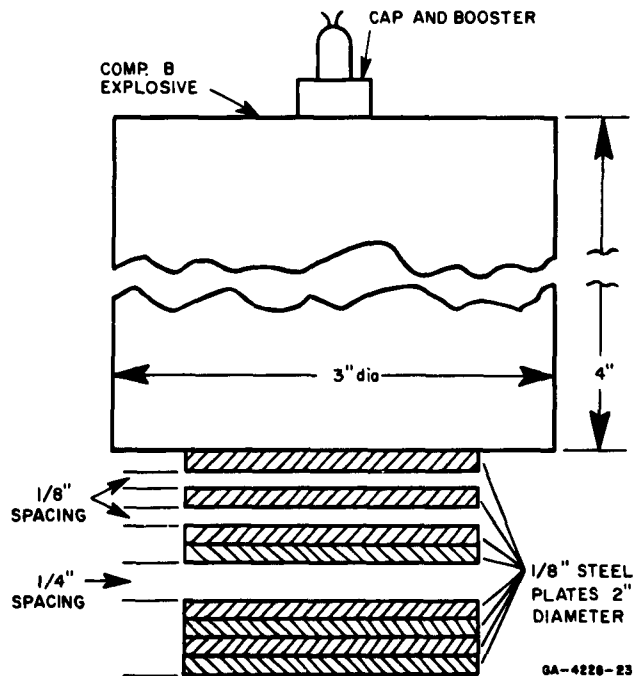


FIGURE 25 (U) SPACED LAYER SHOT DESIGN (U)  
[Figure and caption combined (U)]

# CONFIDENTIAL

large enough to allow the shock waves induced by each impact to die down before the next one. Such a design will be designated here as a 1-1-2-4 design in order to specify the plate groupings used. When this design was fired in front of the X-ray it was observed that although as many as three of the plates held together fairly well and moved off at about the same velocity, the remaining plates were severely damaged by the repeated impacts upon one another, and their fragments were quite widespread. Figure 26 shows a particularly bad example of this behavior: a cloud in which only one plate is clearly intact.

(C, gp 4) When a buffer layer of foamed plastic was placed in the spaces between plate groups, both the damage to the plates and the velocity variation were significantly reduced. It therefore seemed worthwhile to shoot some similar shots with fragments, and three such were fired.

(U) Figure 27 shows the parts of the two shots using 60 lb/ft<sup>3</sup> polyurethane foam before assembly. The 2-2-4 and 4-4 configurations tested had been found to behave in essentially the same way in the solid plate tests, so they were chosen over the original 1-1-2-4 design in order to reduce the number of damaging impacts during acceleration.

(U) The records from these two shots are shown in Figure 28 and indicate that a fairly low velocity spread is achieved by these designs.

### 3. Summary

Table 8 lists all the shots fired during the investigation of this method of velocity control. The performance of the last two shots, although not as good as that of some of the more sophisticated methods, may still be adequate for some applications. If so, the simplicity of construction and the high fragment velocity will make this method an attractive choice.

# CONFIDENTIAL

CONFIDENTIAL

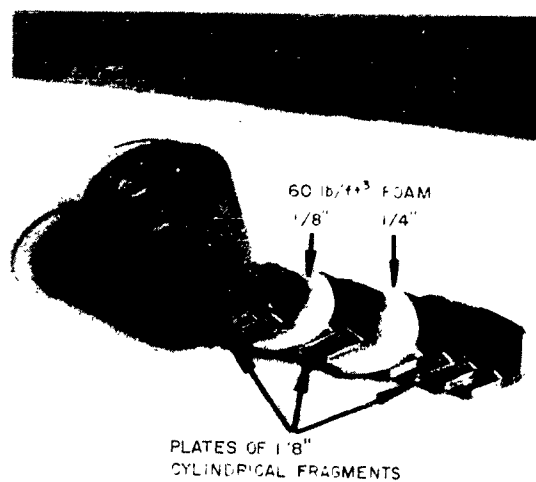


Figure 26 (U) Spaced Plate Shot, No. 9711 (U).

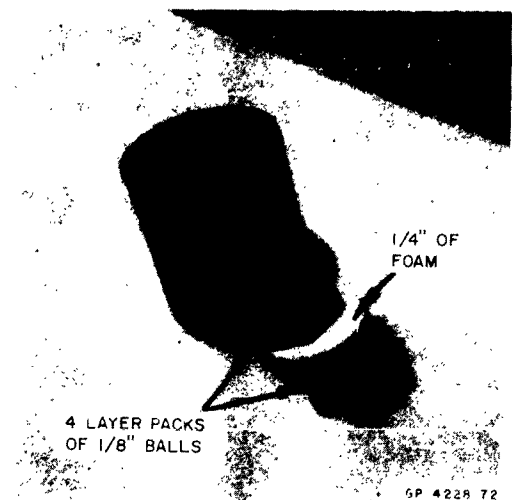
CONFIDENTIAL



CONFIDENTIAL



(a) SHOT 10271



(b) SHOT 10272

Figure 27 (C) Spaced Fragment Plate Shot Assembly (C).

CONFIDENTIAL

CONFIDENTIAL

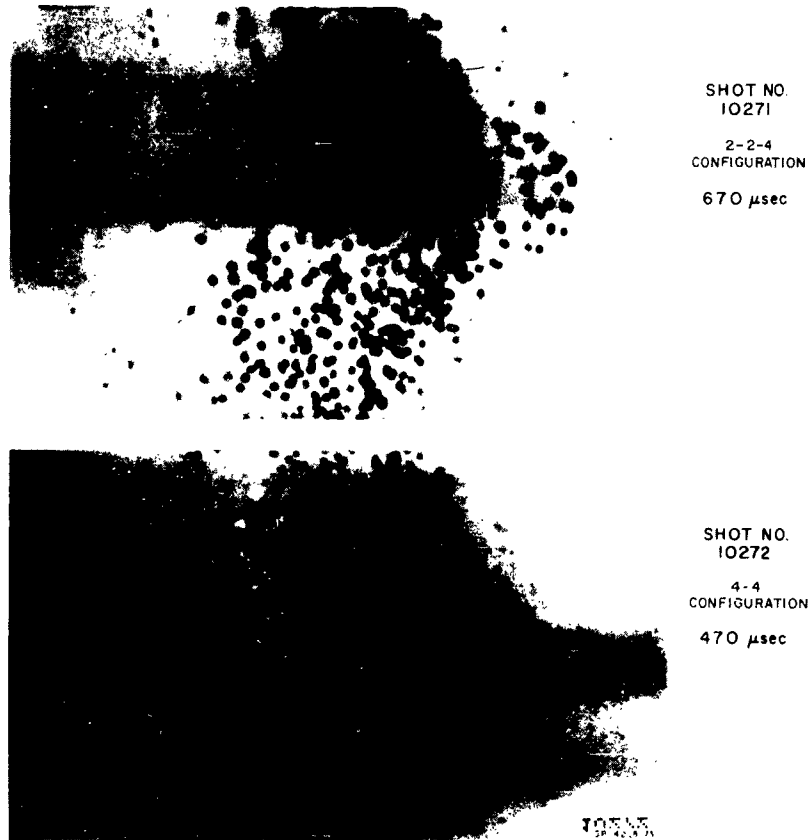


Figure 28 (C) Spaced Plate Shots with Fragments and 60 lb/ft<sup>3</sup> Foam (C).

CONFIDENTIAL

CONFIDENTIAL

Table 8 (C, gp-4)  
SHOTS WITH SPACED AND BUFFERED PLATES (U)

Shot No.	Recording Instrument	Explosive Thickness & Dia. (inches)	Plate Grouping Starting at HE	Foam Density Between Groups (lb/ft <sup>3</sup> )	Pack Makeup	Velocity (mm/μsec)	% Mass in Frag.	Comments
9645	Flash X ray	4 x 3	1-1-2-4	0	1/8 solid plates	0.40 ±12%	35	Plates badly broken up.
9711		4 x 3	1-1-2-4	0		0.38 ±24%	35	Plates badly broken up.
9838		3 x 3	2-2-4	0		0.39 ±34%	41	
9839		3 x 3	2-2-4	20		0.35 ± 7%	41	
9910		3 x 3	2-2-4	20	1/8 frag. plates	-0.40 ±20%	39	Deep bowl-shaped cloud.
10, 237		3 x 3	*	*	1/8 solid plates	Lead 0.55 Trail 0.27	38	Plates badly broken up.
10, 256		3 x 3	2-2-4	60		Avg. - 0.35	40	4 plates 0.34 ± 2% mm/μsec; other frags. 0.2 to 0.5 mm/μsec.
10, 257		3 x 3	4-4	60		Avg. - 0.35	40	5 plates 0.33 mm/μsec ± 5%; other frags. to 0.5 mm/μsec.
10, 271		3 x 3	2-2-4	60	1/8 frag. plates	Avg. 0.42	39	Nose: 0.48 mm/μsec. Main mass: 0.42 mm/μsec. Rim: 0.35 mm/μsec.
10, 272		3 x 3	4-4	60	1/8 ball pack.	Avg. - 0.60	29	Nose: 0.66 mm/μsec. Main mass: 0.60 mm/μsec. Rim: 0.47 mm/μsec.

\* All plates separated by 0.0165 inch lead sheet.

CONFIDENTIAL

# CONFIDENTIAL

## F. NOL TWO-STAGE DESIGN

### 1. Theory

(C, gp 4) H. M. Sternberg and D. Piacesi have described <sup>7</sup> a cylindrical warhead which employs a two-stage construction to achieve high casing velocities with comparatively low peak pressures of long duration. Although their treatment was entirely theoretical, the results of their calculations seemed encouraging enough to justify an experimental attempt to adapt the concept to an end charge such as we are considering.

(C, gp 4) The operation of the two-stage design starts with the detonation of the main explosive charge which, in turn, accelerates a thin steel plate across an air gap. This air gap initially contains a thin additional layer of explosive which is initiated by the shock from the main charge coming through the flying plate as the plate is accelerated. The air shock and explosive product gases from the detonation of this inside layer of explosive traverse the air gap much faster than the flying plate and begin to apply pressure to the opposite wall. This wall is the material to be accelerated — in our case, the fragment pack. As the flying plate continues across the gap, the pressure between it and the fragment pack is maintained by shock waves reflecting back and forth between the two, until eventually the fragment pack has been accelerated to the point where it carries most of the momentum originally in the flying plate.

(C, gp 4) From our point of view the advantage of the above process is that a long pressure pulse can be obtained, even though the flying plate is quite thin, because the product gases from the inside explosive act as a buffer and start applying pressure long before the flying plate arrives at the fragment pack.

### 2. Experiments

(C, gp 4) The examples calculated in the Sternberg-Piacesi report were for a cylindrical warhead in which the cylindrical outer wall was to be accelerated. The pulse durations calculated were considerably shorter than the 10  $\mu$ sec required for our work, so we made a rather arbitrary extrapolation of the design in order to find one more likely to operate satisfactorily. Figure 29 shows the basic design used for shots fired during the early stages of the investigation of this design.

CONFIDENTIAL

CONFIDENTIAL

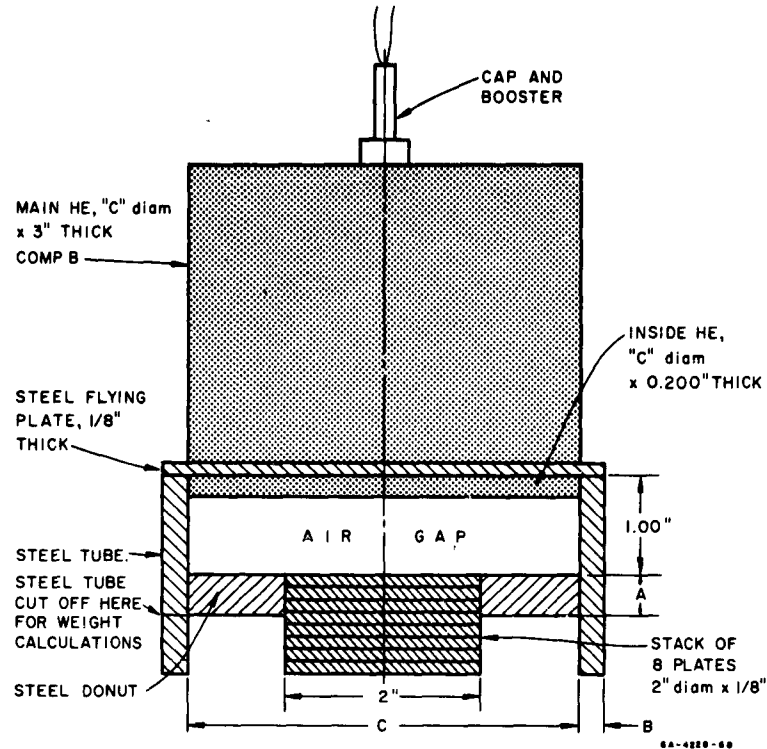


FIGURE 29 (C) NOL DESIGN MODIFIED FOR MULTILAYER ACCELERATION (C)  
[Figure and caption combined (C, gp 4)]

(C, gp 4) Since gas pressure is the main source of accelerating force in this design, it was expected that side confinement to prevent loss of pressure would be quite important. The first shot was designed to reduce pressure loss to a minimum by having a design 4 inches in diameter (to allow an inch all around for edge effects), by surrounding the 2-inch-diameter plate stack by a steel donut of the same 1-inch thickness, and by enclosing the air gap and the donut in a steel cylinder with a 1/4-inch wall.

(C, gp 4) Subsequent shots varied the cylinder wall thickness, the donut thickness, and the diameter in order to assess the importance of these various components. Since the donut of the first shot should go at the same velocity as the plate stack, a second plate was placed below it to slow it down and to allow the plate stack to get ahead where it could be seen on the X ray. All other shots had thinner donuts, so that this addition was not necessary.

CONFIDENTIAL

# CONFIDENTIAL

(U) Figure 30 shows photographs of various shots in this series as they were being assembled and set up for firing. Note that the length of the cylinder was held at 2 inches, even when donuts thinner than 1 inch were used, in order to provide better support for the charge.

(C, gp 4) A selection of some of the X-ray records from the early shots is shown in Figure 31. Of particular note are those pictures in which it appears that the donut has caught a few of the plates and is carrying them along at a velocity higher than the rest of the stack. This process probably accounts for the large overall velocity variation seen in the 1/2-inch donut shots. With either thicker or thinner donuts the separation is smoother, and the velocity variation is very low.

(C, gp 4) Pieces of the flying plate can be seen in several of the shot pictures. In the 4-inch-diameter shots the central section of this plate is formed into a cup, and during the acceleration process this cup apparently serves to seal a volume of compressed gas against the plate stack and thus helps avoid edge effects.

(C, gp 4) When this method was tried with fragment packs instead of the solid plate stack the results were very good. Figure 32 shows that the velocity uniformity achieved by the 3- and 4-inch designs was very good and that even the 2-inch design gave a respectable performance.

### 3. Summary

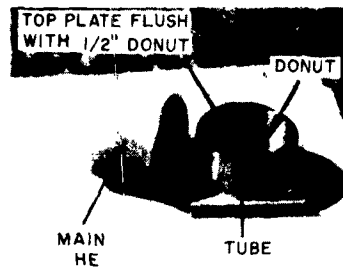
(U) Some twenty shots were fired during the investigation of this method, and the most pertinent examples of these are covered in Table 9. From a study of these shots the following conclusions have been drawn.

(C, gp 4) 1. Reduction of donut thickness from 1 inch to 1/8 inch and of cylinder wall thickness from 1/4 inch to zero reduces a steel plate velocity about 20 percent without appreciable effect on the velocity uniformity.

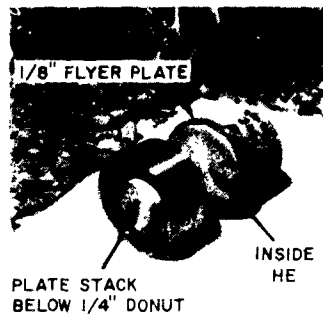
(C, gp 4) 2. Velocity uniformity for steel plates is very good ( $\pm 1$  percent or less) for 4- and 3-inch-diameter designs, but it deteriorates in the 2-inch-diameter design to  $\pm 5$  percent.

# CONFIDENTIAL

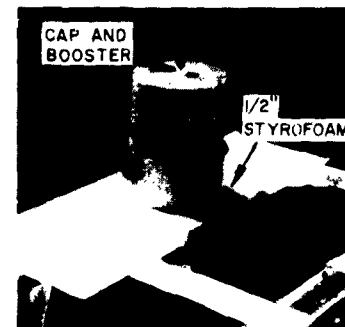
CONFIDENTIAL



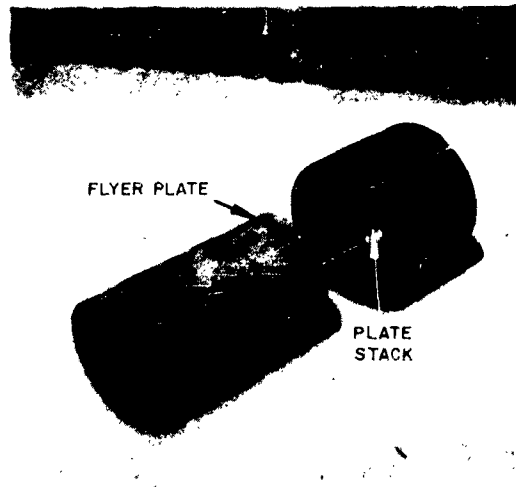
a) SHOT 10265  
NOTE FLUSH TOP



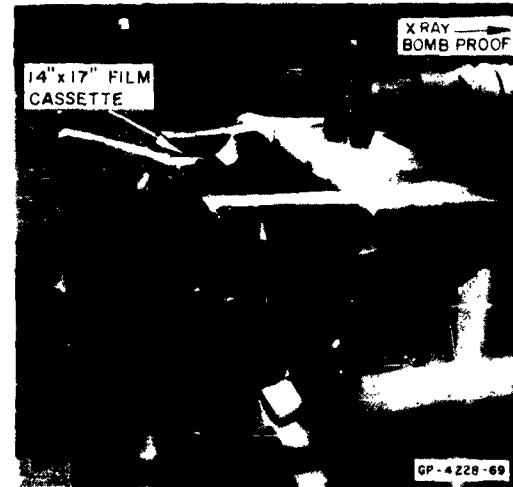
(b) SHOT 10266  
NOTE HE ASSEMBLY



(c) SHOT 10266  
READY TO FIRE



(d) SHOT 10269, ASSEMBLY

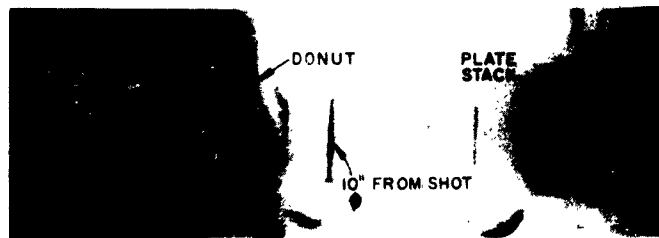


(e) SHOT 10269, FIRING POSITION

Figure 30 (C) Assembly and Setup of NOL Design Shots (U).

CONFIDENTIAL

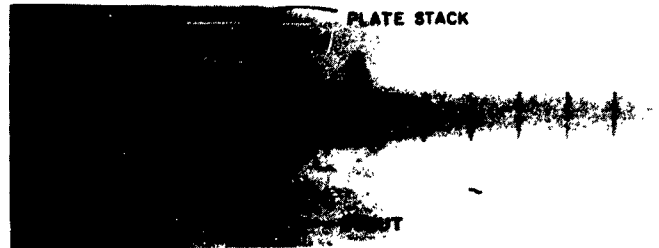
CONFIDENTIAL



SHOT NO 10235

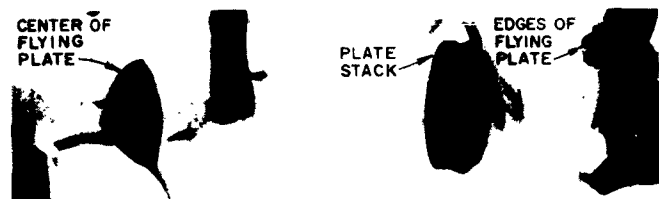
750  $\mu$ sec

1" DONUT



SHOT NO 10265

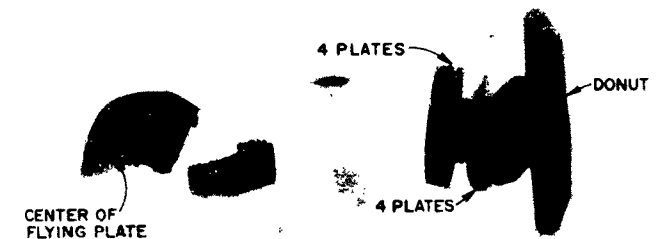
370  $\mu$ sec



SHOT NO 10266

670  $\mu$ sec

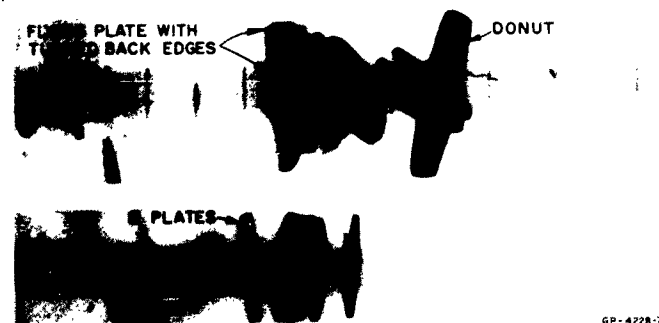
$\frac{1}{4}$ " DONUT



SHOT NO 10267

670  $\mu$ sec

$\frac{1}{8}$ " WALL



SHOT NO 10268

670  $\mu$ sec

3" diam

SHOT NO 10269

970  $\mu$ sec

2" diam

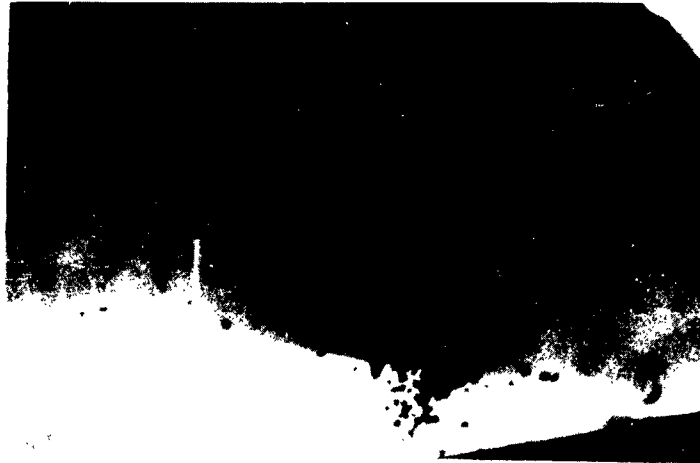
GP-4228-70

Figure 31 (C) NOL Design Shots (U).

CONFIDENTIAL



CONFIDENTIAL



SHOT 10,321  
4", 470  $\mu$ sec



SHOT 10,349  
2", 970  $\mu$ sec



SHOT 10,350  
3", 370  $\mu$ sec

Figure 32 (U) NOL Shots with Fragments (U).

CONFIDENTIAL

# CONFIDENTIAL

Table 9 (C, gp 4)  
SELECTED NOL DESIGN SHOTS (U)

Shot No.	Diam. C (inches)	Cyl Wall B (inch)	Donut A (inch)	HE Height (inches)	Pack Makeup	Inside HE (inch)	Gap + HE (inches)	Velocity (mm/ $\mu$ sec)	% Mass in Pack	Comments
10,235	4	1/4	1	3	8 plates 1/8" x 2" steel	0.20	1.00	0.52 $\pm 2\%$	11	
10,267	4	1/8	1/2	3	8 plates	0.20	1.00	0.53 $\pm 3\%$	15	
10,317	4	1/8	1/8	3	8 plates	0.20	1.00	0.45 $\pm 0\%$	19	
10,321	4	1/4	1/4	3	Ball pack 1636 1/8" brass	0.20	1.00	0.68 $\pm 1\%$	10	Equiv. solid plate shot: 0.50 mm/ $\mu$ sec.
10,268	3	1/4	1/2	3	8 plates	0.20	1.00	0.41 $\pm 7\%$	22	Flying plate overlapped cyl. walls.
10,318	3	1/8	1/4	3	8 plates	0.20	1.00	0.39 $\pm 1\%$	28	No overlap.
10,346	3	0	1/8	3	8 plates	0.20	1.00	0.34 $\pm 1/2\%$	34	No overlap.
10,350	3	1/8	1/4	3	Ball pack	0.20	1.00	0.53 $\pm 1/2\%$	18	No overlap.
10,269	2	1/4	---	3	8 plates	0.20	1.00	0.25 $\pm 5\%$	34	No overlap.
10,319	2	1/8	---	3	8 plates	0.22	1.00	0.23 $\pm 2\%$	43	No overlap.
10,320	2	1/8	---	3	8 plates	0.22	1.20	0.22 $\pm 5\%$	42	No overlap.
10,344	2	1/8	---	2	8 plates	0.22	1.00	0.22 $\pm 2\%$	47	No overlap.
10,345	2	0	---	2	8 plates	0.22	1.00	0.18 $\pm 5\%$	63	No overlap.
10,349	2	1/8	---	2	1636 balls	0.22	1.00	Avg 0.33	34	No overlap, balls loose- cast in cylinder. Nose: 0.45 mm/ $\mu$ sec Bowl: 0.35 mm/ $\mu$ sec Rim: 0.27 mm/ $\mu$ sec
10,351	4	1/8	1/4	3	16 plates 1/8" x 3" steel	0.20	1.00	0.23 $\pm 0\%$	51	
10,364	4	1/4	---	4	16 plates 1/8" x 4" steel	0.44	2.00	0.22 $\pm 5\%$	47	Double-scale of Shot No. 10,344.

CONFIDENTIAL

# CONFIDENTIAL

(C, gp 4) 3. Some improvement in the performance of the 2-inch-diameter design can be made if the inner explosive thickness and the air gap thickness are changed slightly. Velocity variations for plates may be reduced to  $\pm 2$  percent in this way, as shown in Figure 33.

(C, gp 4) 4. The main HE in the 2-inch diameter design can be reduced to 2 inches in length without significant effect on performance.

(C, gp 4) 5. The flying plate in 3-inch-diameter designs should be made so that it will slide inside the cylinder, since this reduces velocity variation to  $\pm 1$  percent from the  $\pm 7$  percent observed when the plate had to shear off before entering the cylinder.

(C, gp 4) 6. Spherical fragments are accelerated very satisfactorily by these designs, either when cast in a close-packed hexagonal array or when randomly potted in a cylindrical shape. The velocities achieved by a pack of 1600 brass balls are 35 to 40 percent higher than those observed for a steel plate stack, and the fragment clouds, as shown in Figure 32, are very well formed and compact, at least for the 3- and 4-inch designs.

(U) 7. The overall design of these shots can be varied considerably without adverse effect on performance. Shot No. 10,351 accelerated 4 1/2

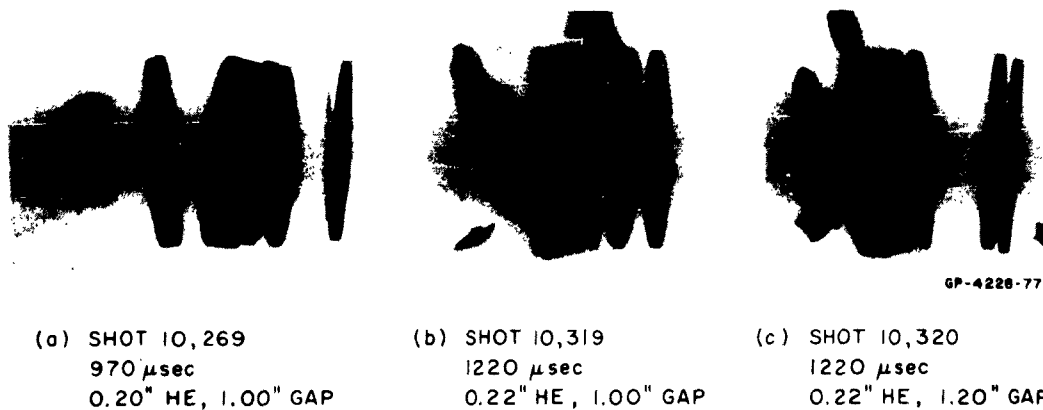


Figure 33 (C) Two-Inch NOL Shots with Various Inner Explosive Arrangements (C).

# CONFIDENTIAL

times the normal mass to 46 percent of the velocity normal for a 4-inch-diameter design. The kinetic energy of the plate stack was equal to that in a normal design although the momentum was increased by a factor of 2.1.

(C, gp 4) 8. If all linear dimensions of a 2-inch design are scaled up by a factor of 2, velocities and velocity uniformities will remain essentially the same.

(C, gp 4) 9. If the design is modified to increase the mass percent in fragments, velocity and velocity uniformity deteriorate so significantly that the electrical or MDF backwards initiation designs begin to be more attractive. Thus, at present, it appears that the NOL design should be used only when high velocities are required, or when the straightforward initiation of the explosive is an advantage.

## G. EXPANDED METAL STUDIES

### 1. Theory

(U) In other projects<sup>8</sup> at these Laboratories it has been shown that when a shock wave is induced in a porous, collapsible material, the material will have been transformed, after passage of the shock, into a thinner layer of material of the collapsed density with all parts of the layer having about the same velocity. In effect, what the porous material does is reshape a peaked shock wave into a square one.

(C, gp 4) This behavior and its application to this project are illustrated in Figure 34 which shows what should happen when a multilayered pack of fragments made of such a porous material is struck by a detonation front. In this case the final result should be a cloud of fragments, now compressed to a normal density, all moving off with a uniform velocity.

### 2. Experiments

(C, gp 4) The porous materials studied in this project were foamed aluminum<sup>9</sup> and felted nickel,<sup>10</sup> each approximately half its solid density. The foamed aluminum was tested because it was readily available even though its compressed density is too low for use in most final designs. The felted nickel was chosen because nickel fragments were expected to perform well in a war-head of this type. It was originally planned to test felted copper and iron as well,

# CONFIDENTIAL

CONFIDENTIAL

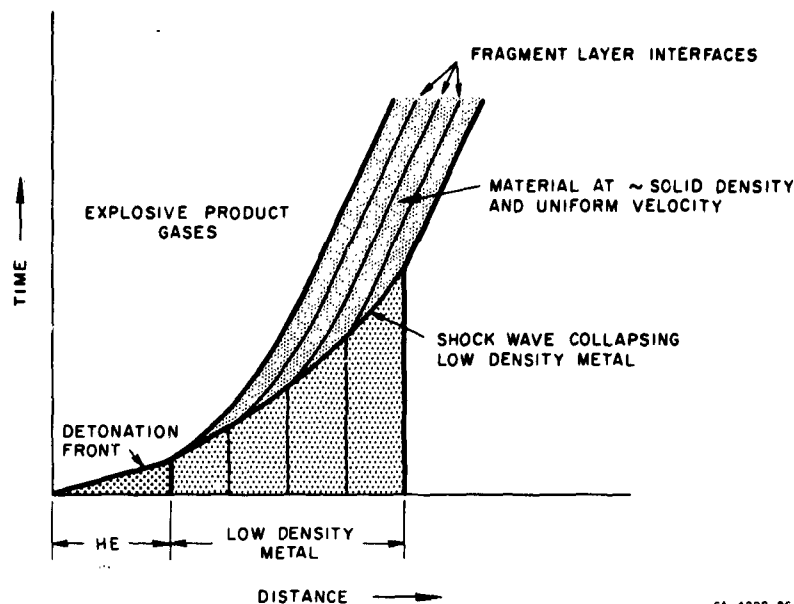


FIGURE 34 (U) DISTANCE-TIME PLOT OF EXPLOSIVELY SHOCKED, LOW-DENSITY METAL (U)  
[Figure and caption combined (U)]

but delivery of these materials was delayed until it became too late to use them in the project and the order was cancelled.

(C, gp 4) The first shots fired attempted to use a high explosive-to-fragment-weight ratio in order to produce high velocities. A plane-wave initiated cylinder of Comp B, 2 inches in diameter and 2 inches long, was used to compress and accelerate four 1/8-inch layers of felted nickel. Figure 35 shows the design of the shots and the way in which the air was evacuated from the felt disks so that air shocks would not interfere with the collapse of the felt. On the outside of the stack of felted plates Shot No. 10,062 included one solid steel plate to determine if its presence would consolidate the spray of fragments. Shot No. 10,061 eliminated this plate and used only a 0.001-inch Mylar diaphragm to provide a vacuum seal.

(C, gp 4) Figure 36 shows the X-ray records from these two shots and the very small fragments produced. It appeared from these shots that even though a velocity on the order of 1 mm/ $\mu$ sec could be reached in this way, sizeable fragments could not be produced.

CONFIDENTIAL

CONFIDENTIAL

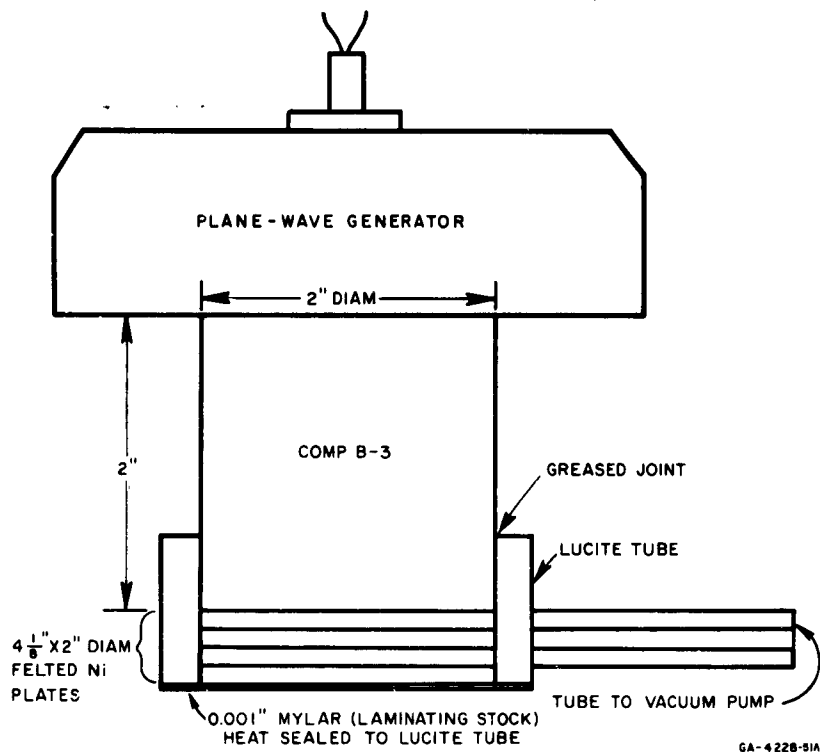


FIGURE 35 (C) EVACUATED METAL FELT SHOT DESIGN (U)  
[Figure and caption combined (C, gp 4)]

(C, gp 4) The next series of four shots tested single and multiple layers of fragments cut out of the two low-density materials. Aluminum foam fragments were cut  $1/4 \times 1/4 \times 1/2$  inch, and nickel fragments were  $1/8 \times 1/8 \times 1/4$  inch. Other details of these shots are given in Table 10 at the end of this section.

(C, gp 4) In order to assure a uniform pressure pulse from the comparatively thin explosive used, initiation was at a point off to one side of the pack of fragments, and the detonation front then ran across the top of the pack laterally. In spite of this arrangement, even the single-layer shots showed considerable velocity variation.

(C, gp 4) The recovered fragments showed that compression too close to solid density and to a compact cubical shape was achieved in all shots with little or no breakup of the fragments or fusing to adjacent fragments. Figure 37 shows typical fragments recovered from the two 4-layer shots.

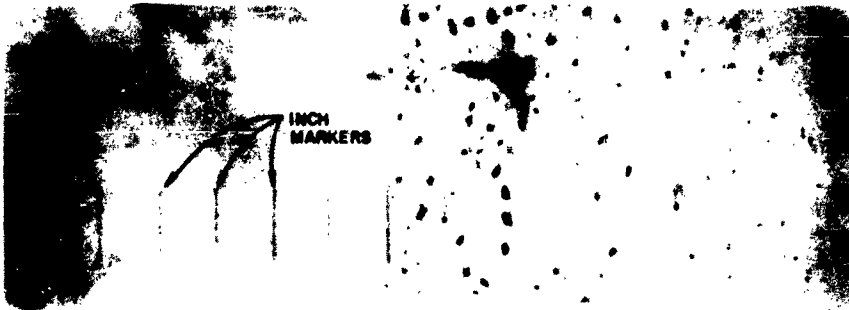
CONFIDENTIAL

CONFIDENTIAL

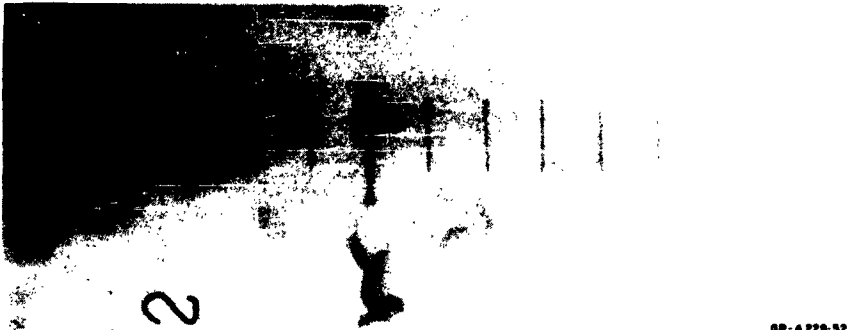


200  
 $\mu$ SEC

SHOT NO.  
10,061,  
MYLAR  
SEAL



400  
 $\mu$ SEC



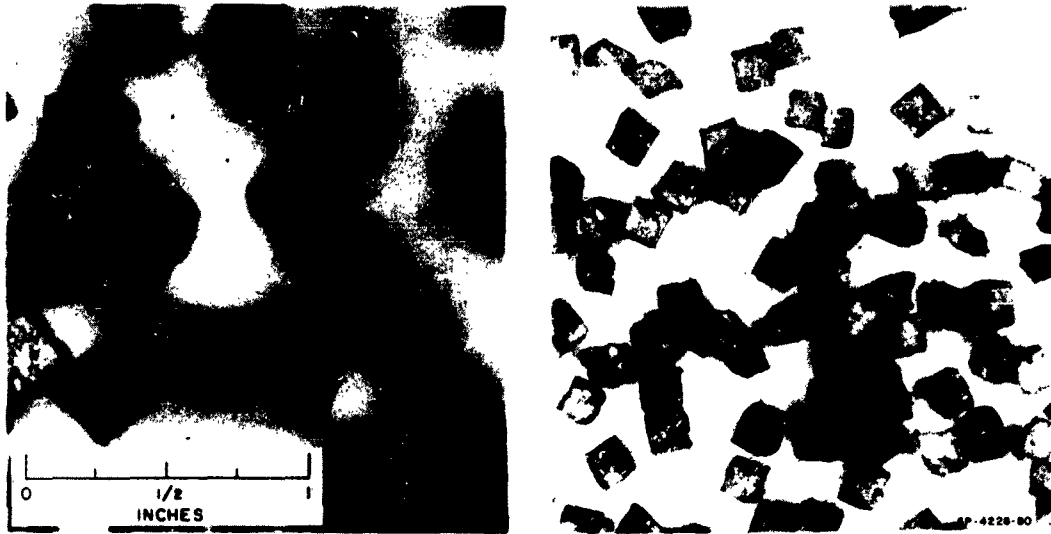
SHOT NO.  
10,062,  
STEEL  
PLATE  
SEAL  
200  
 $\mu$ SEC

GP-4220-52

Figure 36 (U) X-Ray Records of Evacuated Metal Felt Shots (U).

CONFIDENTIAL

# CONFIDENTIAL



(a) SHOT 10,362  
AZ FOAM, 50% DENSITY  
ORIG. 1/4" x 1/4" x 1/2"

(b) SHOT 10,363  
FELTED Ni, 40% DENSITY  
ORIG. 1/8" x 1/8" x 1/4"

Figure 37 (C) Compressed Fragments Recovered from 4-Layer Low-Density Shots (C).

(C, gp 4) On the theory that the velocity variation in this last series was due to the lack of edge confinement and to the running detonation, the shot shown in Figure 38 was fired. The nine pieces of MDF were used to produce a quasi-plane detonation front in the EL-506D sheet explosive. The other change from earlier shots was the addition of steel confinement around the edges of the stack of felt fragments. This confinement was added so that a large diameter warhead would be more completely simulated by this small-scale shot.

(C, gp 4) Figure 39 shows the X-ray record for the shot. The velocity calculated from this record is  $0.32 \text{ mm}/\mu\text{sec} \pm 3 \text{ percent}$ , which is quite good performance. The X ray appears to show that most of the fragments remained separate from each other, but many of the recovered fragments were clustered, even after striking sand. Figure 40 shows a representative sample of these fragments and includes clumps of as many as eight or twelve.

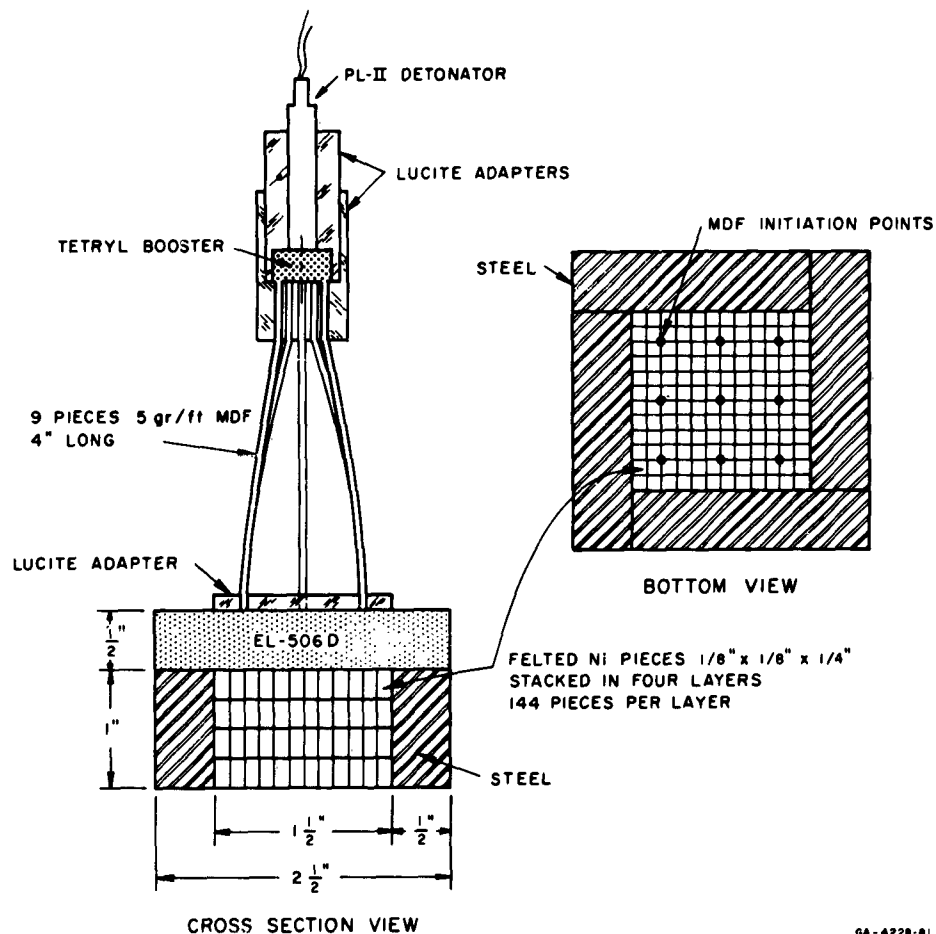
# CONFIDENTIAL



**CONFIDENTIAL**

(C, gp 4) As the project was drawing to a close, there was still time and material to fire one more shot to see if the clustering of fragments could be reduced. Figure 41 shows the half-filled, next-to-last layer of a fragment pack in which each fragment is separated from its neighbors by a 0.005-inch Mylar.

(C, gp 4) Figure 42 shows the fragment cloud produced by this design, and Figure 43 shows some of the recovered fragments. These both show that clustering was virtually eliminated by this change in the design. The increase in velocity variation apparent in Figure 42 as compared to that shown in



GA-4228-81

FIGURE 38 (C) FELTED NICKEL SHOT WITH QUASI-PLANE-WAVE INITIATION (U)  
[Figure and caption combined (C, gp 4)]

**CONFIDENTIAL**

**CONFIDENTIAL**



Figure 39 (U) Felted Nickel X-ray Shot, No. 10,392 - 970  $\mu$ sec (U).

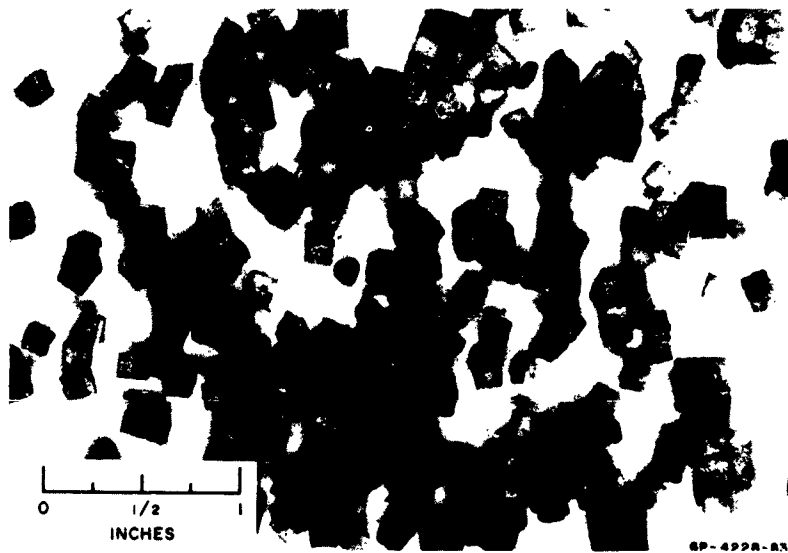


Figure 40 (U) Nickel Fragments Recovered from Shot No. 10,392 (U).

**CONFIDENTIAL**

**CONFIDENTIAL**

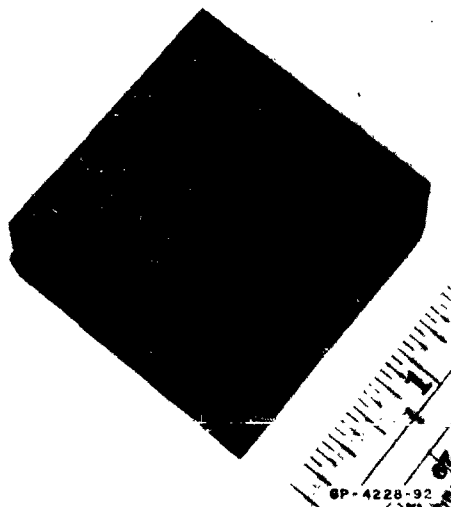


Figure 41 (U) Assembly of Felted Nickel Fragments Separated by 0.005-Inch Mylar, Shot No. 10,480 (C).

Figure 39 may be caused by the addition of the Mylar, but the reduction in fragment pack dimensions to 1 x 1 inch from the 1 1/2 x 1 1/2 inches used earlier may also be a contributing factor.

### 3. Summary

(U) Table 10 gives details of the six last shots fired during this study. Although more work remains to be done before this method becomes fully workable, it does appear feasible to develop a warhead of this kind. The fragment velocities are quite high, even with the low-explosive loading used, and it is quite possible that these can be increased substantially before fragment breakup becomes a problem.

(U) A fairly large selection of porous materials is now becoming available. Huyck Corporation, the supplier of the felted nickel tested here, claims to be able to supply felted iron, nickel, cobalt, copper, and precious metals, as well as all common alloys of these basic metals. Ipsen Industries of Rockford, Illinois, has a contract to develop foamed stainless steel, aluminum, and nickel for NASA, and there are other sources as well. Consequently, there should be little difficulty in obtaining the desired material.

**CONFIDENTIAL**

CONFIDENTIAL



Figure 42 (U) Felted Nickel X-ray Shot with Fragments Separated by 0.005-Inch Mylar, No. 10,480 (C).

CONFIDENTIAL

**CONFIDENTIAL**

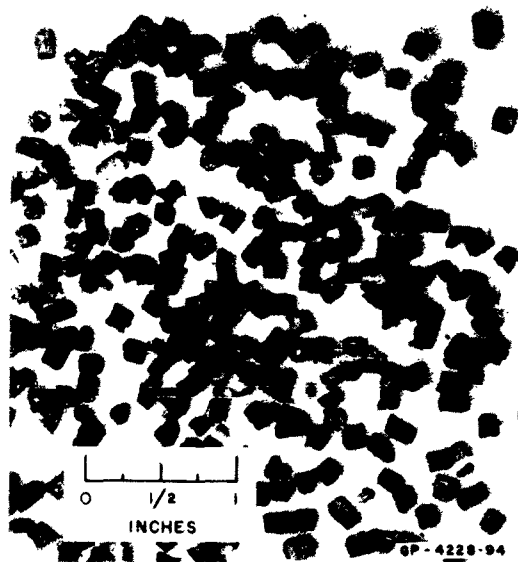


Figure 43 (U) Recovered Fragments from Felted Nickel Shot with Mylar Separation, No. 10,480 (U).

**CONFIDENTIAL**

CONFIDENTIAL

Table 10 (C, gp-4)  
LOW-DENSITY FRAGMENT SHOTS (C, gp-4)

Shot No.	Material	Original Frag. Size	Layer Construction	No. Layers	HE	Results
10, 348	Al	1/4"x1/4"x1/2"	1 1/2"x1 1/2", 36 pcs	1	EL-506D 2"x3"x0.18" Running detonation	Leading group 0.5 mm/sec. Several compressed fragments recovered.
10, 352	Ni	1/8"x1/8"x1/4"	1 1/2"x1 1/2", 144 pcs	1	EL-506D 2"x3"x0.18" Running detonation	Velocities 0.25 to 0.45 mm/μsec. Several compressed fragments recovered.
10, 362	Al	1/4"x1/4"x0.46"	2"x2", 64 pcs	4	Comp B 3"x4 1/2"x0.50" Running detonation	Velocities 0.29 to 0.37 mm/μsec. A few fragment pairs, all compressed.
10, 363	Ni	1/8"x1/8"x1/4"	1 1/2"x1 1/2", 144 pcs	4	Comp B 2 1/2"x4"x0.50" Running detonation	Velocities 0.25 to 0.35 mm/μsec. A few fragment pairs, all compressed.
10, 392	Ni	1/8"x1/8"x1/4"	1 1/2"x1 1/2", 144 pcs	4	EL-506D 2 1/2"x2 1/2"x0.50" 9 point "plane" initiation.	0.32 mm/μsec ±3%. Some clustering of recovered fragments.
10, 480	Ni	1/8"x1/8"x1/4"	1.09"x1.09" 64 pcs sep. by 0.005 Mylar	4	EL-506D 2.09"x2.09"x0.50 9 point "plane" initiation	0.30 mm/μsec ±14%. Clustering greatly reduced.

CONFIDENTIAL

## H. MISCELLANEOUS DESIGNS

(C, gp 4) Three shots were fired to measure for velocity variations resulting from shot designs which do not fit into any of the categories discussed thus far. A brief description of these will therefore be given here.

### 1. Simultaneous Forwards-Backwards Initiation

(C, gp 4) The peak pressure applied to a fragment pack by a backwards initiation design is much lower than that which would be applied by a detonation front arriving at the pack in the normal way from an initiation point at the back of the explosive. It was thought that some of this pressure might be regained if the detonation front were reflected off another detonation front so that a shock wave would be reflected back to the fragment pack through the detonation-product gasses.

(C, gp 4) To test this theory a shot was fired in which a 3-inch-diameter, 2-inch-thick charge, electrically initiated at three points on each circular face simultaneously, was used to accelerate a stack of solid plates from one face.

(C, gp 4) Table 11 shows the results of this shot and of a similar shot of the usual electrical backwards initiation design. No improvement due to the two-surface initiation is seen; in fact there is no significant difference between the two shots. It is possible that the relatively unconfined boosters on the face away from the plate stack failed to detonate, but additional tests were not made to check on this.

Table 11 (C, gp 4)  
SIMULTANEOUS FORWARD-BACKWARD INITIATION (U)

Shot No.	Explosive	Initiation	Average Velocity (mm/ $\mu$ sec)	Velocity Variation (%)
9840	3" dia. x 2" long	Simultaneous electrical forward-backward	0.32	$\pm 1 \frac{1}{2}$
9704	3" dia. x 2" long	1 point electrical backward	0.31	$\pm 1 \frac{1}{2}$

## 2. Aluminum Foam Buffer Shot

(C, gp 4) The construction of an aluminum flying plate shot is complicated by the necessity of providing an air gap between the aluminum and the fragment pack in order to allow shocks in the plate to die down before the plate strikes the pack. Also, there is a minimum amount of explosive which can be used on a 1-inch plate with causing it to spall. This sets a lower limit to the nonfragment weight in the warhead even though the lower velocities achieved by less explosive might be quite acceptable.

(C, gp 4) The shock-loaded behavior of porous materials discussed earlier and illustrated in Figure 34 suggests that if the space between the explosive and the fragment pack is filled with a foamed aluminum buffer which, when compressed, has a thickness equal to the solid flying plate usually used, the pressure pulse experienced by the fragment pack should be identical to that resulting from impact of a solid plate.

(C, gp 4) To test this theory a shot was fired in which 2 inches of foamed aluminum of about half the solid density were placed between the explosive and the fragment pack. The explosive pad was only 1/2 inch thick, and it and the aluminum foam were both 3 inches in diameter.

(C, gp 4) Figure 44 shows the fragment cloud generated by this shot. The velocity calculated from this record is  $0.10 \text{ mm}/\mu\text{sec} \pm 3 \text{ percent}$  if all but some of the extreme fragments are included. It thus appears that this is a quite satisfactory way of building such a shot. In addition to the construction ease, the reduction in diameter required (from 4 to 3 inches) makes possible a design with as much as half the weight appearing as fragments.

## 3. Lead-Interlayer Shot

(C, gp 4) Some calculations on a previous project<sup>11</sup> had suggested that under certain circumstances the insertion of a thin layer of lead between explosive and another material would result in a pressure pulse of lower amplitude and longer duration than that normally produced. Although the present case was quite different from that considered in the calculations, it seemed worthwhile to try one shot to test the effect of lead experimentally.



**CONFIDENTIAL**

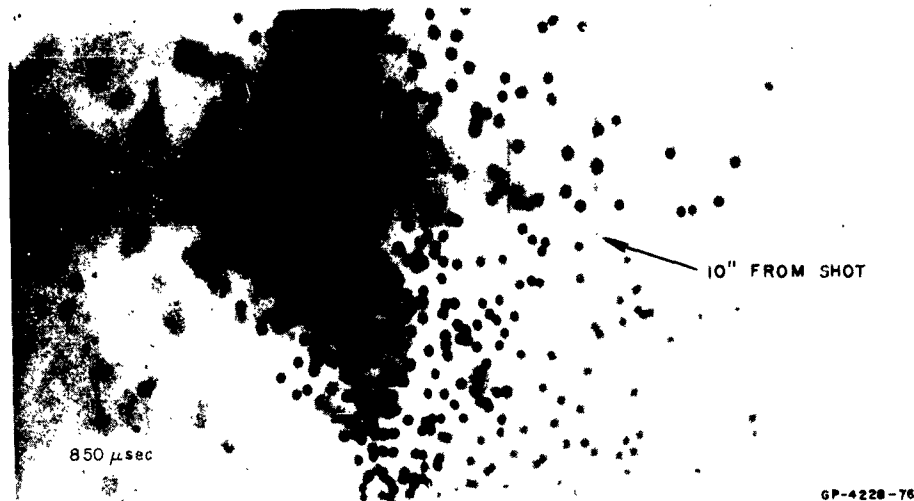


Figure 44 (U) Aluminum Foam Buffer Shot No. 10,270 (U).

(U) Lead foils 0.0165 inch thick were interleaved with 1/8-inch solid steel plates for this shot, and an additional foil was placed between this stack and a 3-inch-diameter x 3-inch-thick Comp B pad. This pad was initiated by a cap and booster on the side away from the plate stack.

(C, gp 4) Figure 45 shows the results of this shot and indicates that the lead does little to reduce the velocity variation normally present in such a design.

**CONFIDENTIAL**

CONFIDENTIAL

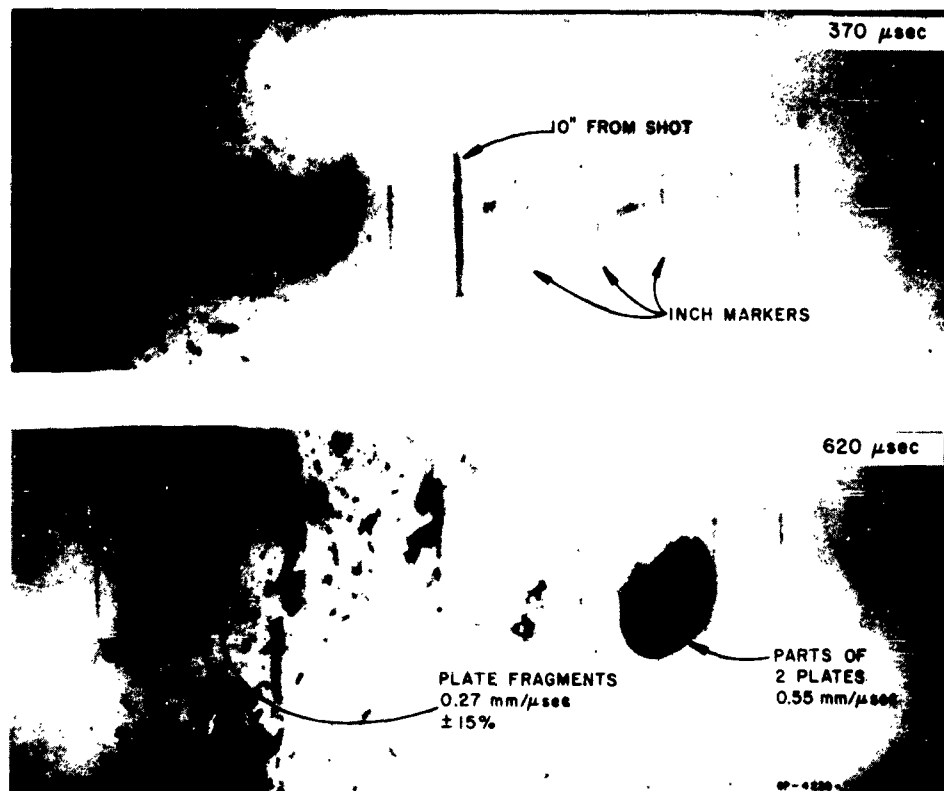


Figure 45 (U) Record from Shot Interlayered with 0.0165-Inch Lead, No. 10,237 (U).

CONFIDENTIAL

# CONFIDENTIAL

## 5. FRAGMENT TRAJECTORY DISTRIBUTION

(C, gp 4) R&D Exhibit No. ASQWR 61-11, which specified the work to be done under the contract initiating this project, stated that a satisfactory war-head should place "80 percent of the total number of pellets within a circular, hexagonal, or square pattern of uniform random distribution." When the contract was extended after the first year, the work to be done was then specified by R&D Exhibit No. ASQWR 61-11A which did not specify the distribution of pellets so exactly but merely said that the density distribution achieved in the fragment pattern is one of the "aspects of a design other than the velocity distribution which are to receive attention."

(C, gp 4) Four of the seven methods devised for velocity control were far enough advanced during the course of the project to justify testing.

(C, gp 4) Based upon these contractual statements and upon discussions with the technical monitoring personnel, the fragment trajectory distribution test program was developed with the primary aim of simply measuring the distributions produced by the various designs. Only when an obvious defect in the pattern appeared, usually a gap or hole where the density was much lower than that in the surroundings, was an effort made to modify the pattern.

### A. MEASUREMENT TECHNIQUE

(C, gp 4) Although some idea of the distribution of fragments in a cloud can be gained from the X-ray records, the best way to determine the distribution is to fire a shot against a large target and to record the density of hits as a function of position on the target.

(C, gp 4) Two targets were used during this project. The first, shown in Figure 46, was made of two 4- x 8-foot sheets of plywood painted white. After shooting, the target was divided into circles at radial intervals of 6 inches, and the hits in each segment were counted so that a plot of density vs radius could be prepared.

(C, gp 4) The major drawback of this first target was that unless the fragment cloud was quite compact, a significant fraction of the fragments missed the target and was not recorded. For this reason a second plywood target was built

**CONFIDENTIAL**

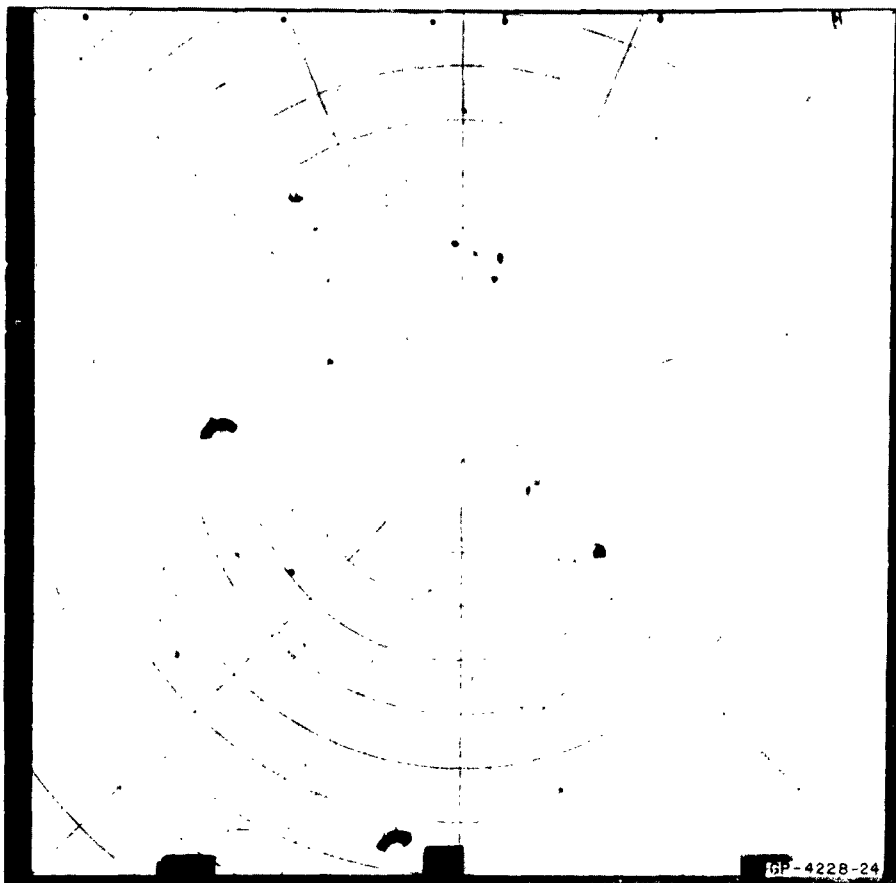


Figure 46 (U) First Fragment Distribution Target, Showing Hits from Shot No. 9607 (U).

which was twice as big, 16 x 16 feet. To make it as sturdy as possible two telephone poles supported the outer edges, and the framework between was arranged so that no beams were required in the central area where most fragment damage occurred.

(C, gp 4) All shots were fired about 13 feet from this target, except for one which was known to give a compact pattern and which was therefore moved back to 24 feet. This target survived shots with explosive weights up to 2-1/2 lbs at the 13-foot position, and suffered only minor damage with 11 lbs of explosive at the 24-foot position. These shots were fired from a mound of such

**CONFIDENTIAL**

# CONFIDENTIAL

a height that the firing point was roughly on a level with the target center. The exact firing position was pinpointed by finding the intersection of three strings of equal length attached at the midpoint of the bottom and two sides of the target.

(U) Since the shots were usually cylindrical and were to be fired with the axis horizontal, a wooden supporting cradle was mounted first. This cradle was placed on a wooden stand on the firing mound, and then a sighting tube with two sets of cross wires was placed in the shot position in the cradle in order to align the axis of the shot with the center of the target. Fresh sheets of white cardboard were stapled to the front of the target before firing to provide a clean surface for each test. After the shot, dark green nylon cords which were permanently attached at 1-foot intervals around the periphery of the target were stretched across the face of the target to form a grid of 1-foot squares. The target and grid were then photographed on Kodak High Contrast Copy Film (Pan), because this film is practically grainless and large blow ups could be made for future study of the impact pattern. Finally, the hits in each square were counted and recorded.

## 1. Data presentation

(C, gp 4) The best method for specifying and displaying the results of these experiments has received considerable study during this project. The raw data of hits per square can be converted into a graph of hits/ft<sup>2</sup> vs radius, such as that shown in Figure 47 for the target shown in Figure 46. This sort of graph presents information about only the radially symmetrical parts of the pattern, however. Misalignment of the aim point with target center will not show up. Likewise any nonsymmetry due, for example, to multipoint initiation of the explosive, will be hidden. To avoid these drawbacks the presentation method shown in Figure 48 was developed. In this figure the blackness of the dot pattern in each square corresponds to the density of the fragment hits in the corresponding square of the target. The particular shot shown was one of the three-point, backwards initiation shots, and there is some indication in the figure that the fragment trajectory pattern may have been slightly affected by this. Three arms of slightly higher hit-density appear to be going horizontally to the left and diagonally to the upper and lower right. This trend can hardly

# CONFIDENTIAL

**CONFIDENTIAL**

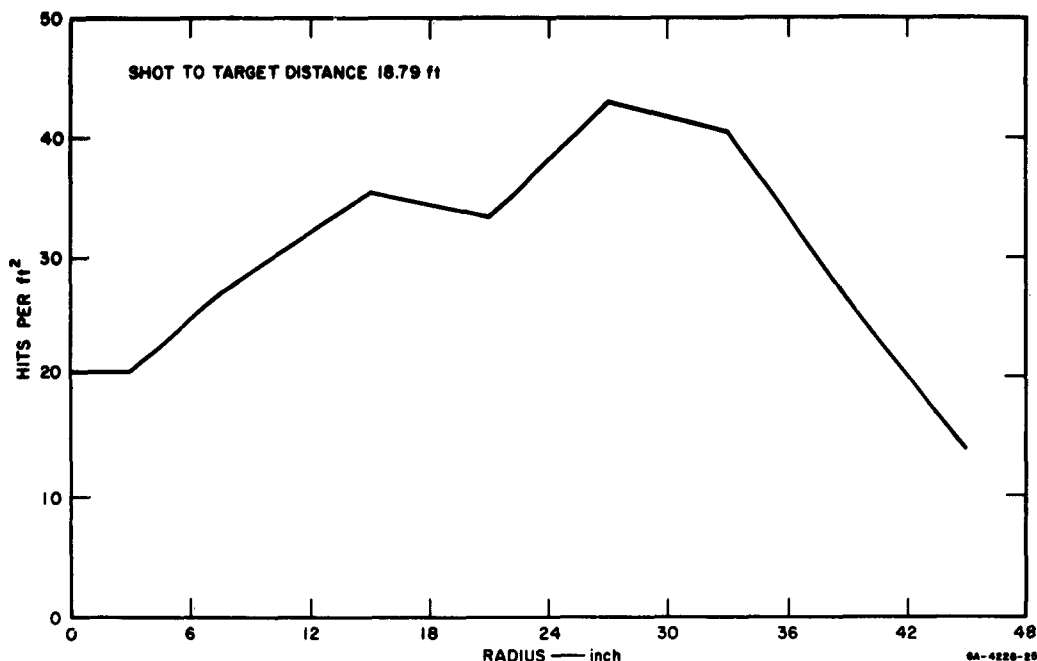
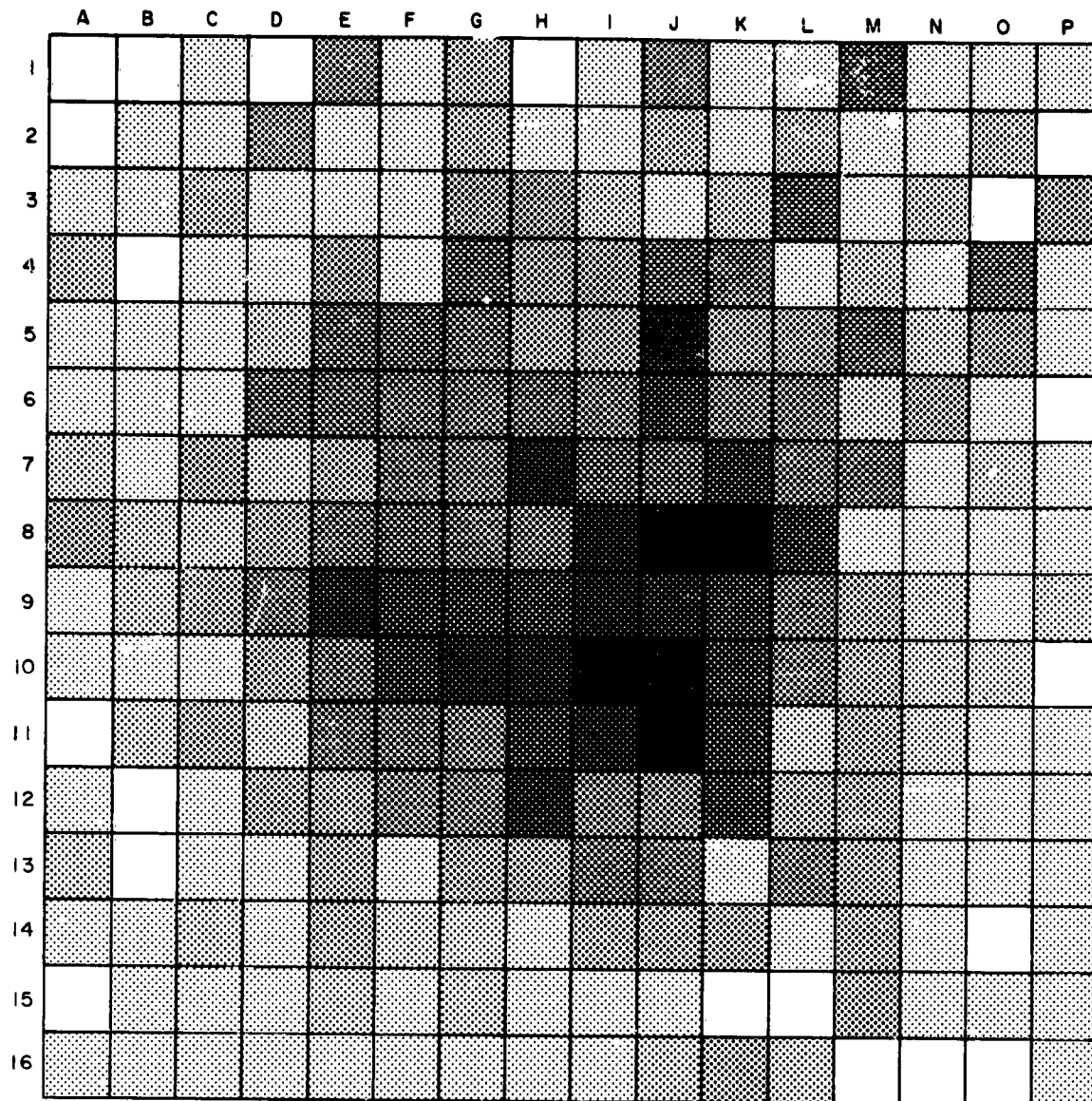


FIGURE 47 (U) FRAGMENT HIT DISTRIBUTION, SHOT NO. 9607 (U)  
[Figure and caption combined (U)]

be described as strong, however, since even in this sort of presentation it is hardly noticeable.

(U) Even the presentations of the type shown in Figure 48 still suffer from lack of space resolution. A single square on the large target often contained parts of two features of the pattern, and there were therefore averaged out in the data. The best method of presentation thus appears to be a verbal description of the pattern, supplemented by photographs where necessary.

**CONFIDENTIAL**



HITS/ft:	0	1-2	3	4-5	6-7	8-10	11-15	16-22	23-35	OVER 35
PATTERN:										

GA-4028-34A

FIGURE 48 (U) FRAGMENT HIT DISTRIBUTION, SHOT NO. 9771 (U)  
 [Figure and caption combined (U)]

# CONFIDENTIAL

## B. SUMMARY OF RESULTS

(U) Table 12 presents a summary of the 20 shots fired against the two targets during this project, and a short discussion of the performance of each method will be given here.

(C, gp 4) Most of the direct electrical backwards initiation shots show a fairly smooth distribution, peaked at the center and tapering gradually toward the extremities (Shots 9693, 9755, 9764, and 9771). No serious dips or holes show up in any of the shots fired to date. When three initiation points are used on 2-inch-thick explosive, the peak is somewhat flattened so that a uniform density is approximated out to about a 2-foot radius (Shots 9694 and 9756).

(C, gp 4) The basic behavior of the MDF backwards initiation designs was expected to be the same as that of similar electrical shots, and therefore identical shots were not fired. Most of the MDF shots were designed to try to concentrate the fragments more toward the center of the pattern. Figure 49 shows the design of the most unusual shot fired in this attempt. This peripherally initiated shot did give a smooth pattern, but it actually decreased the central-hit density. Pack insertions greater than 1/4 inch had some effect on central-hit density, but they always produced undesirable low density areas somewhere in the pattern.

(C, gp 4) All the steel flying plate shots show a fairly good distribution. When the steel is inserted all the way into the explosive there appears to be a slight dip at the center (Shots 9696 and 9806), but this is not serious and can apparently be eliminated by inserting the steel only halfway into the explosive (Shot 9920).

(C, gp 4) Aluminum flying plate shots gave more trouble. The ordinary design with central initiation results in a quite serious hole in the middle of the pattern (Shot 9607). This was rectified by going to peripheral initiation as shown in Figure 50, but then a fairly serious empty ring developed (Shot 9799). This also was finally eliminated by going to plane-wave initiation of the explosive (Shot 9934).

(C, gp 4) The NOL designs gave a very concentrated pattern with a sharp cutoff at a 3- to 4-foot radius. Within this cutoff there was some tendency for a

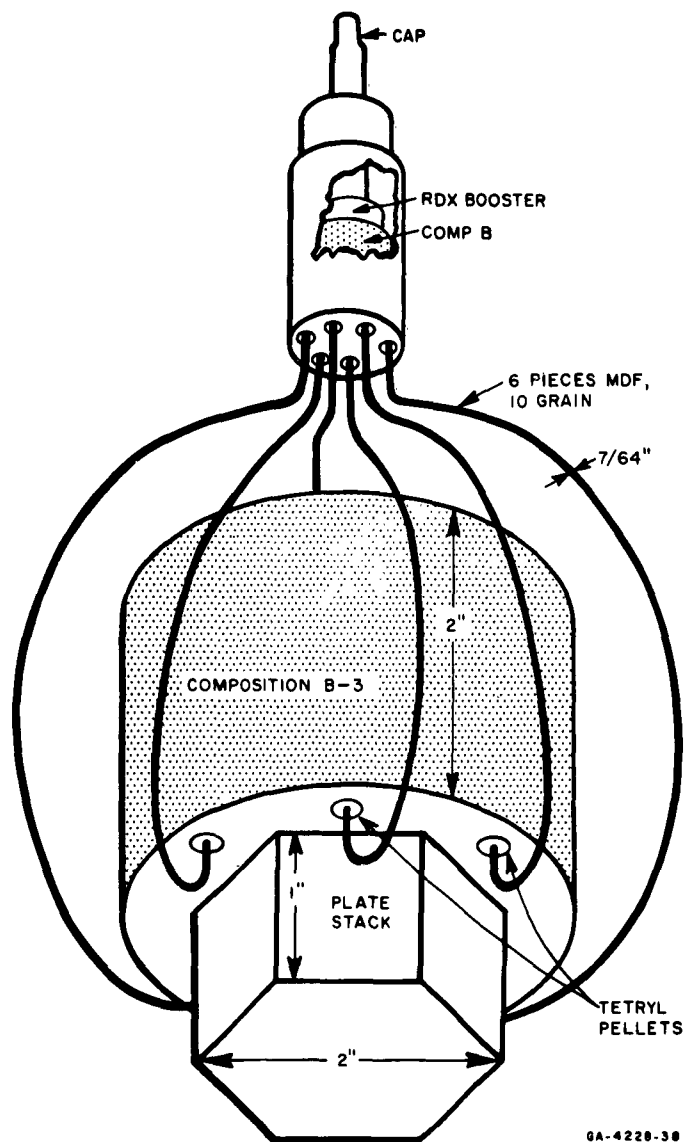
# CONFIDENTIAL



# CONFIDENTIAL

Table 12 (C, gp-4)  
FRAGMENT TRAJECTORY SHOTS (U)

Shot No.	Make Up (Explosive dimensions are thickness behind metal x diameter)	Target Distance Ft., In.	Target Size Ft.	Percent Recorded	Results
ELECTRICAL BACKWARDS INITIATION					
9693	2 x 3-inch HE, 1 point.	18 9-1/2	8 x 8	34	One bunch slightly off center, otherwise smooth. Center: -30/ft <sup>2</sup> ; 4 ft radius: -5/ft <sup>2</sup> .
9694	2 x 3-inch HE, 3 point.	12 6-1/2	8 x 8	53	Very smooth, fairly uniform to 2 ft radius. Center: 25-30/ft <sup>2</sup> ; 4 ft radius: -10/ft <sup>2</sup> .
9755	2 x 3-inch HE, 1 point.	12 11-1/2	16 x 16	64	One or two bunches near center otherwise smooth. Center: -30/ft <sup>2</sup> ; 10 ft radius: -1/ft <sup>2</sup> .
9756	2 x 3-inch HE, 3 point.	12 11-1/2	16 x 16	70	Slightly off center but uniform to 2 ft radius. Peak -20/ft <sup>2</sup> ; 10 ft radius -1/ft <sup>2</sup> .
9764	1 x 3-inch HE, 1 point	12 11	16 x 16	65	Smooth peaked pattern, well centered. Center: 25/ft <sup>2</sup> ; 10 ft radius: 1/ft <sup>2</sup> .
9771	1 x 3-inch HE, 3 point	12 6-1/2	16 x 16	68	Smooth peaked pattern, well centered. Center: -25/ft <sup>2</sup> ; 10 ft radius: 1/ft <sup>2</sup> .
MDF BACKWARDS INITIATION					
9836	2 x 3-inch HE, 6-point peripheral	12 8-1/2	16 x 16	57	Low density smooth pattern uniform to 2 ft. Center: -12/ft <sup>2</sup> ; 10 ft radius: -1.4 ft <sup>2</sup> .
9837	2 x 3-inch HE, 1-point, fragment pack inserted 1 inch.	13 3	16 x 16	78	Big bunch in center empty ring at 1.5 ft radius. Center: -110/ft <sup>2</sup> ; 10 ft radius: -0.5 ft <sup>2</sup> .
10,003	2 x 3-inch HE single point, fragment pack inserted 1/4-inch	12 8-1/4	16 x 16	71	Smooth peaked pattern well centered. Center: 30/ft <sup>2</sup> ; 10 ft radius: -1/ft <sup>2</sup> .
10,120	2 x 3-inch HE single point, fragment pack inserted 1/2 inch	12 7	16 x 16	77	Low density hole in center: 10/ft <sup>2</sup> . Maximum at 1-1/2 ft radius 27/ft <sup>2</sup> . Down to 1/ft <sup>2</sup> @ 10 ft radius.
FLYING PLATES					
9607	1 x 4-inch HE, 1-point initiation, 4-in-dia. A1 plate	18 9-1/2	8 x 8	92	Low density hole in center, 20/ft <sup>2</sup> . Maximum at 2 ft radius 40-50/ft <sup>2</sup> down to 10-15/ft <sup>2</sup> @ 4 ft.
9696	2 x 4-inch HE, 1 point initiation, 3-inch-dia. steel plate fully inserted	18 9-1/2	8 x 8	52	Quite uniform, smooth distribution. Center: 20-25/ft <sup>2</sup> ; 4 ft radius: 12/ft <sup>2</sup> .
9799	1 x 4-inch HE, peripheral initiation, 4-inch-dia. A1 plate.	12 7	16 x 16	79	Empty ring at 2.5 ft radius otherwise smooth. Center: 20-25/ft <sup>2</sup> ; 10 ft radius: -1.6/ft <sup>2</sup> .
9806	2 x 4-inch HE, 1 point initiation, 3-inch-dia. steel plate fully inserted	12 8-1/2	16 x 16	95	Rather spotty, closely grouped pattern. Center: 30-50/ft <sup>2</sup> ; down almost to zero at 8 ft radius.
9920	2 x 4-inch HE, 1 point initiation, 3-inch-dia. steel plate half inserted	12 9-3/4	16 x 16	84	Quite uniform, smooth distribution out to 4 ft. Center: 12-14/ft <sup>2</sup> ; 10 ft radius: -0.5/ft <sup>2</sup> .
9934	1 x 4-inch HE, Plane wave initiation 4-inch diameter A1 plate.	12 8-3/4	16 x 16	64	Quite uniform central region 10-15/ft <sup>2</sup> out to 3 ft off center spot of 20/ft <sup>2</sup> . Down to 2/ft <sup>2</sup> @ 10 ft radius.
NOL DESIGN					
10,398	Standard 3-inch design. Cylinder wall 1/8-inch, donut 1/4-inch. Hex pack of 1/8-inch balls approx. 0.84 x 2 inch	12 5	16 x 16	93	Very small pattern may have low density ring. Peak -100/ft <sup>2</sup> . 1 ft radius: -50/ft <sup>2</sup> . 2 ft radius: -60 then very rapid drop to 2.5 ft <sup>2</sup> @ 4 ft radius. See Figure 51.
10,447	2-inch design. Cylinder wall 1/8-inch. 0.220-inch inner explosive in a 1.00-inch gap. 1636 balls loose cast in epoxy in a 2-inch cylinder.	12 8	16 x 16	94	Fairly even center with high density ring @ 2 ft radius. Center: 40/ft <sup>2</sup> . Ring: -60/ft <sup>2</sup> . Rapid drop to 2/ft <sup>2</sup> @ 5 ft radius.
10,457	Standard 4-inch design. Cylinder wall 1/8-inch, donut, 1/4-inch. Hex pack of 1/8-inch balls approx 0.84 x 2 inches.	12 8	16 x 16	93	Very small pattern, fairly uniform at 70-100/ft <sup>2</sup> out to 1.8 ft; then very rapid drop to 1/ft <sup>2</sup> @ 4 ft radius.
10,458	Double scale of 3-inch design used for Shot 10,398. Hex pack of 1/4-inch balls approx. 1.68 x 4 inches	23 11	16 x 16	81	Pattern somewhat blotchy. Fairly uniform central area with 15-20/ft <sup>2</sup> out to 4.5 ft; then down to 1/ft <sup>2</sup> except for 8 bunches due to hex pack which have -10/ft <sup>2</sup> and cover -8 ft <sup>2</sup> each.



QA-4228-38

FIGURE 49 (U) SIX-POINT MDF PERIPHERAL BACKWARDS INITIATION (U)  
 [Figure and caption combined (U)]

CONFIDENTIAL

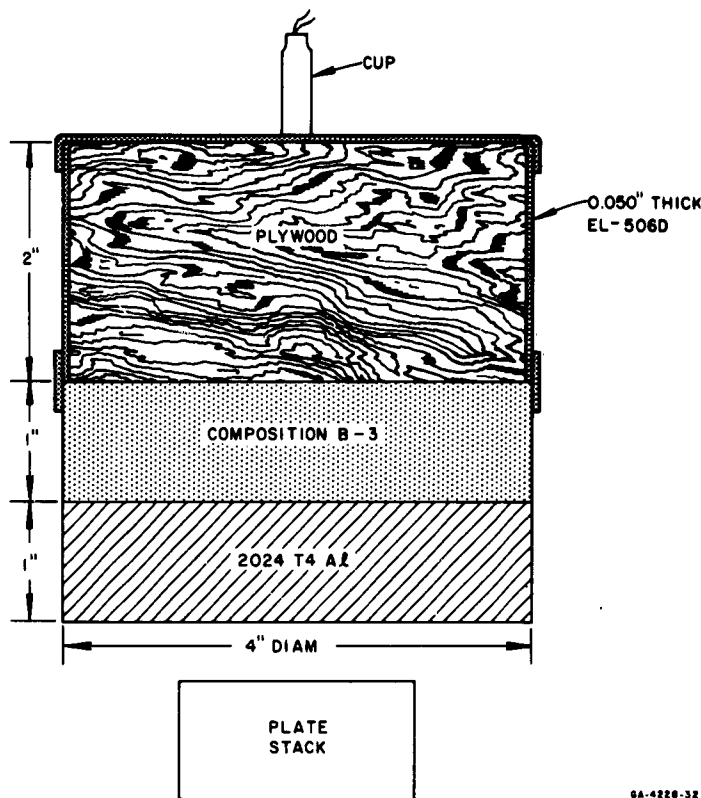


FIGURE 50 (U) PERIPHERAL INITIATION DESIGN, SHOT NO. 9799 (U)  
[Figure and caption combined (U)]

high density area at the very center and another high density ring just inside the cutoff radius. This variation was not too great, however, as can be seen in Figure 51, which is the pattern made by a 3-inch design (Shot 10,398).

(C, gp 4) One shot (10,458) was fired to check on the scaling laws for this process. It was a double-scale duplicate of the 3-inch design, and it was fired at about twice the distance from the target. The pattern it produced was quite well scaled from that of the 3-inch shot, both in pattern size and in hit density. The only major difference was that the hexagonal shape of the fragment pack seemed to have more effect on the pattern of the large shot than on that of the small, as is noted in Table 12. This effect will be eliminated when round fragment packs are used and is, therefore, unimportant.

CONFIDENTIAL

**CONFIDENTIAL**

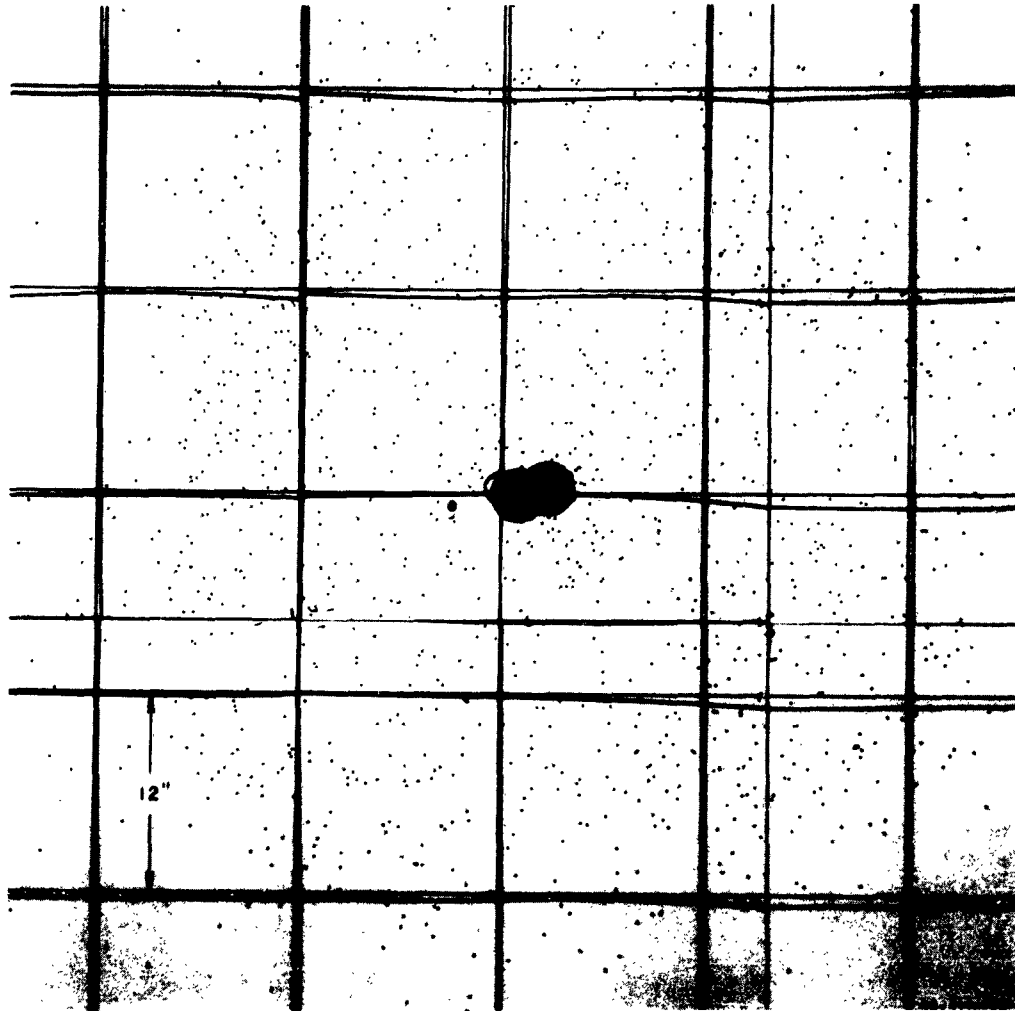


Figure 51 (U) Hit Pattern from 3-Inch NOL Design, Shot No. 10,398 (U).

**CONFIDENTIAL**

## 6. FRAGMENT DAMAGE

(U) Most of the fragments used during this project are well described by R&D Exhibit No. ASQWR 61-11, attached to the original contract as: pre-formed fragments "of at least the density of titanium" which might "be spheres, cubes, cylinders, etc. of a compact (length/diameter = 1) configuration." The fragment shapes actually used in the majority of the designs were cylinders and spheres, and the material was brass.

(C, gp 4) Such chunky fragments are quite resistant to damage during acceleration by explosives in any case, and, when accelerated by the low amplitude, long duration pressure pulses required for uniform velocity, can be expected to fare even better. For this reason, little extra effort was made to control such damage, and only when designs were fired which were expected to produce damage was recovery of the fragments made. The information gained is summarized below.

### A. FLYING PLATE SHOT

(C, gp 4) Figure 52 shows some fragments which were recovered from a shot in which an aluminum plate accelerated brass cylindrical fragments. These fragments can be divided into three distinct classes. On the left is a fragment which had one face heavily coated with aluminum, indicating that it was on the surface struck by the flying plate. The next fragment in the figure shows a curious type of damage that apparently is caused by some form of jetting between

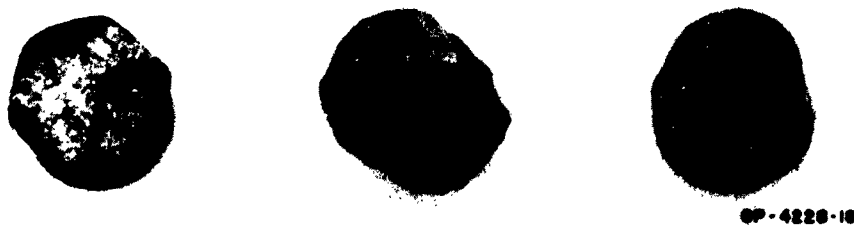


Figure 52 (U) Typical Fragments Recovered from Range Shot No. 9445 (U).

# CONFIDENTIAL

fragments of the adjacent layer. These layers were not exactly registered over each other, and portions of the outlines of three fragments can be seen on this one. The third example in Figure 52 shows an essentially undamaged fragment which apparently came from much farther inside the pack.

(C, gp 4) None of this damage is severe enough to warrant concern, especially since weapons of this type will probably be employed outside most of the earth's atmosphere so that the drag parameter of the fragments will not be important. Even the fragments nearest the flying plate were deformed only slightly. The most extreme deformation among those recovered in this group was a reduction in thickness by about 30 percent, and the other reductions averaged about 10 percent.

## B. FELTED METAL SHOT

(C, gp 4) Figures 37 and 40 showed recovered fragments from shots which employed felted nickel fragments. Although a detailed weight analysis of these has not been made, it appears that 90 to 95 percent of the original mass is present in these compressed fragments.

## C. HOLLOW SPHERE SHOTS

(C, gp 4) Investigations of the penetration of spaced plates by various hyper-velocity projectiles have shown that hollow metal spheres may perform much better in such applications than other shapes of projectile.<sup>12</sup> For this reason, two shots which accelerated hollow brass balls were fired during this project. One shot employed the MDF backwards initiation technique, and one the aluminum flying plate technique. The balls used were made of brass and were supplied by J. T. Healy and Son, Inc., of Attleboro, Mass. They were 0.122 inch in diameter and had a wall thickness of 0.020 inch. They were encapsulated in the usual way -- by stacking eight layers in a hexagonal mold and surrounding by ordinary epoxy resin. (Since these balls have no holes, no epoxy got inside.)

(C, gp 4) The velocities resulting from these shots have been covered in Section 4 of this report (see Tables 3 and 5). As expected, the velocities were significantly higher than those resulting from similar solid ball shots. To check on damage to the balls, the shots were fired into a water-filled barrel with 4 inches of dense styrofoam and 8 inches of light styrofoam above the water,

# CONFIDENTIAL

# CONFIDENTIAL

so that the balls could be recovered with as little additional damage as possible. Figure 53 shows typical selections of the recovered balls. The balls from the MDF shot appeared to be battered but still in fairly good condition, although many of them were punctured. The aluminum flying plate balls were in slightly better condition, with fewer punctures. Balls from both shots are probably still round enough to perform well, although additional hypervelocity tests would be required to confirm this.

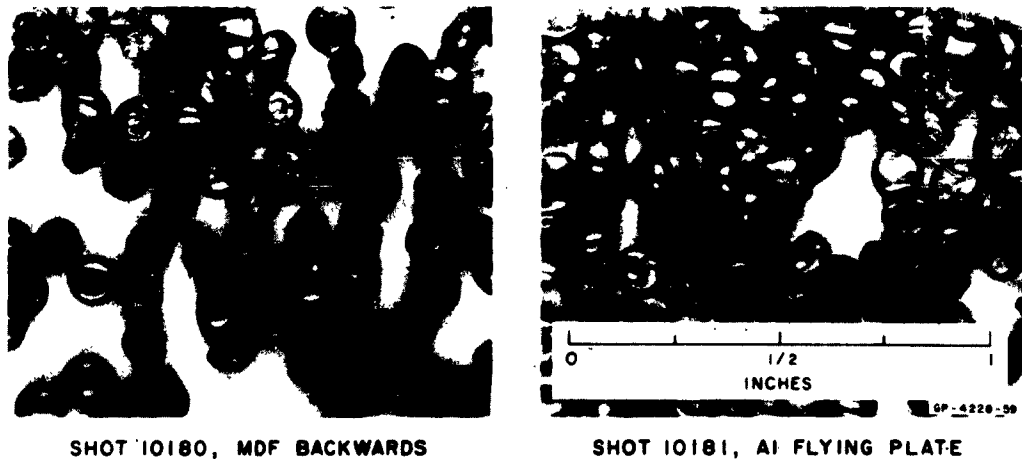


Figure 53 (C) Recovered Hollow Brass Balls (U).

# CONFIDENTIAL

## 7. CONCLUSIONS AND RECOMMENDATIONS

### A. CONCLUSIONS

(C, gp 4) The main conclusion of this study is that multiple layers of fragments can be projected by explosive systems so as to form clouds of the desired flat shape. The actual flatness produced is only one of a group of variables such as fragment velocity, mass percent in fragments, and many others. Although the seven basic methods discussed in this report are far from completely developed, certain characteristics of each have become clear so that an intelligent choice can be made for a particular end item. To aid in that choice, Table 13 has been prepared to point out the more glaring strengths and weaknesses of each.

Table 13 (C, gp 4)

COMPARISON OF VARIOUS DESIGNS (U)

	Velocity Uniformity	Velocity	Mass % in Frags.	Fuzing	Mechanical Structure	Explosive Structure
Steel Flying Plate	B	B	C	A	B	A
Aluminum Flying Plate	A	C	B	A	B	A
Electrical Backwards	B	B	A	C	A	C
MDF Backwards	B	B	A	A	A	C
Shock Backwards	B	B	B	A	B	B
Spaced Plates	C	A	A	A	A	A
Expanded Metal Fragments.	B	B	A	A	A	A
NOL Design	A	A	B	A	C	B

A = above average

B = average

C = below average



# CONFIDENTIAL

(U) In addition to the characteristics we have already discussed, the three included in Table 13 are:

1. fuzing complexity, primarily included so that the major drawback of the electrical backwards initiation design can be emphasized,
2. mechanical complexity, included as some measure of the construction cost of a warhead exclusive of the explosive and its fuzing,
3. explosive complexity, to emphasize the expense of complex explosive machining or high quality control on the explosive.

(U) Each design has been rated A, B, or C according to whether it is above average, average, or below average in the particular characteristic being considered.

## B. RECOMMENDATIONS

(U) Five of the eight methods listed in Table 13 have been developed about as far as they can be until the requirements of a definite end item are established. Those which might benefit from additional research are listed here, with a short outline of the work which might be done.

### 1. Shock initiated backwards initiation

(C, gp 4) A few shots should be fired with a charge of PBX of a reasonable shape in order to see if plates and fragments are accelerated uniformly as expected. If these shots are satisfactory, simplification of the aluminum plate acceleration system, possibly by use of foamed aluminum, should be accomplished.

### 2. Spaced plates

(C, gp 4) Additional shots with various buffer materials should probably be fired in order to determine the optimal design more accurately.

### 3. Expanded metal fragments

(C, gp 4) Larger scale shots than those fired here are required in this area and other metals should also be tested. The possibility of achieving higher velocities should also be investigated.

# CONFIDENTIAL

# CONFIDENTIAL

## Appendix I

### SIMPLE CALCULATIONS OF FLYING PLATE ACCELERATION

#### 1. INTRODUCTION

(U) In order to get a rough idea of the efficiency to be expected from a design using the flying plate method of acceleration, some calculations were performed based on a simple model of the processes taking place during acceleration. This appendix describes these calculations and tabulates the results.

#### 2. FLYING PLATE ACCELERATION OF THE FRAGMENT PACK

(C, gp 4) The operation of a warhead using the flying plate method can be divided into two parts: the acceleration of the flying plate by the explosive and the acceleration of the fragments by the flying plate. The end result is a cloud of fragments flying off at some velocity and carrying with them some amount of momentum, energy, etc. The actual amount of these quantities will vary with total warhead weight, flying plate weight, and fragment pack weight.

(C, gp 4) Considering first the acceleration of the fragments by the flying plate, we find that two simplifying assumptions about the process make it possible to get a great deal of information out of a few simple calculations:

(a) that both kinetic energy and momentum are conserved during the acceleration process, i. e. , it is a perfectly elastic collision; and (b) that a flying plate thickness exactly equal to the fragment pack thickness is sufficient to achieve the uniformity of fragment velocity desired from the warhead. With these assumptions we can then calculate the average fragment velocity,  $V_t$ , as a function of flying plate velocity,  $V_f$ , and the ratio of the density of the fragment material to the flying plate material,  $R$ .

(U) This gives us the equation.

$$V_t = \frac{2V_f}{R+1} \quad \text{or} \quad \frac{V_t}{V_f} = \frac{2}{R+1}.$$

Similarly the ratios of the momenta,  $M_t/M_f$ , the kinetic energy,  $E_t/E_f$ , and quantities proportional to the mass times the velocity to the 3/2 power,  $L_t/L_f$ , can be calculated as follows:

CONFIDENTIAL

$$\frac{M_t}{M_f} = \frac{2R}{R+1}$$

$$\frac{E_t}{E_f} = \frac{4R}{(R+1)^2}$$

$$\frac{L_t}{L_f} = \frac{2^{3/2} R}{(R+1)^{3/2}}$$

(C, gp 4) The quantity L is included here because it is the quantity which seems to determine the antipersonnel lethality capabilities of weapons and is therefore of interest for warheads designed for this purpose. The quantities which determine the effectiveness of a weapon against other kinds of targets are not known as well as those for human targets, but both energy and momentum are likely candidates.

(C, gp 4) Figure 54 shows these four ratios plotted as a function of R. As expected, all the curves pass through 1.0 when R is 1, since in that case the fragment pack bounces off the flying plate like a billiard ball and moves off with all the properties of the plate, leaving it sitting behind, stationary. At values of R less than 1, the fragment pack velocity is seen to be higher than the original flying plate velocity, but all the other values drop off because of the reduction in fragment mass necessary to achieve such values of R. With R greater than 1, the momentum curve rises above 1 due to the bouncing back of the light flying plate. The comparative constancy of the lethality ratio in this region is interesting and suggests that if this is the most important quantity for a particular application, R can be varied quite widely in order to optimize other aspects of the design without sacrificing lethality.

### 3. EXPLOSIVE ACCELERATION OF THE FLYING PLATE

(C, gp 4) Figure 54 can only be used to choose a value of R when the amount of energy, lethality, velocity, or momentum in the flying plate has already been fixed by other considerations. In the more general case, however, the amount of these quantities in the flying plate will vary as the flying plate and fragment materials are varied, because c/M, the mass ratio of explosive to flying plate, will usually change. In order to look into the more general case, therefore,

CONFIDENTIAL

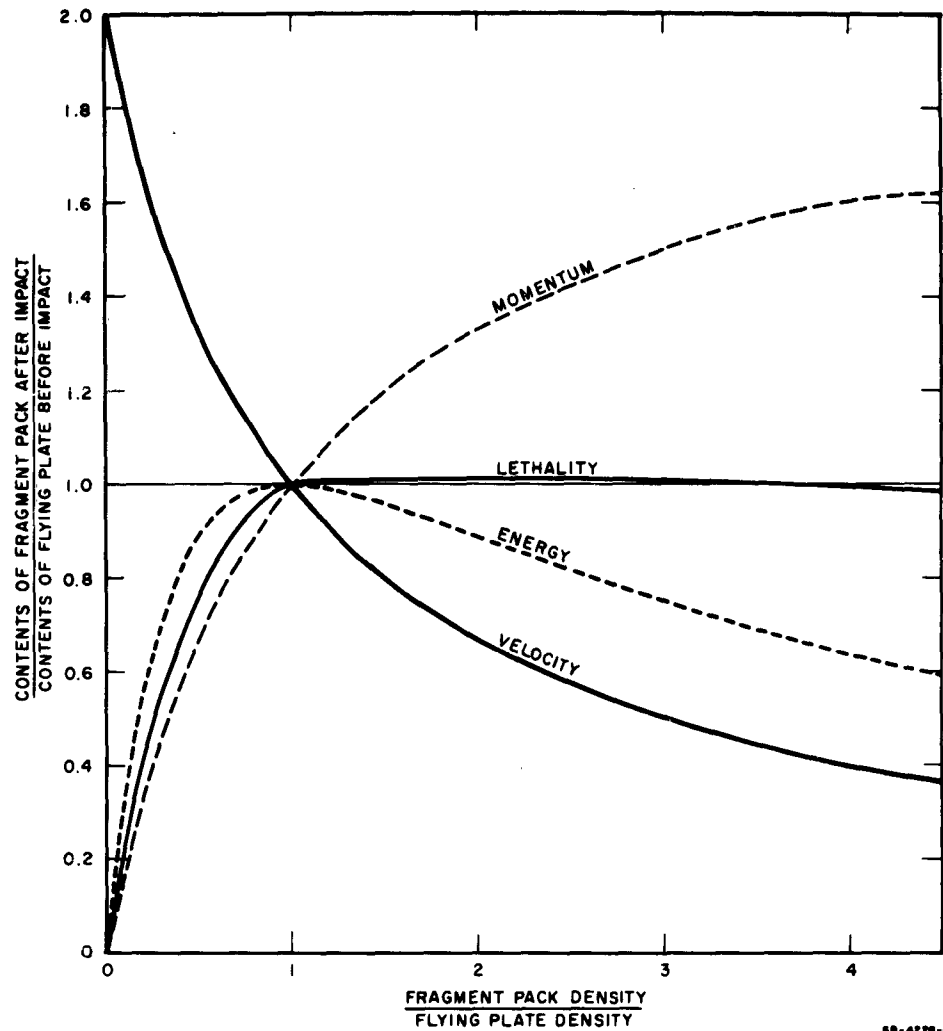


FIGURE 54 (C) TRANSFER RATIOS BETWEEN FLYING PLATE AND FRAGMENT PACK FOR VARIOUS DENSITY RATIOS (C)  
[Figure and caption combined (C, gp 4)]

the acceleration of the plate by the explosive must be considered as well as the effect of the total mass allowed for explosive, flying plate, and fragment pack.

(U) The equation used to calculate the flying plate velocity was the Gurney equation<sup>13</sup> for flat plates:

$$V_f = 2.68 \times 10^5 \sqrt{\frac{3 \frac{c}{M}}{5 + 4 \frac{M}{c} + \frac{c}{M}}}$$

where  $c$  is the explosive mass per unit area and  $M$  is the metal mass per unit area.

CONFIDENTIAL

# CONFIDENTIAL

## 4. CALCULATIONS AND RESULTS

(C, gp 4) In order to investigate the effects of the choice of various materials for flying plate and fragment pack as a function of total warhead weight, calculations were made of the fragment pack velocity, momentum, energy, and lethality for a warhead of unit fragment pack thickness, unit flying plate thickness, total weight ranging from 75 to 6.0 g/cm<sup>2</sup> of plate area, and plate fragment densities ranging from uranium's 18.7 down to aluminum's 2.7 g/cm<sup>3</sup>. A total of 490 combinations of plate density, fragment density, and total weight were considered. Tables 14 and 15 are an attempt to summarize the results of this calculation.

(C, gp 4) Table 15 presents the data in a way that is designed to answer the following questions: If I wish to accelerate fragments of a particular material, say, for example, copper, and I can have a warhead weighing a fixed total amount, for example, 30 g/cm<sup>2</sup>, what material should the flying plate be made of to get maximum velocity fragments? In the example cited the material is titanium and the velocity achieved is  $1.9 \times 10^5$  cm/sec, or about 6200 ft/sec.

(C, gp 4) It is interesting to note in Table 14 that the material chosen for the flying plate is always denser for the warheads of high total weight, and, therefore, these designs must give a velocity higher than if the flying plate were removed and the fragments were accelerated directly by the explosive. Thus in at least these cases there is a positive return in velocity, as well as in velocity constancy, obtained in exchange for the weight penalty imposed by the addition of the flying plate. However, when the total warhead mass drops to the point where the ratio of explosive mass to total metal mass is nearing 1.5, the optimal flying plate material becomes less dense than the fragments, and this gain is eliminated.

(C, gp 4) Table 15 presents the data to show, for each weight warhead, the combinations of fragment and flying plate densities which will yield the highest momentum, the highest energy, and the highest lethality.

(C, gp 4) There are two interesting observations to be made from an examination of Table 15. First, the diversity of materials contained in a single design is much less than that exhibited in Table 14; generally the materials of

# CONFIDENTIAL

# CONFIDENTIAL

Table 14 (C, gp 4)

## DESIGNS FOR MAXIMUM VELOCITY FOR VARIOUS FRAGMENT MATERIALS AND TOTAL WEIGHT (U)

Fragment		War-head	Optimum Flyer		Velocity cm/sec	Final Fragment			Mass Ratios, Charge to		
Material	Density gm/cm <sup>3</sup>	Weight gm/cm <sup>3</sup>	Material	Density gm/cm <sup>3</sup>					Flyer	Frag	Flyer
Uranium	18.7	75	--	15	$2.3 \times 10^5$				2.8	2.2	1.2
		60	Lead	11.3	$1.9 \times 10^5$				2.7	1.6	1.0
		45	Steel	7.8	$1.4 \times 10^5$				2.4	1.0	.70
		30	Titanium	4.5	$7.3 \times 10^4$				1.5	.38	.29
		25	Aluminum	2.7	$4.4 \times 10^4$				1.3	.19	.15
		15	--	15	$2.6 \times 10^5$				3.0	3.0	1.5
--	15	60	Lead	11.3	$2.3 \times 10^5$				3.0	2.3	1.3
		45	Copper	8.9	$1.8 \times 10^5$				2.4	1.4	.88
		30	Titanium	4.5	$1.1 \times 10^5$				2.3	.70	.54
		25	Titanium	4.5	$7.7 \times 10^4$				1.2	.37	.28
		20	Aluminum	2.7	$4.0 \times 10^4$				.85	.015	.013
		15	Aluminum	2.7	$2.7 \times 10^4$						
Lead	11.3	75	Lead	11.3	$3.1 \times 10^5$				3.2	4.2	1.8
		60	Lead	11.3	$2.7 \times 10^5$				3.3	3.3	1.7
		45	Copper	8.9	$2.2 \times 10^5$				2.8	2.2	1.2
		30	Titanium	4.5	$1.5 \times 10^5$				3.2	1.3	.90
		25	Titanium	4.5	$1.3 \times 10^5$				2.0	.81	.58
		20	Aluminum	2.7	$8.9 \times 10^4$				2.2	.53	.43
Copper	8.9	15	Aluminum	2.7	$2.7 \times 10^4$				.37	.089	.071
		75	Lead	11.3	$3.5 \times 10^5$				4.8	6.1	2.7
		60	Lead	11.3	$3.1 \times 10^5$				3.5	4.5	2.0
		45	Copper	8.9	$2.7 \times 10^5$				3.1	3.1	1.5
		30	Titanium	4.5	$1.9 \times 10^5$				3.7	1.9	1.2
		25	Titanium	4.5	$1.6 \times 10^5$				2.6	1.3	.86
Steel	7.8	20	Titanium	4.5	$1.2 \times 10^5$				1.5	.74	.49
		15	Aluminum	2.7	$7.9 \times 10^4$				1.3	.38	.29
		12	Aluminum	2.7	$1.5 \times 10^4$				.15	.045	.035
		75	Lead	11.3	$3.7 \times 10^5$				4.9	7.1	2.9
		60	Lead	11.3	$3.4 \times 10^5$				3.6	5.2	2.1
		45	Steel	7.8	$2.9 \times 10^5$				3.8	3.8	1.9
Titanium	4.5	30	Titanium	4.5	$2.1 \times 10^5$				3.9	2.3	1.4
		25	Titanium	4.5	$1.9 \times 10^5$				2.8	1.6	1.0
		20	Titanium	4.5	$1.5 \times 10^5$				1.7	.99	.63
		15	Aluminum	2.7	$1.0 \times 10^5$				1.7	.58	.43
		12	Aluminum	2.7	$5.0 \times 10^4$				.56	.19	.14
		7.5	Aluminum	2.7	$1.8 \times 10^4$				.11	.067	.042
Aluminum	2.7	75	Copper	8.9	$4.6 \times 10^5$				6.9	14	4.6
		60	Copper	8.9	$4.3 \times 10^5$				5.2	10	3.5
		45	Steel	7.8	$3.8 \times 10^5$				4.2	7.3	2.7
		30	Titanium	4.5	$3.1 \times 10^5$				4.7	4.7	2.3
		25	Titanium	4.5	$2.8 \times 10^5$				3.6	3.6	1.8
		20	Titanium	4.5	$2.4 \times 10^5$				2.4	2.4	1.2
Aluminum	2.7	15	Aluminum	2.7	$1.9 \times 10^5$				2.9	1.7	1.1
		12	Aluminum	2.7	$1.5 \times 10^5$				1.8	1.1	.66
		7.5	Aluminum	2.7	$1.8 \times 10^4$				.11	.067	.042
		75	Steel	7.8	$5.3 \times 10^5$				8.3	24	6.1
		60	Steel	7.8	$5.0 \times 10^5$				6.3	18	4.7
		45	Titanium	4.5	$4.5 \times 10^5$				8.4	14	5.2
Aluminum	2.7	30	Titanium	4.5	$4.0 \times 10^5$				5.1	8.4	3.2
		25	Titanium	4.5	$3.7 \times 10^5$				4.0	6.6	2.5
		20	Aluminum	2.7	$3.2 \times 10^5$				5.4	5.4	2.7
		15	Aluminum	2.7	$2.8 \times 10^5$				3.6	3.6	1.8
		12	Aluminum	2.7	$2.4 \times 10^5$				2.4	2.4	1.2
		7.5	Aluminum	2.7	$1.2 \times 10^5$				.78	.78	.39
Aluminum	2.7	6.0	Aluminum	2.7	$4.5 \times 10^4$				.22	.22	.11

# CONFIDENTIAL

Table 15 (C, gp 4)

**DESIGNS FOR VARIOUS TOTAL WARHEAD WEIGHTS WHICH MAXIMIZE  
MOMENTUM, ENERGY, OR LETHALITY (C)**

Fragment		War-Head	Optimum Flyer		Final Fragment				Mass Ratios, Charge to:		
Material	Density gm/cm <sup>3</sup>	Weight gm/cm <sup>2</sup>	Material	Density gm/cm <sup>3</sup>	Velocity cm/sec	Momentum gm <sup>2</sup> /cm <sup>2</sup> ·sec	Energy gm <sup>2</sup> /cm <sup>2</sup> ·sec <sup>2</sup>	Lethality gm <sup>3</sup> /cm <sup>2</sup> ·sec <sup>3</sup>	Flyer	Frag	Total
Uranium	18.7	75	--	15	2.3x10 <sup>8</sup>	4.2x10 <sup>6</sup>	4.8x10 <sup>11</sup>	2.0x10 <sup>9</sup>	2.8	2.2	1.2
Copper	8.9	75	Lead	11.3	3.5x10 <sup>8</sup>	3.1x10 <sup>6</sup>	5.5x10 <sup>11</sup>	1.8x10 <sup>9</sup>	4.8	6.1	2.7
--	15	75	--	15	2.6x10 <sup>5</sup>	3.9x10 <sup>6</sup>	5.2x10 <sup>11</sup>	2.0x10 <sup>9</sup>	3.0	3.0	1.5
Uranium	18.7	60	Lead	11.3	1.9x10 <sup>5</sup>	3.5x10 <sup>6</sup>	3.3x10 <sup>11</sup>	1.5x10 <sup>9</sup>	2.7	1.6	1.0
Steel	7.8	60	Lead	11.3	3.4x10 <sup>5</sup>	2.6x10 <sup>6</sup>	4.4x10 <sup>11</sup>	1.5x10 <sup>9</sup>	3.6	5.2	2.1
Lead	11.3	60	Lead	11.3	2.7x10 <sup>5</sup>	3.1x10 <sup>6</sup>	4.2x10 <sup>11</sup>	1.6x10 <sup>9</sup>	3.3	3.3	1.7
--	15	45	Copper	11.3	1.8x10 <sup>5</sup>	2.7x10 <sup>6</sup>	2.3x10 <sup>11</sup>	1.1x10 <sup>9</sup>	2.4	1.4	.88
Titanium	4.5	45	Steel	7.8	3.8x10 <sup>5</sup>	1.7x10 <sup>6</sup>	3.2x10 <sup>11</sup>	1.0x10 <sup>9</sup>	4.2	7.3	2.7
Copper	8.9	4.5	Copper	8.9	2.6x10 <sup>5</sup>	2.4x10 <sup>6</sup>	3.1x10 <sup>11</sup>	1.2x10 <sup>9</sup>	3.1	3.1	1.5
Lead	11.3	30	Titanium	4.5	1.5x10 <sup>5</sup>	1.7x10 <sup>6</sup>	1.3x10 <sup>11</sup>	6.8x10 <sup>8</sup>	3.2	1.3	.90
Titanium	4.5	30	Titanium	4.5	3.1x10 <sup>5</sup>	1.4x10 <sup>6</sup>	2.1x10 <sup>11</sup>	7.7x10 <sup>8</sup>	4.7	4.7	2.3
Copper	8.9	25	Titanium	4.5	1.7x10 <sup>5</sup>	1.5x10 <sup>6</sup>	1.2x10 <sup>11</sup>	6.0x10 <sup>8</sup>	3.7	1.9	1.2
Aluminum	2.7	25	Titanium	4.5	3.7x10 <sup>5</sup>	9.9x10 <sup>5</sup>	1.8x10 <sup>11</sup>	6.0x10 <sup>8</sup>	4.0	6.6	2.5
Titanium	4.5	25	Titanium	4.5	2.8x10 <sup>5</sup>	1.2x10 <sup>6</sup>	1.8x10 <sup>11</sup>	6.7x10 <sup>8</sup>	3.6	3.6	1.8
Steel	7.8	20	Titanium	4.5	1.5x10 <sup>5</sup>	1.2x10 <sup>6</sup>	8.5x10 <sup>10</sup>	4.4x10 <sup>8</sup>	1.7	.99	.63
Aluminum	2.7	20	Aluminum	2.7	3.2x10 <sup>5</sup>	8.7x10 <sup>5</sup>	1.4x10 <sup>11</sup>	5.0x10 <sup>8</sup>	5.4	5.4	2.7
Titanium	4.5	20	Titanium	4.5	2.4x10 <sup>5</sup>	1.1x10 <sup>6</sup>	1.3x10 <sup>11</sup>	5.3x10 <sup>8</sup>	2.4	2.4	1.2
Titanium	4.5	15	Aluminum	2.7	1.9x10 <sup>5</sup>	8.7x10 <sup>5</sup>	8.5x10 <sup>10</sup>	3.9x10 <sup>8</sup>	2.9	1.7	1.1
Aluminum	2.7	15	Aluminum	2.7	2.8x10 <sup>5</sup>	7.6x10 <sup>5</sup>	1.1x10 <sup>11</sup>	4.0x10 <sup>8</sup>	5.4	5.4	2.7
Titanium	4.5	12	Aluminum	2.7	1.5x10 <sup>5</sup>	7.0x10 <sup>5</sup>	5.4x10 <sup>10</sup>	2.7x10 <sup>8</sup>	1.8	1.1	.66
Aluminum	2.7	12	Aluminum	2.7	2.4x10 <sup>5</sup>	6.5x10 <sup>5</sup>	7.8x10 <sup>10</sup>	3.2x10 <sup>8</sup>	2.4	2.4	1.2
Aluminum	2.7	7.5	Aluminum	2.7	1.2x10 <sup>5</sup>	3.3x10 <sup>5</sup>	2.1x10 <sup>10</sup>	1.2x10 <sup>8</sup>	.78	.78	.39
Aluminum	2.7	6.0	Aluminum	2.7	4.5x10 <sup>4</sup>	1.2x10 <sup>5</sup>	2.8x10 <sup>9</sup>	2.6x10 <sup>7</sup>	.22	.22	.11

# CONFIDENTIAL

# CONFIDENTIAL

flying plate and fragment pack are either identical or, at most, two steps apart in the density series. Second, the chosen values of  $c/M$  are all quite high, falling consistently below 1.0 only when the total warhead weight is reduced drastically. The optimal  $c/M$  for maximum momentum seems to be about 1.0; that for energy, around 2.0 to 2.5; and that for lethality, about 1.5 to 2.0.

(C, gp 4) Full use of the information contained in Tables 14 and 15 cannot really be made until a more nearly final warhead design is being determined. However, the tables can give suggestions about the design of the experiments to perform. At the time these calculations were made, aluminum and steel flying plates were being studied. Two values of  $c/M$  were being used for each material: for the aluminum, 0.31 and 0.92; and for the steel, 0.21 and 0.42. Obviously these values are much lower than the optimum except for very light warheads, and for such warheads steel is not an appropriate material. Therefore, the shots with aluminum were continued, directed toward the goal of an aluminum-steel or aluminum-copper warhead yielding massive fragments at a low velocity. The steel experiments were changed so as to have a much higher  $c/M$ , directed toward the goal of a steel-on-steel warhead similar to one of the optimal designs in Table 15 of about  $45 \text{ g/cm}^2$  weight.

(C, gp 4) Various refinements could be made in the calculations which have been discussed in this section. For example, the different shock and rarefaction velocities of the various materials considered might be taken into account since these affect the thicknesses of flying plate required for uniform acceleration of the fragments. Also, the kinetic energy loss during fragment acceleration might be estimated so that more realistic velocities would be calculated. However, since the primary aim of the calculations has been to give quite general guidelines, and the relative performance of the various designs is probably quite accurately described by the calculations in their present form, this additional work did not appear justified.

# CONFIDENTIAL



# CONFIDENTIAL

## Appendix II Q CODE CALCULATIONS (U)

(C, gp 4) In connection with other projects at these Laboratories, methods have been developed for making accurate and detailed calculations of the processes taking place during and after impact of a flying plate. These methods reached a stage during this project where it appeared worthwhile to employ them, particularly as the behavior predicted by the calculations has several features which may affect quite seriously the uniformity of fragment velocity achieved by the flying plate warhead designs being considered.

(U) By way of introduction, the description of the computer program and some of the early results achieved in a calculation of aluminum flying plate impact on a thick aluminum target will be reprinted here, copied from a report dated January 21, 1963, by John O. Erkman to the Defense Atomic Support Agency.

(U) "The primary reason for initiating this project was concern over the fact that rigidity was not being taken into account when high pressure events in solids were treated theoretically. That is to say, it was assumed that solids behaved as fluids, and the hydrodynamic theory was applied. Work on this project as well as other projects in these Laboratories indicates that hydrodynamics cannot be applied with accuracy; for example, to calculate the flow induced in an aluminum target when it is struck by an aluminum plate having a velocity of from 0.1 to 0.2 cm/ $\mu$ sec. For this reason, some attempt has been made to use an elastic-plastic model in the calculations.

(U) "Some of the work performed on a related project by Curran was given in an appendix of an earlier report. Curran found that he could obtain reasonable agreement between the results of his experiments and theoretical results if he used the elastic-plastic theory. He found it necessary to assume a variation in the tensile yield strength from 2.5 kbar at atmospheric pressure to 12.5 kbar at a pressure of 175 kbar. This early work used the method of characteristics, and the calculations were done by hand.

(U) "Elastoplastic problems can be solved with some degree of success by the use of a computing scheme which represents the differential equations for supersonic flow by finite difference equations. This scheme was developed by von Neumann and Richtmyer, and is often called the artificial viscosity method or the 'Q method.' Results of this method are seldom as satisfactory as those obtained from the application of the method of characteristics because shock fronts are smeared over a finite distance. However, the method is easily adapted to a wide variety of problems, so

# CONFIDENTIAL

that its use has become popular. As originally applied, the Q method was strictly hydrodynamic, i. e. , a hydrodynamic equation of state was used. A code has now been written which employs the Q method and which provides for elastic-plastic flow for the case of the impact of a flying plate on a target.\* This code can be used on the Burroughs 220 computer or on the IBM 7090 computer. An early version of the code used the stress-strain relation assumed by Morland. Results of this code did not fit the data from the plate-slap experiments; the attenuation of the wave proceeded too slowly. This result is in agreement with the findings of Curran. The present version of the code allows the yield strength, Y, to vary in the manner proposed by Curran; i. e. ,

$$Y = 0.0025 + 0.0055 P,$$

where Y and P are in megabars. Poisson's ratio,  $\gamma$ , is assumed to be constant, and Young's modulus is represented by:

$$E = -3(1-2\nu) V \frac{dP}{dV}$$

where the pressure P and the specific volume V are related by what Morland calls a hydrostatic compression formula. In the present work, the Hugoniot is used for relating these variables. Because the bulk modulus, K, and the shear modulus,  $\mu$ , can be expressed in terms of  $\nu$  and E, they do not appear explicitly in the equations on which the code is based.

(U) "Some of the results given by the elastic-plastic code are indicated in Figure 55 where the pressure is shown as a function of the distance into the target. Distance is given by the Lagrangian value; i. e. , the original coordinate of the mass cell, which simplifies the plotting of the data. In Figure 55, results are shown for the case of an aluminum plate 0.3 cm thick and having a velocity of 0.2 cm/ $\mu$ sec colliding with an aluminum target. Initially, the wave is essentially flat across the top -- see the curve labeled 0.3  $\mu$ sec. At 0.77  $\mu$ sec, the elastic relief wave is observed and has an amplitude of about 50 kbar. This elastic relief wave proceeds to overtake the shock front, so that at 3.09  $\mu$ sec the wave is almost triangular. The elastic effects continue, however, as evidenced by the nearly flat part of the wave at 3.9  $\mu$ sec.

(U) "Figure 56 gives the particle velocity as a function of the distance at the same times used in Figure 55. Note that the velocity over much of the pulse is 0.1 cm/ $\mu$ sec when the time is 0.77  $\mu$ sec. At 2.3  $\mu$ sec, the particle velocity of almost all mass cells has been reduced to 0.08 cm/ $\mu$ sec. This is the rapid attenuation of velocity observed in the flying plate experiments. If it is assumed that a free surface is interposed; for example, at  $x = 2.3$  in Figure 56, the free surface would acquire a velocity of about 0.2 cm/ $\mu$ sec,

---

\* (U) This code was written by the author in the course of the research under Contract AF 49(638)-1086 (SRI Project PGU-3731). It is reported here because of its pertinence to the present work.

CONFIDENTIAL

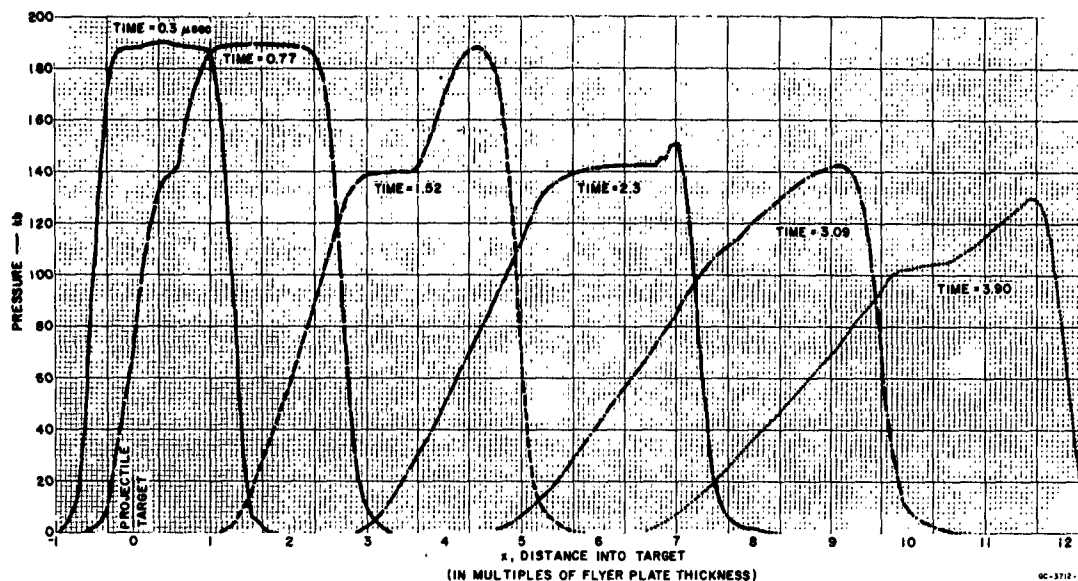


Figure 55 (U) Pressure vs Distance for Shock Wave Induced in an Aluminum Target by the Impact of an Aluminum Plate (Space Coordinates are Lagrangian) (U).

or twice the particle velocity. In this way a plot of the free surface velocity of the target versus the original location of the free surface can be prepared. This plot is shown in Figure 57 which also shows the experimental and theoretical work given by Curran. After making allowance for the different plate velocity used in the new calculations, and with the experimental results, is encouraging."

(C, gp 4) One of the interesting features of these calculations from the point of view of this project is shown in Figure 55. Here it is seen that the pressure pulse in the target material, which would be the fragment pack in our case, is far from the flat-topped square wave that has been assumed up to now. For example, the fragment layer velocity resulting from a wave shape such as that at 1.52  $\mu\text{sec}$  might be expected to vary by over 20 percent depending on the location of the layer. At 2.3  $\mu\text{sec}$ , on the other hand, the wave is much flatter and would probably give much better results.

(U) Another reason for attempting to calculate behavior in this way is that it should be accurate enough to give reliable predictions of shot perform-

CONFIDENTIAL

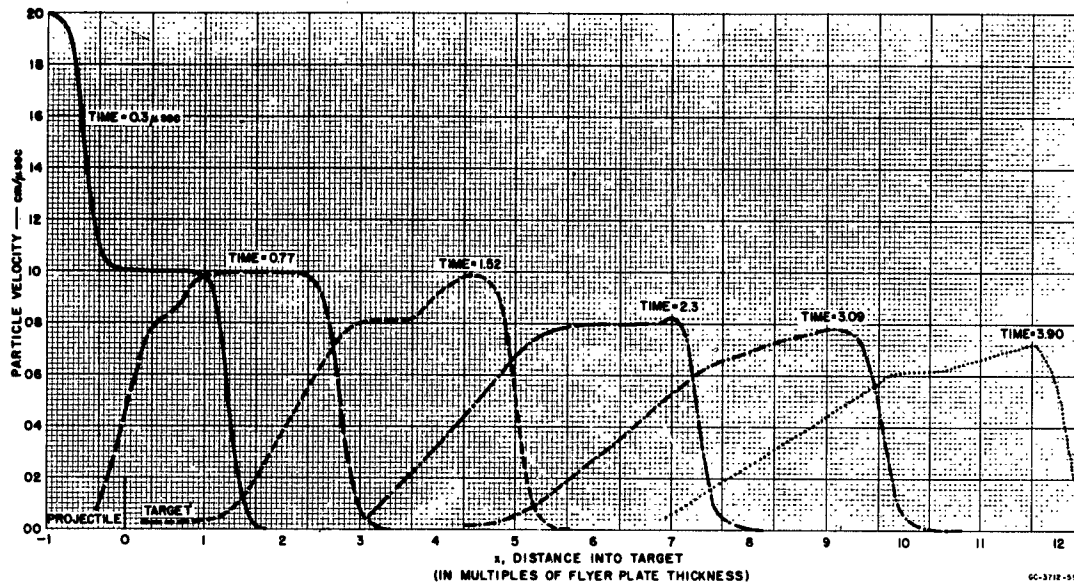


Figure 56 (U) Particle Velocity vs Distance for Shock Wave Induced in an Aluminum Target by the Impact of an Aluminum Plate (Space Coordinates are Lagrangian) (U).

ance without the necessity of firing a shot. Thus various modifications of the design could be made, and the results could be evaluated without the cost of experimentation.

(U) As finally developed, the computer program could describe the processes taking place in a flying plate and in a stack of thinner target plates during the several microseconds immediately after impact of one upon the other. The flying plate was assumed to be shock free before impact and the joints between the plates were assumed to have zero strength.

(U) Figure 58 shows several graphs of pressure and particle velocity which were produced by the computer from the results of calculations of an aluminum flying plate striking a stack of steel plates. As in the other figures in this appendix, the space coordinates are Lagrangian, and, in this case, since steel is more dense than aluminum, the steel plate stack is divided into a larger number of cells than the aluminum flying plate even though they are both 1 inch thick.

(U) The final velocities given to the various parts of this experiment are shown in the last graph. This shows that in this hypothetical experiment the aluminum did bounce off the steel, as was predicted by the simple calculations discussed in Appendix I. The steel plates are moving off at  $0.3 \text{ mm}/\mu\text{sec}$ , except for the last three which are going somewhat slower than this. The average steel plate velocity is about  $0.25 \text{ mm}/\mu\text{sec}$ , which agrees quite well with the  $0.26 \text{ mm}/\mu\text{sec}$  predicted by the simple theory.

(U) The reason for the lower velocities of the last three plates is easy to see. When the two shocks which originate at the impact plane move out, reflect as rarefaction waves, and meet again, their meeting place is not at the impact plane but inside the steel plate stack. Thus the last plates of the stack are slowed down by the rarefaction from the aluminum side, instead of being accelerated by the other rarefaction as all the other plates were.

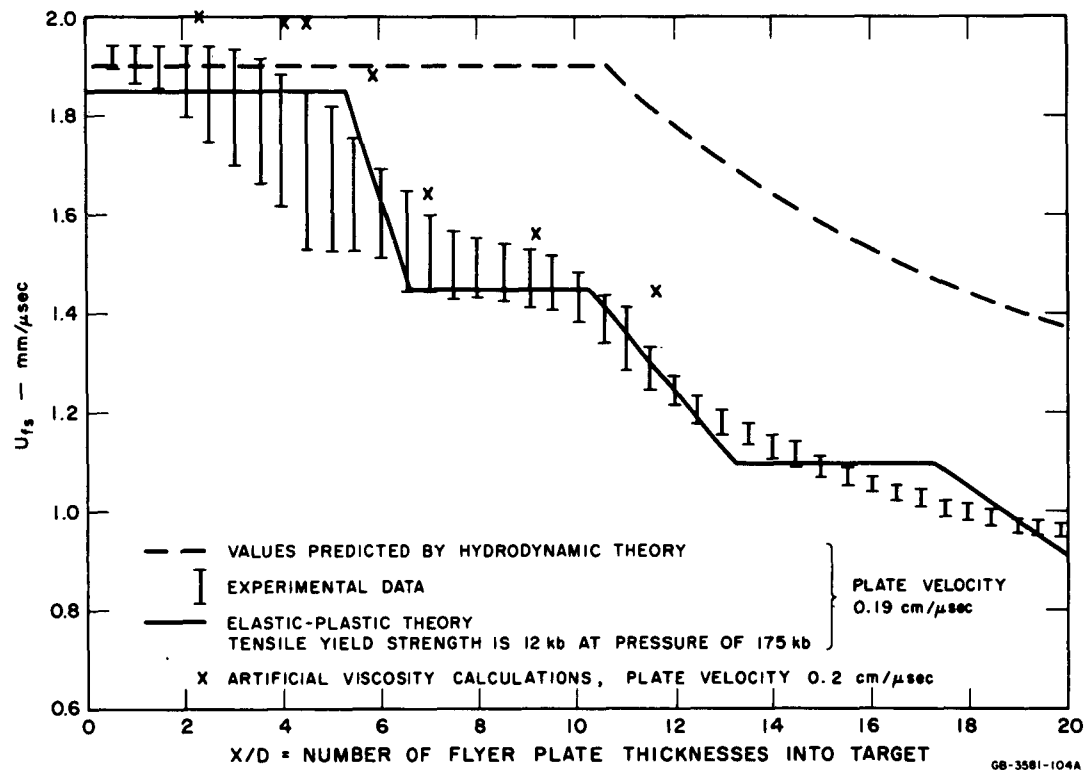


FIGURE 57 (U) FREE-SURFACE VELOCITY vs DISTANCE INTO TARGET (U)  
[Figure and caption combined (U)]

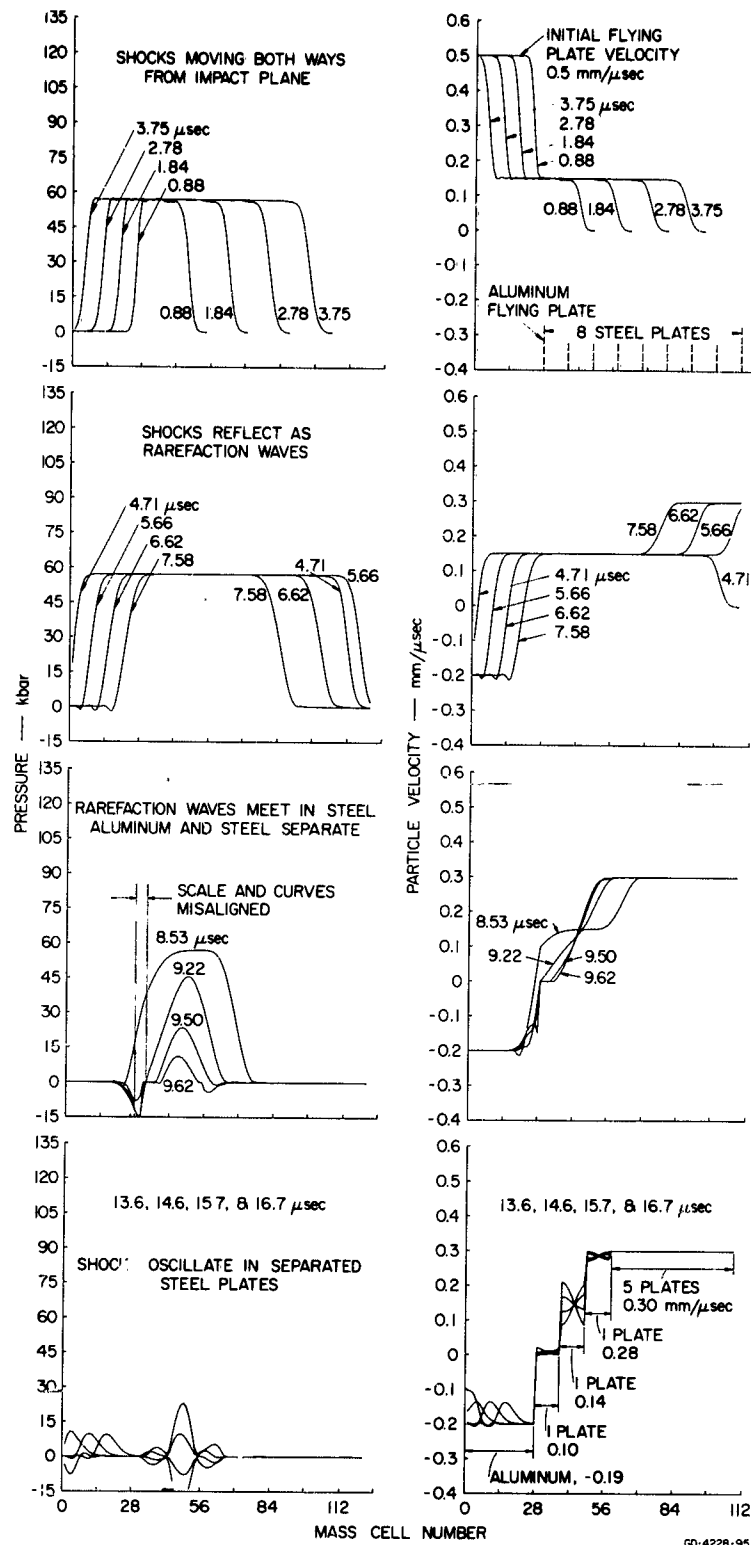


FIGURE 58 (U) CALCULATED IMPACT OF 1-INCH STACK OF STEEL PLATES (U)  
[Figure and caption combined (U)]

(U) When this calculation is compared with actual experiments, we find that the average velocity is in fair agreement but that some of the details do not agree. The flying plate in the actual experiments did not bounce off but travelled along with the plates of the stack. Also, there was much less variation in velocity than that calculated. These discrepancies may be due to several things. First, the flying plate was probably not actually shock free in the shot; second, it may have been accelerated by the explosive product gasses during and after impact; and third, the calculations are one-dimensional, whereas the shot was two-dimensional and edge effects may play an important role.

(U) All of the above discrepancies can be taken care of by a more sophisticated computer program: one which is two-dimensional and which follows the detonation of the explosive and the acceleration of the flying plate, as well as the impact on the plate stack. However, the added expense of writing and running such a program, and the additional difficulty of obtaining reliable equation of state data for some of the materials of interest, prompted the decision to confine this project to experimental rather than computational testing.

# CONFIDENTIAL

## Appendix III INSTRUMENTATION (U)

(U) Most of the instruments used on this project belonged to the normal group often used in explosive research. A framing camera was used primarily in the shock-induced backwards initiation study since the behavior to be expected in any one experiment was unknown, and the maximum amount of visual information was required. A smear camera was also used in the same study when continuous time coverage was required and, in addition, was useful in the early stages of the flying plate study. The flash X-ray machine proved to be the most useful standard instrument during the project, and a short description of it and some of the techniques developed for its use are included below. In addition, two short sections covering a fiber optics technique developed for use with the smear camera and a thin ionization switch technique will also be included.

### 1. Flash X Ray

(U) The X-ray system used during this project is a double unit of the Model 730 series built by the Field Emission Corporation. It has a maximum voltage of 300 Kv and each of the two tubes emits an X-ray pulse with a duration of 0.1  $\mu$ sec.

(U) The two tubes are mounted in a steel-faced bombproof and emit their X rays through two ports facing the firing area. The ports and the tubes can be positioned at varying distances from each other; typically they were spaced about 10 feet apart. The X-ray film with fluorescent intensifying screens in contact with it on both sides is held in an armored cassette typically about 1 foot behind the shot.

(C, gp 4) The film size most commonly used was 14 x 17 inches (the seventeen-inch dimension was vertical). The X-ray tubes, the shot, and the film were arranged so that the shadow of the fragments formed by one flash appeared down one side of the film, and that from the other, on the opposite side. Two steel plates were placed in front of the shot to shield the unused halves of the film from each tube in turn. Figure 59 shows an overhead view of a typical shot setup with strings stretched out to show the path of the two X-ray beams. This particular shot was one of the quasi-plane-wave-initiated, felted nickel shots,

# CONFIDENTIAL



**CONFIDENTIAL**

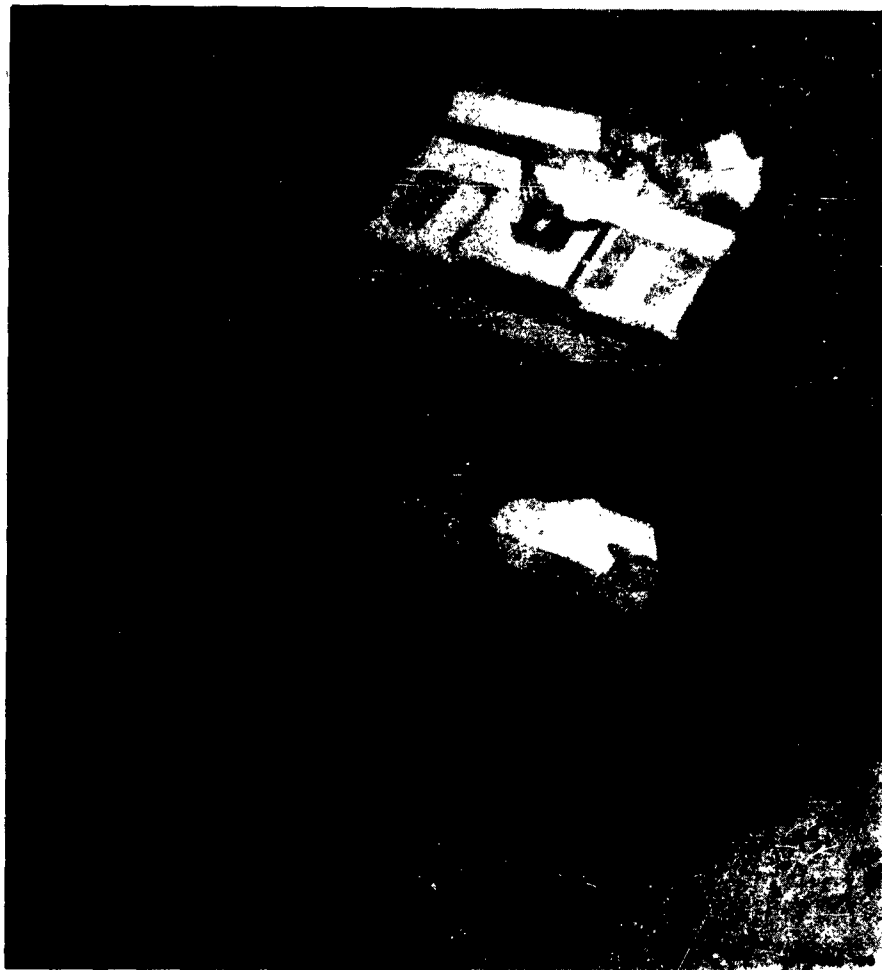


Figure 59 (U) Standard X-ray Setup (U).

and the barrel below the film holder was used to catch the fragments after the pictures were taken. Figure 30(c) in the main body of this report gives a different view of the cassette and shot relationship, this time as used for one of the NOL method shots.

(C, gp 4) In some experiments it was necessary to record an image wider than the 7 inches allowed on half of one film. For these experiments the tubes were moved further apart, so that their beams intersected at the shot at close to a right angle, and two cassettes were used. Figure 60 shows a typical setup of this kind where a double-scale MDF design is being tested.

**CONFIDENTIAL**

# CONFIDENTIAL

The records from this shot are shown in Figure 13 of the main report. Note there and in Figure 60 that the cassette for the second flash has been placed lower than that for the first so that the fragment cloud does not get so far off the film.

(U) To aid in analysis a scale was hung below the shot and an exposure was made before firing. In addition to marking inch intervals, this scale also had a special marker which was some known distance from the face of the shot.

(U) The shot itself was usually supported by a 1/2-inch slab of styro-foam which bridged a hole in the plywood support seen in the figures.

## 2. Fiber optics probes

(C. gp 4) The technique most used during the project to determine the behavior of the shock-initiated backwards initiation designs was to observe with a framing camera what went on at the surface of the charge. While this was generally satisfactory for simple designs, the determination of the internal events in designs which were steel-jacketed and which had an inset brass slug to simulate the fragment pack was often difficult.

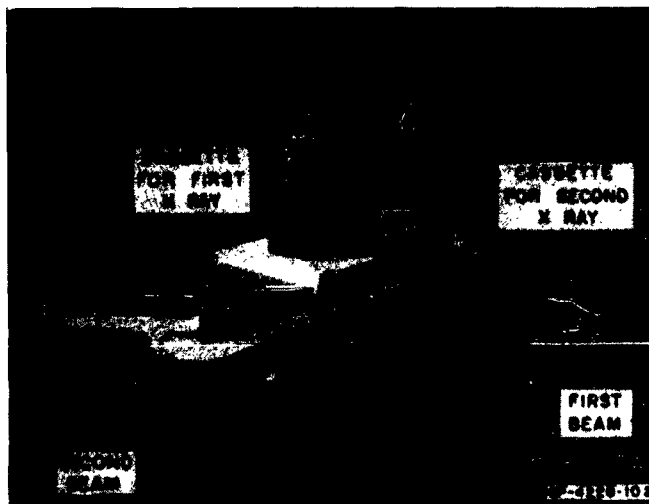


Figure 60 (U) Shot Setup with Two-Film Cassettes, Shot No. 10,203 (U).

**CONFIDENTIAL**

(U) In order to observe directly the shock or detonation arrival at the brass - explosive interface, holes were drilled through the brass so that the smear camera could see through to the interface. Since we did not wish to disturb the shock-to-detonation transition which we hoped was taking place at this interface, the holes were made as small as possible and were then filled with glass fibers potted in epoxy. The glass fibers used were made out of a core of high-index glass surrounded by a sheath of low-index glass. Total internal reflection at the interface between the glasses makes such a fiber an efficient carrier of light from one end to the other. The fibers used in this shot were obtained from a light guide manufactured by American Optical Company and were 0.003 inch in diameter. Approximately 100 fibers were used to fill each 0.040-inch-diameter hole.

(U) Figure 61 shows the still picture and the smear record from one shot using this technique. In this case the switch to high order detonation must have taken place in a small area about an inch or so from the brass plug, thus giving the curved front seen through the fiber optics probes.

(U) A paper has been written describing this technique and will be published in the Review of Scientific Instruments in November or December of this year.

### 3. Thin ionization switches

(C, gp 4) In order to understand fully the processes occurring in a backwards initiation shot such as the one discussed above, it is necessary to monitor the detonation front position within the body of the explosive as well as at the sides and interfaces with fragment packs. For this reason a technique was developed which combines the optical observation methods discussed above with electronic measurements via ionization switches inserted into the explosive to measure the shock and detonation front passage. The ionization switches are inserted by splitting the explosive charge on a plane parallel to and intersecting the axis of the charge and inserting a Mylar sheet, upon which has been evaporated thin gold lines which will act as conductors and as switches. Figure 62 shows the layout of the gold lines and illustrates the way in which the leads for several switches can be threaded out through the bottom of the charge. Since the Mylar is only 1/3 mil thick and the gold is far thinner than that, it was not expected

**CONFIDENTIAL**

**CONFIDENTIAL**



Figure 61 (U) Smear Camera Record of Backwards Initiation, Shot No. 9330 (U).

**CONFIDENTIAL**

CONFIDENTIAL

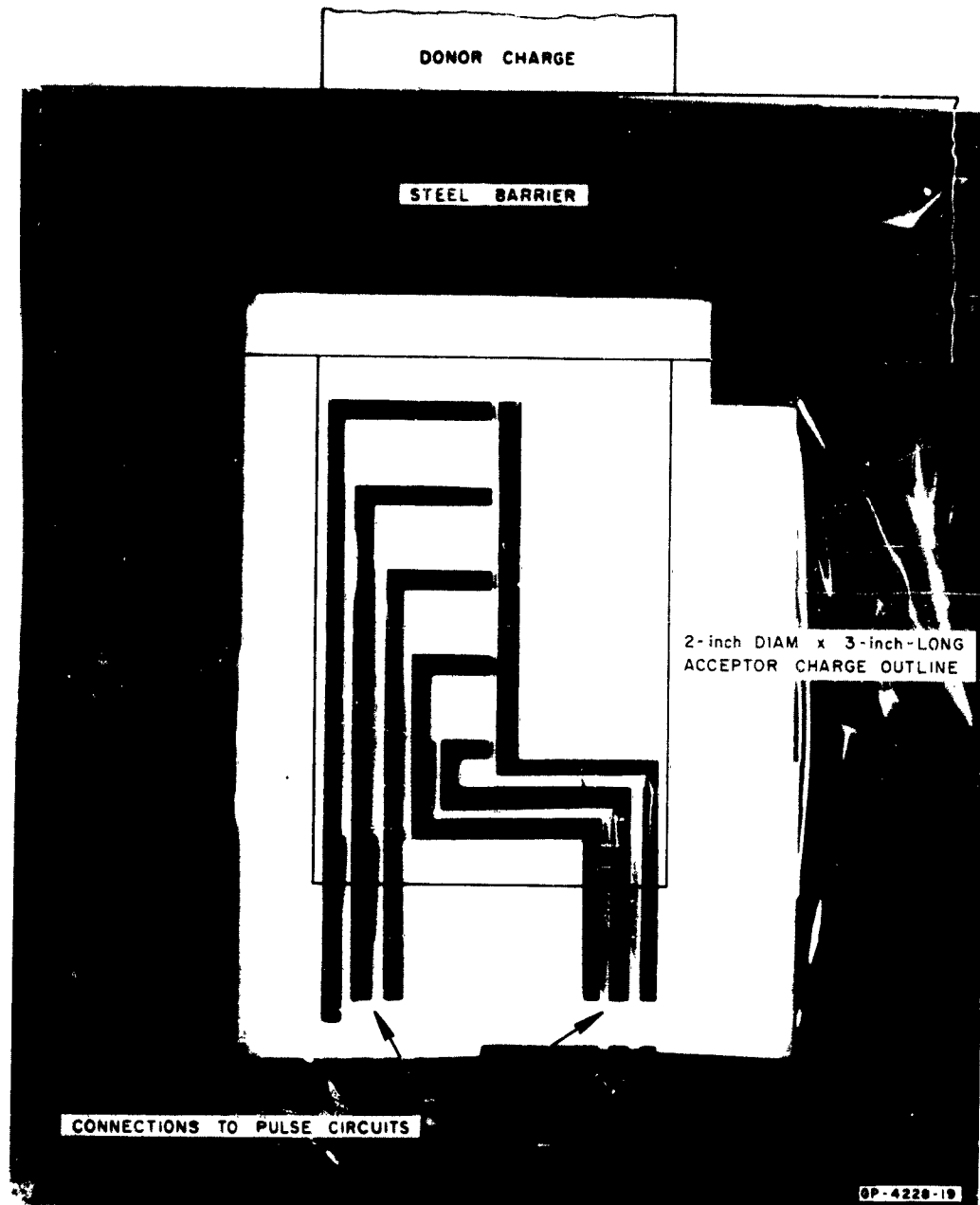


Figure 62 (U) Evaporated Gold-on-Mylar Switch Arrangement (U).

CONFIDENTIAL

# CONFIDENTIAL

that the introduction of this layer would materially alter the processes occurring in the explosive.

(U) A test shot of a fairly simple geometry was fired first; it determined that the shock wave in the explosive will not trip the switches but that a detonation front, with its attendant ionization front, is required to do this. This test shot was made by simply sandwiching the Mylar foil between two blocks of Composition B. Although the results were satisfactory, it was felt that a real test would require that the air gaps between the explosive and the Mylar be filled by a suitable glue to prevent jetting.

(U) The discovery of a suitable glue turned out to be a more difficult problem than was originally anticipated. Glues which are commonly used for attaching explosives to itself or to other materials are Eastman 910 cement, various Furane glues, and epoxy glues. Upon tests, all of these were found to attack Composition B explosive to some extent and were therefore deemed unacceptable since this attack could easily change the sensitivity of the explosive at the joint and hence the behavior of the low-order to high-order transition. A bottled carpenter's glue was tried next, but unless it was exposed to air the solvent in it could not evaporate, and therefore it did not harden. Finally another carpenter's glue, Weldwood Plastic Resin Glue, was tried. This glue comes in powder form, is mixed with water shortly before using, and hardens without being exposed to air. It does not attack the explosive and hardens sufficiently within one-half to one hour to allow careful handling of the charge.

(U) Several test gluings were made, each with Mylar sandwiched between glass and wood, and these showed that for these particular materials the adhesion of the glue to glass or Mylar when completely dried was poor. It was therefore decided to assemble the shot an hour or two before the firing time so that the joint would still be strong at the time of firing. One difficulty with this glue is that it is slightly conductive when the glue is wet. For this reason, and also to strengthen the delicate evaporated switch assembly, the Mylar was laminated in a commercial laminating machine which applied another coat of Mylar over the original one. This added approximately 0.001 inch to the thickness of the assembly.

# CONFIDENTIAL

(U) The assembly of a shot using this technique is shown in Figure 63. The layout of gold lines was changed slightly for this shot so that the leads could be brought out through the 1/2-inch gap between the brass plug and the steel case; three leads were brought out on each side in this way so that five switches could still be used. A sixth switch can be seen at the top of the figure, mounted on a small auxiliary charge which was also viewed by the smear camera. Since the electrical pulse from this switch came at the same time as the light pulse, these could be used to correlate the electronic and optical records.

(U) Figure 64 shows the record from the smear camera with the times and vertical positions of the foil switch closings noted. This record shows that the flipover to high order detonation took place more than 1 1/4 inches away from the brass plug and closed a switch on the axis 2.2  $\mu$ sec before detonation breakout at the surface. The second axial switch closed 1.5  $\mu$ sec before the detonation appeared at the corresponding surface hole, indicating that the front was becoming less curved at this time.

**CONFIDENTIAL**



Figure 63 (U) Foil Switch and Fiber Optics Shot, No. 9497 (U).

**CONFIDENTIAL**



**CONFIDENTIAL**



Figure 64 (U) Smear Camera Record with Foil Switch Closures Entered, Shot No. 9625 (U).

**CONFIDENTIAL**

# CONFIDENTIAL

## Appendix IV

### FRAGMENT PACK FABRICATION TECHNIQUES

#### I. INTRODUCTION

(C, gp 4) The original contract specified that the fragment pack should consist of 8 layers of not less than 200 fragments per layer, or 16 layers of not less than 400 fragments per layer. Stacking this many pieces individually without some method of keeping them together is both time consuming and expensive. This appendix will discuss the various stages in the development of the fragment pack.

##### A. Sliced layers

(C, gp 4) The first methods tried did not start with individual fragments but stacked hexagonal or round rods together. These stacks were then sliced into layers of fragments. Since the geometry chosen for the device was cylindrical it was desirable that the fragment layers approach a circular outline and that the individual fragments should be closely packed with as little space as possible between fragments.

(C, gp 4) Hexagonal rods lend themselves to close packing. An aluminum jig was made that approached a semicylindrical shape. Three-inch-long pieces of hexagonal brass rod, 1/8 inch across the flats, were tinned and stacked in the jig and sweat-soldered together. After two halves were made this way, the halves were soldered together to make a rough cylinder 2 inches in diameter, containing 227 hexagonal brass rods. It was found that this assembly was too fragile to be cut in slices, so it was placed in a 2 1/4-inch-diameter lucite tube and cast in Cerrobend. This provided enough strength so that the assembly could be sliced by using a high speed cut-off saw. The slices were then faced off in a lathe to the specified thickness of 1/8 inch. Figure 65 shows a slice of fragments made in this manner.

(C, gp 4) Although it is possible to make fragment layers by this method the time consumed is great, and the Cerrobend encapsulation results in excess waste weight.

# CONFIDENTIAL

**CONFIDENTIAL**

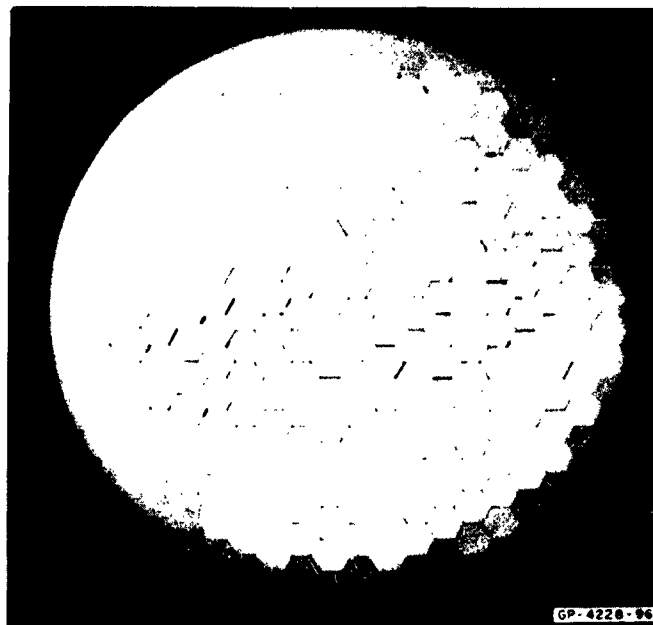


Figure 65 (U) Soldered Hexagonal Fragment Layer Cast in Cerrobend (U).

**B. Stacked rods**

(C, gp 4) The next step in the development of the fragment plates was to stack 209 round brass rods, 1/8 inch in diameter, in a 2-inch-diameter lucite tube and vacuum-cast Cerrobend as a matrix. This was very simple to do and they held together well during the cutting operation. However, the resulting plates contained 21 1/2 percent Cerrobend by weight. In Figure 66 notice the large gaps between some of the fragments which contribute to this wastage.

(U) A refinement of this method was to construct a hexagonal lucite tube (1.870-inches i. d.) across the inside of the flats. Such a tube will hold 217 brass rods 1/8-inch diameter in close hexagonal packing. Cerrobend matrix material was vacuum cast in the tube. By close packing in a hexagonal tube the weight of the Cerrobend matrix was reduced to 14.2 percent of the total weight.

**CONFIDENTIAL**

# CONFIDENTIAL

(C, gp 4) Unfortunately the Cerrobend did not "wet" the brass rods sufficiently to produce a good bond, and the resulting plates were so fragile that only the pressure of the lucite ring kept the pieces from falling apart.

(C, gp 4) In order to obtain sturdier plates, the Cerrobend was replaced with epoxy resin. This technique worked very well and also reduced the matrix weight to 1.6 percent of the total. Figure 67 shows a typical fragment plate made in this way.

## C. Stacked packs

(C, gp 4) Even the relatively efficient fabrication method outlined above was still quite expensive, and the resulting plates, particularly when made in the 1/16-inch thickness out of 1/16-inch rods, were fairly fragile. Since solid brass balls were available at low cost it was decided to attempt fabrication of whole packs by stacking these balls and then potting the stacks in epoxy.

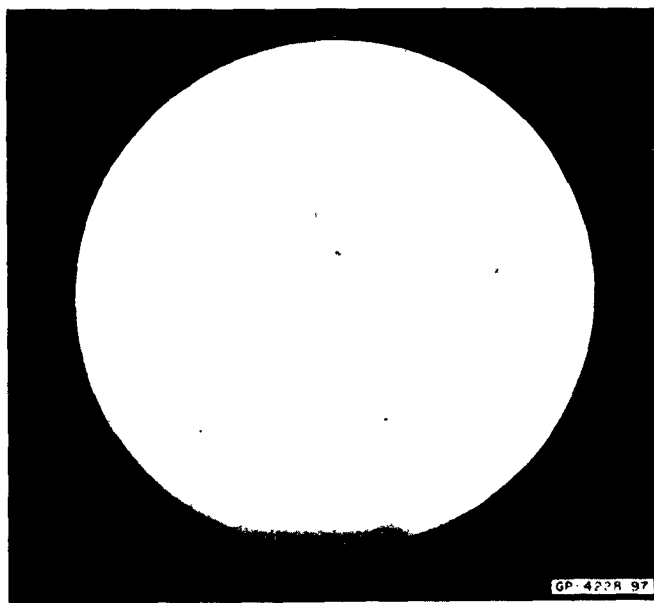


Figure 66 (U) Round Fragments Cast in a Round Tube with Cerrobend Filler (U).

**CONFIDENTIAL**

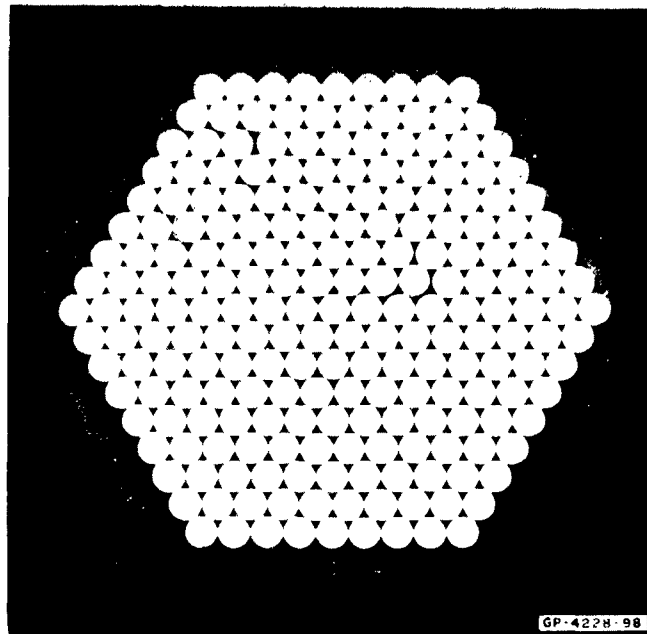


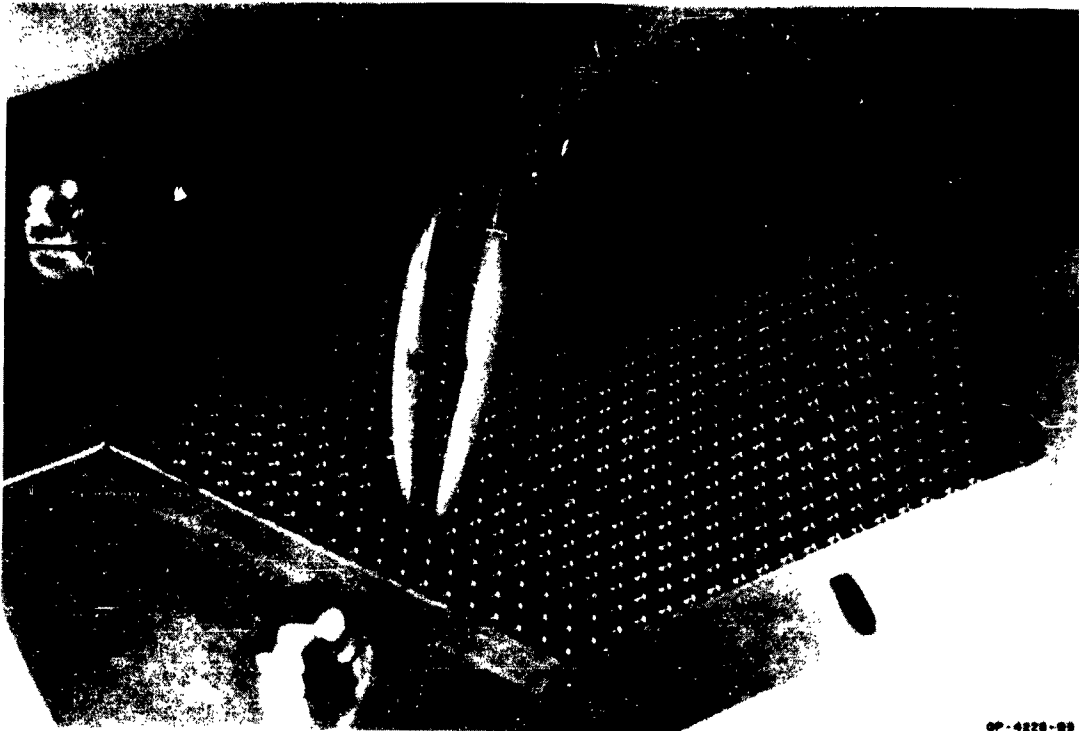
Figure 67 (U) Round Fragments in a Hexagonal Tube Potted in Epoxy (U).

(C, gp 4) Figure 68 illustrates the procedure used to stack the balls. A hexagonal aluminum mold was made and lined with Mylar to insure later release from the epoxy. The first layer of balls covered the entire bottom of the mold in a close-packed hexagonal array. The second layer was slightly displaced so that its balls fell between the balls of the first layer. This displacement meant that about half a row around the edge of the mold was left empty in this layer. The third layer, like the first, filled the entire mold, and the stacking continued in this way, with the two kinds of layers alternating. In Figure 68 a layer which will fill the mold is being added on top of one of the displaced layers. The space between the edge of the displaced layer and the mold can be seen at the right. Tweezers were only required during arrangement of the outer rows of balls; once these were in place the remaining balls could be gently poured into place in the center.

(C, gp 4) Figure 69 shows a typical pack of 1/8-inch balls after potting. The excess epoxy at the top was machined off before firing. Figure 70 shows three packs, the standard size in front and two double-scale packs in the rear.

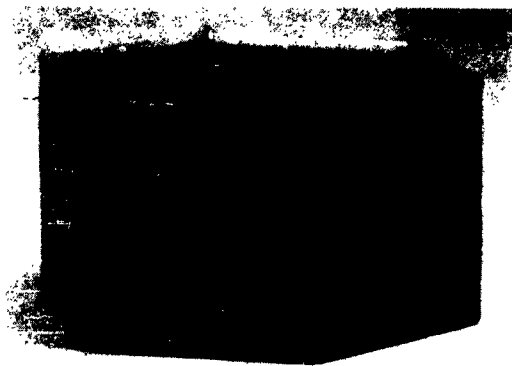
**CONFIDENTIAL**

**CONFIDENTIAL**



GP-4228-99

Figure 68 (U) Stacking 1/8-Inch Balls in the Double-Scale Mold (U).



GP-4228-100

Figure 69 (U) Standard 1/8-Inch Ball Pack (U).

**CONFIDENTIAL**

**CONFIDENTIAL**

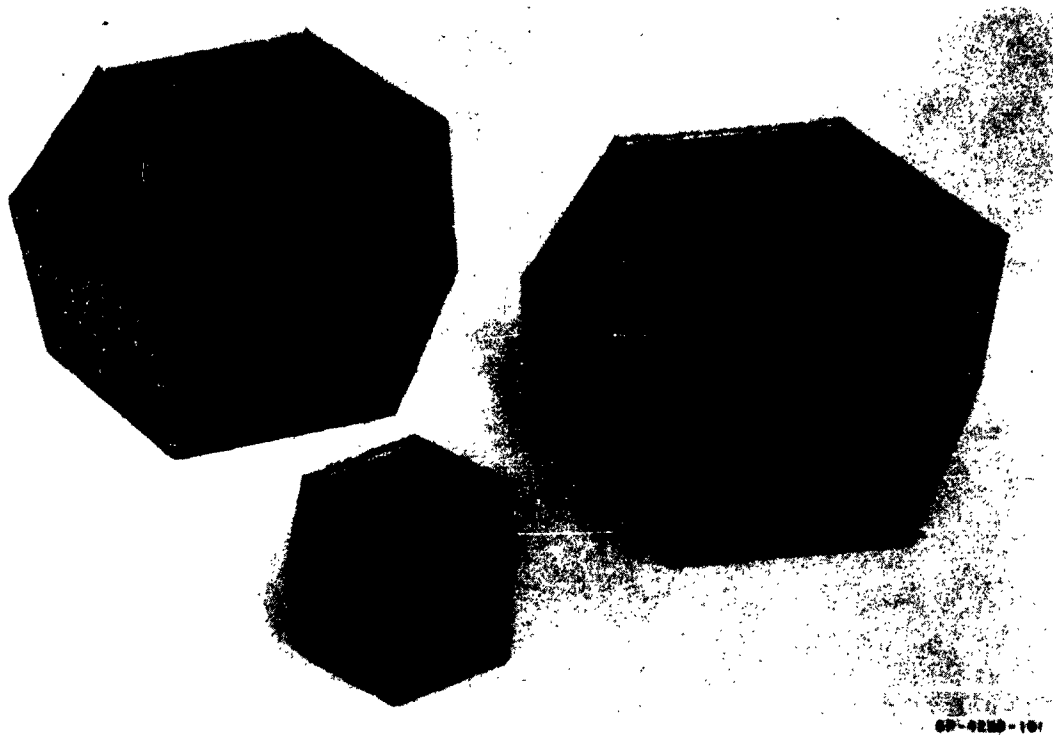


Figure 70 (U) Standard Pack with Two Double-Scale Packs (U).

**CONFIDENTIAL**

**Appendix V**  
**COMPLETE SHOT TABULATION (U)**

(U) The nine tables which comprise this appendix are a complete list of all shots fired on this project. The shots in each table are in chronological order and pertinent data are noted. Separate tables are given for each general class of shot. Additional details of many of these shots can be found in the tables in the body of this report.



CONFIDENTIAL

Table 16 (C gp 4)  
FLYING PLATE SHOTS (U)

Shot No.	Recording Instrument	Plate	Explosive Geometry		Pack Make-Up	Velocity (mm/μsec)	C. Mass in Frag.	Comments
			Thickness Behind x Diameter (inches)	Diameter (inches)				
9185	Smear camera	4" steel	1/2	x 4 <sup>a</sup>	None	0.78		Smooth spall
9186		4" steel	1/2	x 4 <sup>a</sup>	None	0.94		Smooth spall
9187		4" Al	1/2	x 4 <sup>a</sup>	None	1.40		Plate broken into small pieces
9188		4" Al	1 1/2	x 4 <sup>a</sup>	None	2.05		Spalling and melting - small pieces
9189		4" steel	1	x 4	None	0.48		Spall?
9190	Framing camera	4" steel	2	x 4	None	0.61		Smooth spall.
9191		4" Al	1	x 4	None	0.79		Edge spall.
9192		4" Al	2	x 4	None	1.20		Spall
9210		4" Al	1/2	x 4	1/8" solid plates	0.19		
9219		4" Al	1/2	x 4	1/8" solid plates	-0.28	36	
9243	Flash X ray	4" Al	1 1/2	x 4	1/8" solid plates	0.25 = <1%	36	
9246		4" steel	1	x 4	1/8" solid plates	0.23 = 3 1/2%	27	
9247		4" steel	2	x 4	1/8" solid plates	0.34 = 3.5%	17	
9266		4" Al	1 <sup>b</sup>	x 4	1/8" frag. plates	0.23 low spread	15	
9267		3" Al	1 <sup>b</sup>	x 4	1/8" frag. plates	0.25 large spread	30	
9255	Frag. range Flash X ray	3" steel	4 <sup>b</sup>	x 4	1/8" solid plates	0.34 = 3%	32	
9301		3" Al	1 <sup>b</sup>	x 4	1/16" solid plates	-0.28 = 16%	14	
9302		3" steel	4 <sup>b</sup>	x 4	1/16" solid plates	0.34 = 2.5%	33	
9340		3" steel	4 <sup>b</sup>	x 4	None	-----	14	
9341		3" steel	4 <sup>b</sup>	x 4	None	0.80	---	No X rays.
9445	Frag. range Flash X ray	4" Al	1 1/2	x 4	1/8" frag. plates	0.80	---	Flyer broken into 3 parts.
9449		3" steel	4	x 3	None	-0.51	26	Velocity too low to measure
9450		3" steel	4	x 3	None	-0.40		1/2" foam rubber buffer - spall.
9490		3 3/8" steel	4	x 3 3/8	None	0.56		1" foam rubber - spall
9491		3 3/8" steel	4	x 3 3/8	None	0.70		1/2" foam rubber - spall.
9521		3 1/2" steel	3	x 3 1/2 <sup>a</sup>	None	-1.13		No foam - spall.
9644		4" Al	1	x 4	1/16 frag. plates	0.24 low spread	29	Steel broken up
9911		4" Al	1 <sup>c</sup>	x 4	BB cast in plaster	0.28 = 2 1/2%	26	16 layer 1/16" x 1 1/16" press cylinders
9935		3" steel	2	x 4	1/8 frag. plates	0.26 ± 9%	19	352/laver
9978		4" Al	1	x 4	1/8 frag. plates	0.24 small spread	30	910 BBs cast in plaster
9979		3" steel	2	x 4	None	0.56 (spall vel.)	---	Spall - 0.6" thick
9980		3" steel	2 <sup>c</sup>	x 4	1/8 frag. plates	0.28 ± 6%	19	Plate inserted 1/2"
10,146		3" brass	3	x 4	None	0.9 (spall vel.)	---	Very thin spall followed by small pieces
10,181		4" Al	1	x 4	1/8" hollow balls	0.41 low spread	14	1636 balls in close Hex Pack cast in epoxy
10,255		3" Ni d.	3	x 3	None	0.75 (spall vel.)	---	Thin spall followed by small pieces
10,270			1/2	x 3	1/8" balls	0.10 ± 3%	38	1636 balls case in epoxy

CONFIDENTIAL

Table 16 (C gp 4) (Continued)

PRESSURE TRANSDUCER SHOTS									
Shot No.	Recording Instrument	Plate	Explosive Geometry Thickness Behind x Diameter (inches)	Radial Distance in Gage (inch)	Pressure in Gage (kbar)	Plate Velocity (mm/ $\mu$ sec)	Spall Thickness (mm)	Comments	
9774	Oscilloscope	3" steel	3 <sup>b</sup> x 4	0 3/8	-	-	-	Plate spalled and struck transducer at an angle	
9775	Oscilloscope	3" steel	3 <sup>b</sup> x 4	0 3/8	-	-	-	Plate spalled and struck transducer at an angle	
9817	Oscilloscope	6" steel	3 x 6	0 3/8	100 95	1.25 1.20	2.5 2	6"-diameter plane-wave initiation	
9818	Oscilloscope	4" steel	3 x 4	0 3/8	41 39	0.63 0.60	-	Two-part steel plate (see Figure 8, Point Initiation)	

FRAGMENT TRAJECTORY SHOTS									
Shot No.	Recording Instrument	Plate	Explosive Geometry Thickness Behind x Diameter (inches)	Pack Make-up	% Mass in Pack	Target		% Recovered	Results
						Size (ft)	Distance (ft-inches)		
9607	Target	4" Al	1 x 4	1/8" frag. plates	30	8 x 8	18 - 9 1/2	92	Low density at center: max. 20 ft <sup>3</sup> at 2 ft radius; 40 - 50 ft <sup>2</sup> at 4 ft radius.
9696	Target	3" steel	2 <sup>b</sup> x 4	1/8" frag. plates	18	8 x 8	18 - 9 1/2	52	Uniform smooth distribution; center 20 - 25 ft <sup>2</sup> ; 12 ft <sup>2</sup> at 4 ft radius.
9799	Target	4" Al	1 x 4 <sup>c</sup>	1/8" frag. plates	30	16 x 16	12 - 7	79	Empty ring at 2.5 ft radius; otherwise smooth.
9806	Target	3" steel	2 <sup>b</sup> x 4	1/8" frag. plates	18	16 x 16	13 - 1	95	Center: 20 - 25 ft <sup>2</sup> 10 ft radius/ -1.6 ft <sup>2</sup>
9920	Target	3" steel	2 <sup>c</sup> x 4	1/8" frag. plates	19	16 x 16	12 - 9 3/4	84	Rather spotty; close pattern at center - almost 0 ft <sup>2</sup> at 8 ft radius.
9934	Target	4" Al	1 x 4 <sup>a</sup>	1/8" frag. plates	19	16 x 16	12 - 8 3/4	64	Uniform to 4 ft. Center 12 - 14 ft <sup>2</sup> ; 10 ft - 1/2 ft <sup>2</sup> Smoother than Shots 9607 and 9799; Center 10 - 15 ft <sup>2</sup>

<sup>a</sup> P-40 Initiated PWG weighs 1.5 lbs.

<sup>b</sup> Plate inserted 1".

<sup>c</sup> Plate inserted 1/2".

<sup>d</sup> 3" diameter 1.90" foamed Al, density 1.3 g/cm<sup>3</sup> in contact with HE and ball pack.

<sup>e</sup> Peripherally initiated.

Table 17 (C, gp 4)  
ELECTRIC BACKWARDS INITIATION (U)

Shot No.	Recording Instrument	Explosive Thickness and Diameter (Inches)	Initiation Points	Pack Make-up	Velocity (mm/msec)	% Mass in Frag.	Comments
9606	Flash X ray	4 x 3	1	1/8" solid plates	0.32 ± 0.2%	35	No X rays
9608		4 x 3	1	1/8" solid plates	0.32 ± 0.2%	35	
9609		4 x 3	3	1/8" solid plates	0.32 ± 0.2%	35	
9623		4 x 3	1	1/8" Frag. plates	0.38 ± 0.2%	33	Domed cloud.
9624		4 x 3	3	1/8" Frag. plates	0.39 ± 0.2%	33	Domed cloud.
9643		4 x 2	1	1/8" solid plates	0.19 ± 0.4%	54	
9703		3 x 3	1	1/8" solid plates	0.32 ± 0.1%	41	
9704		2 x 3	1	1/8" solid plates	0.31 ± 1.1/2%	51	
9705		1 x 3	1	1/8" solid plates	0.28 ± 0.2%	68	
9706		3 x 2	1	1/8" solid plates	0.19 ± 0.4%	62	
9707		2 x 2	1	1/8" solid plates	0.19 ± 0.5%	70	
9708		1 x 2	1	1/8" solid plates	0.17 ± 0.9%	82	
9709		2 x 2	1	1/8" solid plates	0.25 ± 0.3%	51	HE clad with 1/8" steel.
9710		2 x 2	1	1/8" solid plates	0.30 ± 2.1/2%	40	Clad with 1/4" steel.
9840		2 x 3	6*	1/8" solid plates	0.32 ± 1.1/2%	51	

FRAGMENT TRAJECTORY SHOT						
Shot No.	Recording Instrument	Explosive Thickness and Diameter (Inches)	Initiation Points	Pack Make-up	% Mass in Frag.	Target
						Size ft. Distance ft-in
9683	Target	2 x 3	1	1/8" Frag. plates	49	8 x 8 18 - 9 1/2
9684		2 x 3	3	1/8" Frag. plates	49	8 x 8 12 - 6 1/2
9755		2 x 3	1	1/8" Frag. plates	49	16 x 16 12 - 11 1/2
9756		2 x 3	3	1/8" Frag. plates	49	16 x 16 12 - 11 1/2
9764		1 x 3	1	1/8" Frag. plates	66	16 x 16 12 - 11
9771		1 x 3	3	1/8" Frag. plates	66	16 x 16 12 - 6 1/2

\* Simultaneous forward backward initiation.

# CONFIDENTIAL

Table 18 (C, gp-4)  
MDF BACKWARDS INITIATION (U)

Shot No.	Recording Instrument	Explosive (Thickness & Diameter (inches))	Initiation Geometry (see Fig)	Pack Makeup	Velocity (mm/ $\mu$ sec)	% Mass in Frag.	Comments
9753	Framing Camera	2 x 2	Fig. 12(a)	1" steel slug	----	70	MDF did not crack Comp B.
9754	Framing Camera	2 x 2		1" steel slug	----	70	MDF in spaghetti in 1/8" hole did not crack Comp B.
9772	Flash X ray	2 x 2		1/8" solid plates	0.18 $\pm$ 6%	70	
9773		2 x 2		1/8" solid plates	0.18 $\pm$ 6%	70	
10, 180		2 x 2		1/8" hollow balls	0.51	45	Domed cloud.
10, 191	Framing Camera	4 x 3		1" steel slug	----	35	MDF did not crack Comp B.
10, 203	Flash X ray	4 x 4		1/4" ball pack	Nose 0.43 Bowl 0.38 Rim 0.28	55	1636 brass/balls in 8 layers. Domed cloud.
10, 204		4 x 4		1/8" ball pack	Nose 0.47 Bowl 0.39 Rim 0.26	58	14,152 balls in 16 layers.
10, 213		2 x 2		1/8" ball pack	Nose 0.42 Bowl 0.36	58	Exact 1/2 scale of 10, 203.
10, 214		2 x 2		1/8" ball pack	0.26 $\pm$ 7%	58	Much flatter cloud.
10, 215		2 x 4		1/8" ball pack	0.19 small spread	26	Comp B did not go high order.
10, 236		2 x 3		1/8" ball pack	---	38	Shot did not detonate.
10, 254		2 x 3		1/8" ball pack	0.42 $\pm$ 6%	38	

## Fragment Trajectory Shots

Shot No.	Recording Instrument	Explosive (Thickness & Diameter (inches))	Initiation Geometry	Pack Makeup	% Mass in Frag.	Target		% Recovered	Results
						Size ft	Dist. ft-inches		
9836	Target	2 x 3	a	1/8" frag plates	49	16 x 16	12 - 8 1/2	57	Smooth though low concentration.
9837		2 x 3 <sup>b</sup>	Fig. 12(a)	1/8" frag plates	43	16 x 16	13 - 3	78	Over 100/ft <sup>2</sup> at center. Drops to ~10/ft <sup>2</sup> at 2 foot radius.
10, 003		2 x 3 <sup>c</sup>	Fig. 12(a)	1/8" frag plates	48	16 x 16	12 - 8 1/4	71	Center ~30/ft <sup>2</sup> Tapers smoothly to ~1/ft <sup>2</sup> at 10 foot radius.
10, 120		2 x 3 <sup>d</sup>	Fig. 12(a)	1/8" frag plates	46	16 x 16	12 - 7	77	Low center density ~10/ft <sup>2</sup> . Max. at 1 1/2 ft radius 27/ft. 2

a 6-point peripheral backward

b Pack inserted 1 inch

c Pack inserted 1/4 inch

d Pack inserted 1/2 inch

CONFIDENTIAL

Table 19 (C, gp 4)  
SHOCK INDUCED BACKWARDS INITIATION (U)

Shot No.	Recording Instrument	Explosive		PETN <sup>a</sup> = 1.0 g/cm <sup>3</sup> Thickness (inch)	Barrier Thickness (inches)	Flipover Distance (inches)	Pack Make up Thickness x Diameter (inches)	Mass in Frag.	Comments
		Donor Thickness x Diameter (inches)	Acceptor Thickness x Diameter (inches)						
9061	Framing camera	3 x 2	3 x 2		1.75	1 1/2	1 x 2 steel	6	
9063		3 x 2	3 x 2		2.00		1 x 2	5	No high order
9064		3 x 2	3 x 2		2.25		1 x 2	5	No high order
9089		3 x 2	3 x 2		1.874	1.3/16	1 x 2	5	
9090		3 x 2	3 x 2		1.938		1 x 2	5	No high order
9091		3 x 2	3 x 2		1.812	1 1/16	1 x 2	5	
9102		3 x 2	2 x 2		2.00	1 7/16	1 x 2	5	
9103		3 x 2	3 x 2		2.00	1 1/4	1 x 2	5	
9104		3 x 2	2 1/2 x 2		2.50		1 x 2	4	No high order
9105		3 x 2	3 x 2		1.8125	3/4	1 x 2	5	
9147		3 x 2	3 x 2 <sup>a</sup>	1/4	2.25	@ PETN	1 x 2	4	
9148		3 x 2	3 x 2	1/4	2.25	@ PETN	1 x 2	5	No high order
9149		3 x 2	1 1/2 x 2	1/4	2.25	@ PETN	1 x 2	5	
9177		3 x 2	3 x 2 <sup>a</sup>	1/4	2.25	@ PETN	1 x 2	4	
9178		1 x 2	3 x 3	1/4	2.25		1 x 3	9	No high order.
9179		1 x 2	3 x 3 <sup>a</sup>	1/4	1.75	Very late	1 x 3	11	
9240		1 x 2	3 x 3 <sup>a</sup>	1/4	1.75	@ PETN (late)	1 x 3	11	
9241		1 x 2	3 x 3 <sup>a</sup>	1/4	1.625		1 x 3	11	No high order.
9242		1 x 2	3 x 3 <sup>a</sup>	1/4	1.50	@ PETN	1 x 3	12	1st plate, 0.51 mm $\mu$ sec
9270	Flash X ray	1 x 2	3 x 3 <sup>a,b</sup>	1/4	1.50		1/8 frag. plates in Cerrobend	5	Last 7 plates, 0.35-0.27 mm $\mu$ sec
9271	Flash X ray	1 x 2	3 x 3 <sup>a,b</sup>	1/4	1.50		1/8" solid plates	6	1st plate, 0.68 mm $\mu$ sec
9298	Framing camera	1 x 2	3 x 3 <sup>a,c</sup>		1.50		1 x 2 steel	6	Last 7 plates, 0.19-0.39 mm $\mu$ sec
9299		1 x 2	3 x 3 <sup>a,c</sup>		1.25	1 1/4	1 x 2 steel	6	No record
9315		1 x 2	3 x 3 <sup>a,c</sup>		1.375	1 1/4	1 x 2 steel	6	Definitely flipped before 3" travel
9316		1 x 2	2 x 3 <sup>a,c</sup>		1.50	2	1 x 2 steel	6	Front may be curved.
9330	Smear camera	1 x 2	3 x 3 <sup>a,c,d</sup>		1.50	1 3/4	1 x 2 brass w/fiber optics	6	Curved front
9331	Smear camera	1 x 2	3 x 3 <sup>a,c,d</sup>		1.625			6	Shot failed
9451	Framing camera	3 x 2	3 x 2 <sup>d</sup>		1.50	1 1/4-1 3/4 <sup>e</sup>	None		No framing pictures.
9473	Framing camera	3 x 2	3 x 2 <sup>d</sup>		1.75	-1	None		Good correlation between pictures and pins.
9487	Smear camera	1 x 2	3 x 3 <sup>a,c,d</sup>		1.50	1.2-1.7 <sup>e</sup>	1 x 2 brass w/fiber optics	6	
9625	Smear camera	1 x 2	3 x 3 <sup>a,c,d</sup>		1.50	-1 1/4	1 x 2 brass w/fiber optics	6	

<sup>a</sup> 1/8" wall steel case around acceptor.  
<sup>b</sup> Packs and PETN recessed 1 1/4" (flush) in Comp B.  
<sup>c</sup> Pack inserted 1" (flush) in Comp B.  
<sup>d</sup> Split for foil switch insert.  
<sup>e</sup> Based on foil switch data.

CONFIDENTIAL

Table 20 (U)  
FLYING PLATE SHOCK-INDUCED BACKWARDS INITIATION (U)

Shot No.	Recording Instrument	Driving Explosive Thickness (inch)	Accelerator			Plate Velocity mm/μsec.	Flip over point: inches from top	Comments
			Type	Thickness x Diameter (inches)	Booster Under Acceptor			
9984	Flash X ray	0.100	---	---	---	---	---	Test shot.
9985	Flash X ray	0.100	---	---	---	0.37	---	Test shot.
10,088	Framing camera	0.100	Comp B	2 x 3	PETN	0.37	None	Some reaction, no detonation.
10,089	Framing camera	0.145	Comp B	2 x 3	PETN	0.52	2.0	PETN went first.
10,108	Flash X ray	0.145	Comp B	2 x 3	PETN	0.26	---	
10,119	Flash X ray	0.145	Comp B	2 x 3	PETN	-0.42	---	Large velocity spread.
10,153	Framing camera	0.145	Comp B	2 x 3	None	---	---	
10,159		0.145	Comp B	1 x 3	None	---	-1.2 @ metal	Shock at angle to Comp B surface.
10,186		0.137	Comp B	2 x 3	None	0.47	None	
10,187		0.148	Comp B	2 x 3	None	0.52	1.4	
10,196		0.137	Comp B	2 x 3	None	0.47	1.4	
10,197		0.148	Comp B	1 x 3	None	0.52	None	
10,219		0.148	PBX	3 x 3	None	0.52	1.0	
10,220		0.100	PBX	3 x 3	None	0.37	None	
10,232		0.137	PBX	3 x 3	None	0.47	1.3	
10,233		0.116	PBX	3 x 3	None	0.42	2.2	
10,276		0.116	PBX	3 x 3	None	0.42	2.0	
10,277		0.116	PBX	3 x 3	None	0.42	3.0	
10,303		0.110	PBX	3 x 3	None	---	---	Shot failed.
10,304		0.110	PBX	3 x 3	None	0.40	2.1	
10,355		0.107	PBX	3 x 3	None	0.40	None	

CONFIDENTIAL

Table 21 (C, gp-4)  
SPACED AND BUFFERED PLATE SHOTS (C, gp-4)

Shot No.	Explosive Geometry (length x diam)	Plate Grouping Starting at HE	Foam Density between Groups (lb/ft <sup>3</sup> )	Plate Type	Velocity (mm/μsec)	% Mass in Frags.	Comments
9645	4" x 3"	1 - 1 - 2 - 4	0	Solid steel	0.40 ±12%	35	Badly broken.
9711	4" x 3"	1 - 1 - 2 - 4	0	Solid steel	0.38 ±24%	35	Badly broken.
9838	3" x 3"	2 - 2 - 4	0	Solid steel	0.39 ±34%	41	
9839	3" x 3"	2 - 2 - 4	20	Solid steel	0.35 ±7%	41	
9910	3" x 3"	2 - 2 - 4	20	1/8" cyl. frag.	-0.40 ±20%	39	Deep, bowl-shaped cloud.
10, 256	3" x 3"	2 - 2 - 4	60	Solid steel	avg - 0.35	40	4 plates 0.34 mm/μsec ± 2%. Other frags. 0.2 to 0.5 mm/μsec.
10, 257	3" x 3"	4 - 4	60	Solid steel	avg - 0.35	40	5 plates 0.33 mm/μsec ± 5%. Other frags. to 0.5 mm/μsec.
10, 271	3" x 3"	2 - 2 - 4	60	1/8" cyl. frag.	avg - 0.42	39	Nose: 0.48 mm/μsec Main mass: 0.42 mm/μsec Rim: 0.35 mm/μsec
10, 272	3" x 3"	4 - 4	60	Two 4 layer, 1/8" ball packs	avg - 0.60	29	Nose: 0.66 mm/μsec Main mass: 0.60 mm/μsec Rim: 0.47 mm/μsec

CONFIDENTIAL

CONFIDENTIAL

Table 22 (C, gp-4)  
NOL DESIGN (U)

Shot No.	Recording Instrument	Diam. C (inches)	Cylinder Wall B (inches)	Donut A (inches)	HE Height (inches)	Flying Plate Overlaps Cylinder	Pack Make up	Inside HE (inches)	Gap plus HE (inches)	Velocity (mm/μsec)	Mass in Frag.	Comment
10, 235	Flash X ray	4	1/4	1	3	Yes	8 1/8" x 2" steel plates	0.20*	1.00	0.52 ± 2%	11	Donut traveling 1.2 mm. μsec.
10, 265		4	1/4	1/2	3	Yes		0.20	1.00	0.53 ± 10%	13	
10, 266		4	1/4	1/4	3	Yes		0.20	1.00	0.50 ± < 1%	16	
10, 267		4	1/8	1/2	3	Yes		0.20	1.00	0.53 ± 3%	15	
10, 268		3	1/4	1/2	3	Yes		0.20	1.00	0.41 ± 7%	22	1636 brass balls in loose cylinder casting. Nose velocity: 0.45 mm μsec; Bowl velocity: 0.35 mm μsec; Rim velocity: 0.17 mm μsec.
10, 269		2	1/4	--	3	No		0.20	1.00	0.25 ± 5%	34	
10, 316		4	1/8	1/4	3	Yes		0.20	1.00	0.49 ± 1/2%	18	
10, 317		4	1/8	1/8	3	Yes		0.20	1.00	0.45 ± 0%	19	
10, 318		3	1/8	1/4	3	No		0.20	1.00	0.39 ± 1%	28	1636 brass balls in close packing.
10, 319		2	1/8	--	3	No		0.22	1.00	0.23 ± 2%	43	
10, 320		2	1/8	--	3	No		0.22	1.20	0.22 ± 5%	42	
10, 321		4	1/4	1/4	3	Yes	1/8" ball pack	0.20	1.00	0.68 ± 1%	10	
10, 344		2	1/8	--	2	No	8 1/8" x 2" steel plates	0.22	1.00	0.22 ± 2%	47	1636 brass balls in loose cylinder casting. Nose velocity: 0.45 mm μsec; Bowl velocity: 0.35 mm μsec; Rim velocity: 0.17 mm μsec.
10, 345		2	0	--	2	No		0.22	1.00	0.18 ± 5%	63	
10, 346		3	0	1/8	3	No		0.20	1.00	0.34 ± 1/2%	34	
10, 349		2	1/8	--	2	No	1/8" ball pack	0.22	1.00	Avg. 0.33	34	
10, 350		3	1/8	1/4	3	No	1/8" ball pack	0.20	1.00	0.53 ± 1/2%	18	Double scale of Shot No. 10344.
10, 351		4	1/8	1/4	3	Yes	15 1/8" x 3" steel plates	0.20	1.00	0.23 ± 0%	51	
10, 364		4	1/4	--	4	Yes	16 1/8" x 4" steel plates	0.44	2.00	0.22 ± 5%	48	

\* EL-500D. All remaining are Comp B.

CONFIDENTIAL



Table 22 (C, gp-4) (Continued)

FRAGMENT TRAJECTORY SHOTS														
Shot No.	Recording Instrument	Diam. C (inches)	Cylinder Wall B (inches)	Donut A (inches)	HE Height (inches)	Flying Plate Overlaps Cyl.	Pack Make-up	Inside HE (inch)	Cap plus HE (inches)	% Mass in Frag.	Target		Comment	
											Size (ft)	Diameter (ft-inches)		% Recovered
18, 388	Target	3	1/8	1/4	3	No	1/8" ball pack	0.20	1.00	18	16 x 16	12 - 5	93	1836 brass balls in close hex packing. Hit pattern small with 85-90 ft <sup>2</sup> at center. Very few beyond 2 1/2 ft radius.
18, 427		3	1/8	--	3	No		0.22	1.00	34	16 x 16	12 - 8	94	1836 brass balls in loose cylinder packing. -40 hits/ft <sup>2</sup> to radius of 2 1/2 ft. Few beyond 3 ft radius.
18, 487		4	1/8	1/4	3	Yes		0.20	1.00	11	16 x 16	12 - 8	93	1836 brass balls in close hex packing. -90 hits/ft <sup>2</sup> to radius of 1 1/2 ft. Few beyond 2 ft radius.
18, 488		6	1/4	1/2	6	No	1/4" ball pack	0.40	2.00	17	16 x 16	23 - 11	81	1836 brass balls in close hex packing. -15-20 hits/ft <sup>2</sup> to radius of 4 1/2 ft. Slopes smoothly out to 8 1/2 ft.

Table 23 (C, gp 4)  
LOW-DENSITY FRAGMENT SHOTS (C, gp 4)

Shot No.	Recording Instrument	Explosive (inches)	Material and Density (gm/cm <sup>3</sup> )	Original Frag. Size (inches)	Layer Construction	No. of Layers	Velocity (mm/μsec)	% Mass in Frags	Results
9912	Flash X ray	1 1/2 x 1 1/2 Dia. Comp B central initiation	Ni 3.5	1 x 1 x 1/8	1" x 1" 1 piece	4	0.8 leading edge of cloud	28	Large velocity spread; some recovered frags show density 7 to 8 gm/cm <sup>3</sup>
10, 061		2 x 2 Dia. Comp B + 3" flower pot PWG	Ni 3.5	2 dia. x 1/8	2" dia.	4	1.1 leading edge of cloud	-10	Large velocity spread.
10, 062		2 x 2 Dia. Comp B + 3" flower pot PWG	Ni 3.5	2 dia. x 1/8	2" dia.	4 + 1 steel	1.0 leading edge of cloud	-10	Large velocity spread.
10, 343		EL 500D 2 x 3 x .18 flaming detonation	Al 1.3	1/4 x 1/4 x .46	1 1/2" x 1 1/2" 36 pcs	1	-----	45	No record
10, 346		EL 500D 2 x 3 x .18 flaming detonation	Al 1.3	1/4 x 1/4 x 1/2	1 1/2" x 1 1/2" 36 pcs	1	0.5 leading group	45	Compressed frags. recovered.
10, 352		EL 500D 2 x 3 x .18 flaming detonation	Ni 3.5	1/8 x 1/8 x 1/4	1 1/2" x 1 1/2" 144 pcs	1	0.25 to 0.45	50	Compressed frags. recovered.
10, 362		Comp B 2 x 4 1/2 x 1/2 flaming detonation	Al 1.3	1/4 x 1/4 x .46	2" x 2" 64 pcs	4	0.29 - 0.37	51	A few frag. pairs, all compressed.
10, 363		Comp B 2 1/2 x 4 x 1/2 flaming detonation	Ni 3.5	1/8 x 1/8 x 1/4	1 1/2" x 1 1/2" 144 pcs	4	0.25 - 0.35	53	A few frag. pairs, all compressed.
10, 392		*EL 500D 2 1/2 x 2 1/2 x 1/2 9 point "plasma" initiation	Ni 3.5	1/8 x 1/8 x 1/4	1 1/2" x 1 1/2" 144 pcs	4	0.32 ± 3%	18	Some clustering of recovered frags.
10, 400		*EL 500D 2.00 x 2.00 x 1/2 9 point "plasma" initiation	Ni 3.5	1/8 x 1/8 x 1/4	1.09" x 1.09" 64 pcs	4	0.30 ± 14%	11	No pairs. All frags. compressed. Clustering greatly reduced.

\* Shot confined by steel box 2 1/2" x 2 1/2" x 1"

o Shot confined by steel box 2.00" x 2.00" x 1.00"

o Each fragment was in an "egg crate" made of 0.005" Mylar; 0.005" Mylar; 0.005" Mylar separators between layers and top and bottom.

CONFIDENTIAL

Table 24 (C, gp 4)  
MISCELLANEOUS SHOTS (U)

Shot No.	Recording Instrument	High Explosive		Pack Makeup	Average Velocity (mm/μsec)	% Mass in Frag.	Comments
		Thickness Behind Pack (Inches)	Diameter (Inches)				
8923	Flash X ray	9.73*	2	8, 1/8" steel plates	- 0.43	34	Very poor record.
8924		4.01*	3.12		- 0.61	34	
8925		2.43*	4.00		- 0.46	34	
8949		4.28*	3.01		- 0.61	34	Spalled and fragmented. Pack inserted 1", plates broken badly.
9023		4.32*	3.00		- 0.85	32	Packed inserted 1", large velocity spread.
9024		4.32*	3.00	steel hemisphere 1/16" wall	- 0.88	32	Pack inserted 1", large velocity spread.
9040		4.32*	3.00		- 0.64	32	Pack inserted 1", large velocity spread.
9041		4.32*	3.00		- 0.58	32	Pack inserted 1", large velocity spread.
9443	Frag. range	2" dia. hemi.*		steel hemisphere 1/16" wall	---	50	Test shot on fragmentation range.
9444	Frag. range	2" dia. hemi.*		steel hemisphere 1/16" wall	---	50	Test shot on fragmentation range.
10,234	Flash X ray	3.00 <sup>0</sup>	3.00	8, 1/8" steel plate	- 0.54	41	Shot mistimed so only first plate recorded.

\* C-3  
0 Composition B

CONFIDENTIAL

## REFERENCES

1. Rinehart, J. S. , "Some Quantitative Data Bearing on the Scabbing of Metals under Explosive Attack", J. Appl. Phys. 22, 555-560 (1951)
2. Erkman, J. O. , "Smooth Spalls and the Polymorphism of Iron", J. Appl. Phys. 32, 939-944 (1961)
3. Keough, D. D. , Pressure Transducer for Measuring Shock Wave Profiles, Stanford Research Institute, Project PGU-3713, Final Report, 1963, DASA Report No. 1414
4. Cosner, L. N. , Determination of Pressure-Time Curves in a Donor-Steel-Receptor Explosive System, paper presented at the Symposium on Warhead Research (Surface Target) 17-18 April 1962 at the U. S. Naval Ordnance Test Station, China Lake, California. NOTS Technical Publication No. 2958, 1962 (C)
5. Jacobs, S. J. , T. P. Liddiard, and B. E. Drimmer, "The Shock-to-Detonation Transition in Solid Explosives", Ninth International Symposium on Combustion, Academic Press, N. Y. , 1963
6. Seay, G. E. and L. B. Seely, Jr. , "Initiation of a Low-Density PETN Pressing by a Plane Shock Wave", J. Appl. Phys. , 32, 1092-1097 (1961)
7. Sternberg, H. M. and D. Piacesi, Explosion Hydrodynamic Calculations for a Two-Stage Guided Missile Warhead (U), NOLTR 63-72, 1963 (C)
8. Originally investigated under Air Force Contract AF 29(601)-4363 for AFSWC.
9. Manufactured by Emerson and Cuming, Inc. , and designated "Eccofoam MD AO" (1.3 g/cc density).
10. Manufactured by Huyck Corporation, Milford, Connecticut, and designated Nickel "Feltmetal" (type A30 fiber, 40 percent density).
11. Crosby, J. K. et al. , Feasibility of Simulating the Mechanical Effects of a Nuclear Explosion Using Nonnuclear Explosives, Stanford Research Institute, Project No. 3276, Final Report, 1961, DASA Report No. 1264
12. Christman, D. R. and J. W. Gehring, Study of Lethality of Hollow Spheres, ASD-TDR-63-44, Oct. 1963
13. Sterne, T. E. , A Note on the Initial Velocities of Fragments from Warheads, BRL-648, Sept. 1947

## INITIAL DISTRIBUTION LIST

1	DOD R&E	1	AU (AUL-9764)
3	ADVANCED RSCH PROJ AGENCY	1	NASA
1	WPNS SYS EVAL GP	1	NASA/LEWIS RESCH CTR
1	DASA (DDC LIB BR)	1	NASA/AMES RESCH CTR
1	HQ USAF (AFORQ-Q1)	1	NASA/LANGLEY RESCH CTR
1	HQ USAF (AFRSTE)	1	NASA/MARSHALL SPACE FLT CTR
1	HQ USAF (AFRSTB)	2	OFFICE OF NAVAL RESCH
1	HQ USAF (AFCIN)	1	US NAVAL ORD LAB (Lib)
1	HQ USAF (AFRDP)	1	US NAVAL WPNS EVAL FACILITY
1	HQ USAF (AFOCE)	1	US NAVAL WPNS LAB (Lib)
1	AFSC (SCTR)	1	NAVAL RESCH LAB (CODE 6240)
1	AFSC (MSFA)	2	NAVAL RSCH LAB (Tech Lib)
1	AFSC (SCSA)	1	US NAVAL ORD LAB
1	ASD (ASJ)	2	NAVAL ORDNANCE TEST STN
1	AFAL (AVN)	1	US ARMY ENGR R&D LABS
1	AFML (MAA)	1	USA MSL COMD (Tech Lib)
1	AFML (MAY)	1	ARMY MATERIEL COMMAND
2	AFFDL (FDTS)	1	ARMY WEAPONS COMMAND
1	FTD (TDFA)	1	FIELD COMMAND DASA (FCDR)
1	FTD (TDCE)	2	PICATINNY ARSENAL (Tech Lib)
1	FTD (TDFS)	2	PICATINNY ARSENAL (SMUPA-DWB)
1	FTD (TDBTL)	1	FRANKFORD ARSENAL (Lib)
1	FTD (TDEA)	1	SPRINGFIELD ARMORY
2	FTD (TDEWA)	1	US ARMY RESCH OFFICE-DURHAM
1	SEG	1	BALLISTIC RESCH LAB
1	SEG (SETGF)	2	BALLISTIC RESCH LAB (Tech Lib)
1	SEG (SEDC)	1	BALLISTIC RESCH LAB (AMXBR-WC)
1	SEG (SEBA)	20	DDC
1	SEC (SEPRR)	2	DIR USAF PROJ RAND
1	RTD (RTNW)	2	GENERAL MOTORS CORP
2	RTD (TECH LIB)	1	THE BOEING CO.
2	SSD (SSTAS/Capt Hayford)	1	GENERAL ELEC CO MSVD
1	SSD (SSTDS)	1	AVCO CORP RAD (M. Rockowitz)
1	SSD (SSTIE/Capt Boverie)	1	MARTIN-MARIETTA CORP
1	SSD (SSTRT/Capt K.R.Hughey)	1	NORTRONICS DIV-NORTHROP CORP
2	BSD (BSVDA)	1	RAYTHEON CO.
1	BSD (BSVDA/Capt Baker)	1	RSCH INST-ILLINOIS INST OF TECH
1	ESD (ESAT)	1	BATTELLE MEMORIAL INSTITUTE
1	AFCRL (CRXL)	1	FALCON R&D
1	RADC (RAALD)	3	AEROSPACE CORP
1	AEDC (AETV/Maj Brown)	1	SHOCK HYDRODYNAMICS INC
1	AEDC (Tech Lib)	1	SCIENTIFIC & TECH INFO FAC
2	AFWL (WLL)	1	LOCKHEED AIRCRAFT CORP
1	AFWL (WLRPT/Capt Gillespie)	1	GENERAL AMERICAN TRANSPORTATION CO
1	AFWL (WLAX)	2	AEROSPACE CORP (Tech Lib)
1	AFWL (WLRPD)	1	AEROSPACE CORP (Dr. J. Brown)
1	AFMTC (MTBAT)	1	AEROSPACE CORP (Mr. C. Kelley)
1	AFFTC (FTOOT)	1	AEROSPACE CORP (Mr. R. Farrin)
1	SAC (OA)		

1 AEROSPACE CORP (Mr. V. Frost)  
1 AEROSPACE CORP (Applied Mech Div)  
4 STANFORD RESCH INSTITUTE  
2 PHYSICS INTER. (J. HARLAN)  
1 PGF  
4 PGBAP-1  
1 ATBT  
1 ATG  
1 ATTR  
6 ATWR

~~Confidential~~

Security Classification

**DOCUMENT CONTROL DATA - R&D**

(Security classification of title, body of abstract and indexing annotation must be entered when the overall report is classified)

**1. ORIGINATING ACTIVITY (Corporate author)**

Air Proving Ground Center  
Eglin Air Force Base, Florida

**2a. REPORT SECURITY CLASSIFICATION**  
**CONFIDENTIAL**

**2b. GROUP**  
**4**

**3. REPORT TITLE**

RESEARCH ON THE PROJECTION OF MULTILAYERED FRAGMENTS.

**4. DESCRIPTIVE NOTES (Type of report and inclusive dates)**

**5. AUTHOR(S) (Last name, first name, initial)**

Poston, Edward C., Jr.

**6. REPORT DATE**

November 1964

**7a. TOTAL NO. OF PAGES**

160

**7b. NO. OF REFS**

13

**8a. CONTRACT OR GRANT NO.**

AF08(635)-2951

**b. PROJECT NO.**

2835

**c.**

Task 283501

**d.**

**9a. ORIGINATOR'S REPORT NUMBER(S)**

**9b. OTHER REPORT NO(S) (Any other numbers that may be assigned this report)**

ATL-TR-64-74

**10. AVAILABILITY/LIMITATION NOTICES**

Qualified requesters may obtain copies of this report from DDC.

**11. SUPPLEMENTARY NOTES**

**12. SPONSORING MILITARY ACTIVITY**

Detachment 4, Research and Technology Div.  
Eglin Air Force Base, Florida

**13. ABSTRACT**

(C) This report describes a research program directed toward developing methods for explosive acceleration of multiple fragment layers to a uniform velocity. Seven methods which achieve such velocity uniformity in varying degrees are described. Other aspects of these methods which received attention included fragment density in the fragment cloud, fragment velocity, fragment cloud growth rate, and damage of fragments. Appendices are included which discuss theoretical calculations of the performance of one method, special instrumentation developed and used during the project, and fabrication methods for the fragment pack. A final appendix gives a complete listing of the shots fired during the project.

Op-

DD FORM 1473  
1 JAN 64

~~Confidential~~

Security Classification

Confidential

Security Classification

14.

KEY WORDS

Fragmentation  
Warheads  
Antipersonnel weapons  
Explosion effects  
Projectors (ordnance)

LINK A

LINK B

LINK C

ROLE

WT

ROLE

WT

ROLE

WT

### INSTRUCTIONS

1. **ORIGINATING ACTIVITY:** Enter the name and address of the contractor, subcontractor, grantee, Department of Defense activity or other organization (*corporate author*) issuing the report.

2a. **REPORT SECURITY CLASSIFICATION:** Enter the overall security classification of the report. Indicate whether "Restricted Data" is included. Marking is to be in accordance with appropriate security regulations.

2b. **GROUP:** Automatic downgrading is specified in DoD Directive 5200.10 and Armed Forces Industrial Manual. Enter the group number. Also, when applicable, show that optional markings have been used for Group 3 and Group 4 as authorized.

3. **REPORT TITLE:** Enter the complete report title in all capital letters. Titles in all cases should be unclassified. If a meaningful title cannot be selected without classification, show title classification in all capitals in parenthesis immediately following the title.

4. **DESCRIPTIVE NOTES:** If appropriate, enter the type of report, e.g., interim, progress, summary, annual, or final. Give the inclusive dates when a specific reporting period is covered.

5. **AUTHOR(S):** Enter the name(s) of author(s) as shown on or in the report. Enter last name, first name, middle initial. If military, show rank and branch of service. The name of the principal author is an absolute minimum requirement.

6. **REPORT DATE:** Enter the date of the report as day, month, year, or month, year. If more than one date appears on the report, use date of publication.

7a. **TOTAL NUMBER OF PAGES:** The total page count should follow normal pagination procedures, i.e., enter the number of pages containing information.

7b. **NUMBER OF REFERENCES:** Enter the total number of references cited in the report.

8a. **CONTRACT OR GRANT NUMBER:** If appropriate, enter the applicable number of the contract or grant under which the report was written.

8b, 8c, & 8d. **PROJECT NUMBER:** Enter the appropriate military department identification, such as project number, subproject number, system numbers, task number, etc.

9a. **ORIGINATOR'S REPORT NUMBER(S):** Enter the official report number by which the document will be identified and controlled by the originating activity. This number must be unique to this report.

9b. **OTHER REPORT NUMBER(S):** If the report has been assigned any other report numbers (either by the originator or by the sponsor), also enter the number(s).

10. **AVAILABILITY/LIMITATION NOTICES:** Enter any limitations on further dissemination of the report, other than those

imposed by security classification, using standard statements such as:

- (1) "Qualified requesters may obtain copies of this report from DDC."
- (2) "Foreign announcement and dissemination of this report by DDC is not authorized."
- (3) "U. S. Government agencies may obtain copies of this report directly from DDC. Other qualified DDC users shall request through \_\_\_\_\_."
- (4) "U. S. military agencies may obtain copies of this report directly from DDC. Other qualified users shall request through \_\_\_\_\_."
- (5) "All distribution of this report is controlled. Qualified DDC users shall request through \_\_\_\_\_."

If the report has been furnished to the Office of Technical Services, Department of Commerce, for sale to the public, indicate this fact and enter the price, if known.

11. **SUPPLEMENTARY NOTES:** Use for additional explanatory notes.

12. **SPONSORING MILITARY ACTIVITY:** Enter the name of the departmental project office or laboratory sponsoring (paying for) the research and development. Include address.

13. **ABSTRACT:** Enter an abstract giving a brief and factual summary of the document indicative of the report, even though it may also appear elsewhere in the body of the technical report. If additional space is required, a continuation sheet shall be attached.

It is highly desirable that the abstract of classified reports be unclassified. Each paragraph of the abstract shall end with an indication of the military security classification of the information in the paragraph, represented as (TS), (S), (C), or (U).

There is no limitation on the length of the abstract. However, the suggested length is from 150 to 225 words.

14. **KEY WORDS:** Key words are technically meaningful terms or short phrases that characterize a report and may be used as index entries for cataloging the report. Key words must be selected so that no security classification is required. Identifiers, such as equipment model designation, trade name, military project code name, geographic location, may be used as key words but will be followed by an indication of technical context. The assignment of links, rules, and weights is optional.

Confidential

Security Classification